BILINGUAL PUBLISHING GROUP

Journal of Botanical Research

Volume 5 | Issue 3 | July 2023 | ISSN 2630-5054（Online）

Volume 5 Issue 3 • July 2023 • ISSN 2630-5054 (Online)

Journal of Botanical Research

BILINGUAL PUBLISHING GROUP

BILINGUAL PUBLISHING GROUP

Volume 5 | Issue 3 | July 2023 | Page1-66

Journal of Botanical Research

Contents

Articles

BILINGUAL PUBLISHING GROUP

Journal of Botanical Research

https://journals.bilpubgroup.com/index.php/jbr

ARTICLE

Effects of Arbuscular Mycorrhizal Fungi on the Physiology and Saponin Synthesis of *Paris polyphylla* var. *yunnanensis* at Different Nitrogen Levels

***Can Huang*[1,5], *Shubiao Qian*[1], *Xiaoxian Li*[3], *Xiahong He*[1], *Shuhui Zi*[1,2], *Congfang Xi*[1], *Rui Shi*[4*], *Tao Liu*[1*]**

[1] *College of Agriculture and Biotechnology, Yunnan Agricultural University, Kunming, Yunnan, 650201, China*

[2] *State Key Laboratory of Conservation and Utilization of Bio-resources in Yunnan, National & Local Joint Engineering Research Center on Gemplasm Innovation & Utilization of Chinese Medicinal Materials in Southwest China, Yunnan Agricultural University, Kunming, Yunnan, 650500, China*

[3] *Kunming Institute of Botany, Chinese Academy of Sciences, Kunming, Yunnan, 650201, China*

[4] *Southwest Forestry University, Kunming, Yunnan, 650224, China*

[5] *Guangxi Subtropical Crops Research Institute, Nanning, Guangxi, 530001, China*

ABSTRACT

Arbuscular mycorrhizal fungi (AMF) are important members of the plant microbiome and affect the uptake and transfer of mineral elements by forming a symbiotic relationship with plant roots. Nitrogen (N), as an important mineral element, can directly affect plant growth and development at different N levels. It has been confirmed that inoculation with AMF can improve the efficiency of N utilization by plants. However, there are still fewer reports on the dynamic relationship between arbuscular mycorrhizal and plant secondary metabolites at different nitrogen levels. In this experiment, the physiological indexes and genes related to saponin synthesis were determined by applying different concentration gradients of nitrogen to the medicinal plant *P. polyphylla* var. *yunnanensis* infested by AMF as the test material. It was found that nitrogen addition increased the biomass, chlorophyll content, and nutrient content of above- and below-ground plant parts and increased the content of saponin content of *P. polyphylla* var. *yunnanensis* to some extent, but AMF inoculation increased the saponin content of *P. polyphylla* var. *yunnanensis* more significantly. AMF inoculation also promoted the expression of genes related to the saponin synthesis pathway, including 3-hydroxy-3-methylglutaryl coenzyme A synthase (HMGS), squalene epoxidase 1 (SE1), and cycloartenol synthase (CAS), which is in according with the accumulation of saponin in plants. It also may increase the saponin content of AMF plants by altering the expression of P450s and UGTs related to saponin synthesis.

Keywords: Nitrogen; Arbuscular mycorrhizal fungi; Saponin; *P. polyphylla* var. *yunnanensis*

*CORRESPONDING AUTHOR:

Rui Shi, Southwest Forestry University, Kunming, Yunnan, 650224, China; Email: shirui0227@sina.com.cn

Tao Liu, College of Agriculture and Biotechnology, Yunnan Agricultural University, Kunming, Yunnan, 650201, China; Email: lt-lxx@163.com

ARTICLE INFO

Received: 7 March 2023 | Revised: 6 May 2023 | Accepted: 6 May 2023 | Published Online: 26 May 2023

DOI: https://doi.org/10.30564/jbr.v5i3.5518

CITATION

Huang, C., Qian, S.B., Li, X.X., et al., 2023. Effects of Arbuscular Mycorrhizal Fungi on the Physiology and Saponin Synthesis of *Paris polyphylla* var. *yunnanensis* at Different Nitrogen Levels. Journal of Botanical Research. 5(3): 1-26. DOI: https://doi.org/10.30564/jbr.v5i3.5518

1. Introduction

Nitrogen (N) fertilizer application has long been one of the main tools for agricultural yield improvement [1]. But along with the increased use of nitrogen levels comes an increasingly high economic and environmental cost. However, excessive N can cause dramatic changes in the plant growth environment and can lead to soil acidification and salinization, which in turn can lead to significant loss of soil carbonate [2]. Excessive N application can also reduce soil microbial activity, decreasing the bacterial community composition [3] and enhancing the spread of soil diseases [4]. In recent years, many studies have shown that soil symbiotic fungi with plants, especially arbuscular mycorrhizal fungi, play an important role in helping plants to absorb nitrogen and phosphorus nutrients [5,6]. How to apply nitrogen fertilizer to plants more scientifically, rationally and efficiently can more effectively reduce nitrogen deposition in natural ecosystems, enhance the synergistic effect of nutrient transport between plants and microorganisms, and achieve longer-term sustainable development, are important issues that continue to be explored.

Arbuscular mycorrhizal fungi (AMF) are widely symbiotic in terrestrial plants, and when AMF are symbiotic with plants, AMF can help plants to absorb more water and mineral elements through mycelial transport, which can account for the majority of the total nutrients absorbed by plants [7]. As an important nutrient required for plant growth, the main N in soil is ammonium nitrogen (NO^{3-}) and nitrate nitrogen (NH^{4+}). Many studies have found that AMF can take up ammonium and nitrate nitrogen from the soil, as well as other forms of organic nitrogen. N is taken up by AMF and enters the AMF mycelium and is assimilated into arginine (arg), which is transported through the mycelium to the periplasmic cavity (PAM), where it is hydrolyzed to form NH^{4+}, which enters the plant cell through the PAM and is then transported by cellular NH^{4+} transporters (AMTs) transport [8-11]. In addition, AMF inoculation can also promote plant growth and increase the secondary metabolite content of plants. For example, AMF inoculation significantly increased the yield as well as vitamin content of strawberry at low phosphorus levels [12]. The relationship between microorganisms and secondary metabolites is also complex; for example, certain microorganisms are capable of producing some active ingredients themselves, including secondary metabolites of plants [13]. In medicinal plants, secondary metabolites mainly help plants to resist ecological conditions. The common ones are triterpene saponins, steroid saponins, alkaloids, phenolics, etc. AMF plants are able to alter the accumulation of phenolics in the plant by increasing the uptake of P [14]. In response to biotic stresses and to improve plant adaptations, mycorrhizalization can increase the content of plant alkaloids such as camptothecin [15], in studies on terpenoids, it was found that mycorrhizal symbiosis facilitates the expression of genes on the terpenoid synthesis pathway in medicinal plants [16,17]. In medicinal plants, AMF enhances the accumulation of medicinal components in licorice by inducing the genes SQS1, β-AS, CYP88D6 and CYP72A154 on the glycyrrhetinic acid and glycyrrhizin synthesis pathways [18]. Field trials also demonstrated that AMF inoculation increased artemisinin content in *Artemisia annua* leaves while improving the nutritional status of the plant, and that different AMFs differed significantly in enhancing artemisinin accumulation [19]. Although numerous studies have shown that AMF can effectively increase the content of active chemical components in medicinal plants [20], and regulates the accumulation of secondary plant metabolites by changing root morphology [21], however, the main studies have usually focused on the relationship between P and AMF, the effects of inoculation with mycorrhizal fungi of Artemisia bushes at different nitrogen levels on plant growth and secondary metabolites have not been reported. In addition, there were differences in the effects of different types of AMF on plants, and the analysis of the metabolome revealed significant differences in the effects of different types of AMF on the metabolite accumulation patterns of plants [22]. For example, Glomus caledonium inoculation increased rosmarinic and caffeic acid production in Ocimum basilicum,

while F. mosseae only increased caffeic acid production [23]. In the case of medicinal plants, the promotion effect of AMF symbiosis is also closely related to the growth environment of the plant, as different nutrient conditions, light time, harvesting time and cultivation methods can have significant effects on AMF-plant symbiosis [24]. Through previous studies in the laboratory, it was found that among Glomus moseae, Glomus etunicatum, Glomus eburneum, and Paraglomus occultum, the symbiosis of *P. polyphylla* var. *yunnanensis* rebus with Glomus eburneum and Cryptococcus occultum was better, and the symbiotic colonization rate of the remaining two AMF fungi with *P. polyphylla* var. *yunnanensis* rebus was lower.

P. polyphylla var. *yunnanensis* is a valuable Chinese herb with steroidal saponins as its main active constituents, which have various effects such as antitumor, hemostatic, antibacterial, and immunomodulatory [25]. Steroidal saponins are synthesized mainly through the cytoplasmic mevalonate (MVA) pathway and the plastidic 2-C-methyl-d-erythritol-4-phosphate (MEP) pathway for the biosynthesis of saponin elements, which are then modified by glycosyltransferases and P450 to eventually form different saponins [26,27]. In order to investigate the effect of AMF inoculation on the nitrogen uptake and secondary metabolism synthesis of the plant, the present study was conducted to investigate the effects on the growth physiology and active components of *P. polyphylla* var. *yunnanensis* after symbiosis with different species of AMF under different nitrogen levels and the molecular mechanism behind it.

2. Materials and methods

2.1 Biomaterials and culture

The seedlings were purchased from Yunnan Baotian Agricultural Technology Co. Ltd, and two-year-old seedlings were selected as the test material. The AMF fungi used were purchased from the Germplasm Repository of Congenital Mycorrhizal Fungi (BGC), the Institute of Plant Nutrition and Resources, Beijing Academy of Agricultural and Forestry Sciences (BAAFS), Beijing, China. The purchased fungi were *Glomus eburneum* (Ge) and *Paraglomus occultum* (Po). Mycorrhizal substrates containing approximately 100 spores per 10 g were purchased for subsequent expansion inoculation. The soil substrates used in this experiment were humus, loess, and sand. Humus was purchased from Dounan Flower and Bird Market in Kunming, Yunnan Province, and loess was selected from the test site at Yunnan Agricultural University. The three soils were mixed in a volume ratio of 3:1 (humus: loess) and 2:1 (humus: sand), then sterilized in an autoclave at 121 °C for 1 h, bagged and sealed, and set aside in a cool place. The cooled soil was packed into pots of about 1.5 kg each, with a diameter of 21 cm, bottom diameter of 20 cm and height of 20 cm. 10% sodium hypochlorite was sprayed on the surface for 1 h before use, and then rinsed with sterile water to dry. Two layers of 8-needle shade net were covered in the rain-proof greenhouse, and trays were placed at the bottom of the planting pots to prevent rapid water loss and to ensure no cross-contamination between treatments. Before the test treatment, the *P. polyphylla* var. *yunnanensis* seedlings were transplanted into pots, 2/3 of the substrate soil was poured in first, then the roots of *P. polyphylla* var. *yunnanensis* were put into the soil, and finally the soil was filled, and 3 or 4 *P. polyphylla* var. *yunnanensis* plants were transplanted into each pot. The transplanting was completed in June 2020. Until the second year of seedling emergence regularly watered with sterile water, and to ensure the rate of shade of the greenhouse, control of pests and diseases, keep the greenhouse clean and good air permeability, weed at the right time.

2.2 AMF propagation

AMF was colonized using sandy soil with humus as substrate. Maize seeds were selected in July 2020 after surface disinfection by 10% sodium hypochlorite spraying for 1 h and rinsing and drying with sterile water, buried 5 cm below the surface soil, and 2 g of AMF fungicide was evenly applied around them, 3-4 maize seeds were planted into each pot, a total of 10 pots were cultivated, 5 pots for each type of AMF, and Hoagland nutrient solution was applied

regularly (once every 2 weeks) during the rest of the time, sterile water was poured to ensure that the soil moisture content was maintained between 20% and 30% (measured using a moisture meter) in order to increase the AMF colonization rate.

2.3 AMF inoculation

After 4 months of expansion culture, the aboveground part of the successfully expanded maize was cut, and the roots were cut into root segments of about 1 cm and mixed evenly with the root soil as a follow-up AMF fungicide. AMF was inoculated at the rhizomes of *P. polyphylla* var. *yunnanensis*, the soil at the rhizomes of *P. polyphylla* var. *yunnanensis* prepared for inoculation was removed, and then the spare fungicide (about 50 g) weighed in advance was spread evenly around the rhizomes of *P. polyphylla* var. *yunnanensis* again, and finally, the soil was filled, finish the transplanting and inoculation process. AMF inoculation of *P. polyphylla* var. *yunnanensis* was completed in March 2021.

2.4 Different nitrogen concentration treatment

The nitrogen test was divided into 3 nitrogen addition gradients: N1 (application of 1 mM NH_4NO_3), N2 (application of 2.5 mM NH_4NO_3), and N3 (application of 5 mM NH_4NO_3). Each nitrogen gradient consisted of three inoculation treatments: no AMF (AM^-), inoculation with *Glomus eburneum* (Ge), and inoculation with *Paraglomus occultum* (Po), for a total of nine treatments: N1CK; N1Ge; N1Po; N2CK; N2Ge; N2Po; N3CK; N3Ge; N3Po. Nitrogen was added every 2 weeks by accurately weighing 16.00 g into a 1000 mL volumetric flask, using sterilized pure water to fix the volume to 1000 mL to obtain 16 g/L NH_4NO_3 solution. The NH_4NO_3 solutions of 1 mM/250 mL, 2.5 mM/250 mL and 5 mM/250 mL were obtained by dividing 5 mL, 12.5 mL and 25 mL into 250 mL volumetric flasks and adding sterilized pure water to 250 mL, respectively. After 90 days of nitrogen addition, the corresponding indexes of *P. polyphylla* var. *yunnanensis* were measured. The nitrogen addition was started in June 2021.

2.5 AMF colonization rate

AMF was determined with reference to the Taipan Blue staining method, determination by reference to the method [28]: (1) Fixation: 1 cm root segments (lateral roots) of *P. polyphylla* var. *yunnanensis* rebus were taken and fixed in FAA solution (130 mL formaldehyde, 50 mL glacial acetic acid, 2000 mL 5% ethanol) for 24 h. (2) Transparency: Root segments were cleaned with distilled water, immersed in 10% KOH solution, heated in a water bath at 90 °C for 60 min, and heated until the root color was slightly white and transparent. (3) Acidification: The residual KOH on the roots was cleaned with distilled water, immersed in 2% HCL solution, acidified for 10 min, and then cleaned with distilled water. (4) Staining: Put the washed root segments into 0.05% Taipan blue staining solution, heated in a 90 °C water bath for 30 min, removed and cooled, then put into lactic acid glycerol solution for decolorization for more than 60 min. (5) Filming observation: According to the amount of mycorrhizal structure of each root segment, the infestation rate was graded by 0%, < 5%, < 10%, < 30%, > 50%, > 70%, > 90%.

2.6 Determination of elemental content

Soil nitrogen: The determination was performed by the alkaline solution method. Soil phosphorus: The determination was carried out by atomic absorption spectrometry using ammonium acetate leaching. Soil phosphorus: Molybdenum antimony anti-colorimetric method was used for determination.

Organic matter: The oxidation capacity method of potassium dichromate was used for the determination. Plant nitrogen: Measured with reference to the agricultural industry standard NY/T297-1995 of the People's Republic of China. Plant phosphorus: Measured with reference to NY/T2421-2013, the agricultural industry standard of the People's Republic of China. Plant potassium: Measured with reference to NY/T2420-2013, the agricultural industry standard of the People's Republic of China. Plant organic

matter: Measured with reference to NY/T1121.6-2006, the agricultural industry standard of the People's Republic of China.

2.7 Determination of plant physiological indicators

Determination of chlorophyll content

To determine the photosynthetic pigment content of *P. polyphylla* var. *yunnanensis* plants [29], fresh plant leaves of uniform length were selected, the midvein was removed, cut, and weighed to 0.1 g. The samples were placed in a mortar, and 2-3 mL of 95% ethanol and a small amount of calcium carbonate ($CaCO_3$) was added to make a homogenous slurry, 95% ethanol was added dropwise until the tissue turned white, and left to stand; the filter paper was placed on a funnel, moistened with ethanol, and filtered into a 25 mL volumetric flask. The filter paper was placed on a funnel, moistened with ethanol, and filtered into a 25 mL volumetric flask. Rinse the chlorophyll on the filter paper with 95% ethanol into a volumetric flask, fix the volume to 25 mL, shake well, and set aside. The above samples were taken into the cuvette, and the values of 665 nm, 649 nm and 470 nm were measured with 95% ethanol reagent as blank.

Calculation formula:

$$Ca = 13.95\ A665 - 6.88\ A649$$

$$Cb = 24.96\ A649 - 7.32\ A665$$

$$Cx = (1000\ A470 - 2.05\ Ca - 114.8\ Cb)/245$$

$$\text{Content (mg/g)} = [\text{C(mg/L)} \times \text{total extract (25 mL)}]/[\text{weight of leaf sample (0.1 g)} \times 1000]$$

2.8 Determination of Abscisic Acid (ABA), 3-Indoleacetic acid (IAA) and Proline (Pro) in plants

Determination of ABA and IAA

Both ABA and IAA were determined using enzyme-linked immunoassay kits, and ABA was determined using plant ABA enzyme-linked immunosorbent assay kits [30]. Extraction of primary enzyme solution: Cut the leaf tissue into the grinding bowl, then liquid nitrogen grinding into powder, 1 g of plant tissue plus 9 mL of homogenate (PBS), 4000-5000 rpm/min centrifugation for 15 minutes to take the supernatant. Dilution of standards: The kit provides one original multiple standard, which can be diluted in small test tubes according to the following chart: No. 5 standard: 150 μL of original multiple standard added to 150 μL standard dilution; No. 4 standard: 150 μL of No. 5 standard added to 150 μL standard dilution; No. 3 standard: 150 μL of No. 4 standard added to 150 μL standard dilution; No. 2 standard: 150 μL of No. 4 standard added to 150 μL standard dilution; No. 3 standard: 150 μL of No. 4 standard added to 150 μL standard dilution. Dilution; No. 2 standard: 150 μL of No. 3 standard added to 150 μL standard dilution; No. 1 standard 150 μL of No. 2 standard added to 150 μL standard dilution, the concentrations are 48 pmol/L, 24 pmol/L, 12 pmol/L, 6 pmol/L, 3 pmol/L. Adding samples: Set up blank wells respectively (blank control). The wells were set up as blank control wells (no sample and enzyme reagent were added to the wells, the rest of the steps were the same), standard wells and wells for the samples to be tested. Add 50 μL of standard to the enzyme plate, 40 μL of sample dilution to the sample wells, and then 10 μL of sample to be tested (the final dilution of the sample is 5 times). Add the sample to the bottom of the well of the enzyme plate without touching the wall of the well as much as possible, and gently shake and mix. Warming: Seal the plate with sealing film and incubate at 37 °C for 30 minutes. Configurate liquid: 30-fold washing solution diluted 30-fold with distilled water backup washing: Uncover closure plate membrane, discard liquid, dry by swing, add full washing solution to each well, rest for 30 seconds, repeat 5 times, dry by pat. Add enzyme: Add hrP-conjugate reagent 50 μL to each well, except the blank well. Incubation: Operation with 3. Washing: Operation with 5. Color-developing: Add color developing agent A50 μL and color-developing agent B50 μL to each well, mix gently, and avoid light developing for 10 minutes at 37 °C. Termination: Add 50 μL termination solution to each well to terminate the reaction (at this

time, the blue color turns to yellow). Determination: Set the blank hole to zero, and measure the absorbance (OD value) of each hole in sequence at 450 nm wavelength. The determination should be carried out within 15 minutes after adding termination solution.

Proline determination

Proline was extracted and determined by referring to the method of Bates et al. [31]. The proline content in *P. polyphylla* var. *yunnanensis* was determined by using UV spectrophotometer. About 0.5 g of *P. polyphylla* var. *yunnanensis* leaves were weighed and added to 4.5 mL of homogenization medium, and mechanical homogenization was carried out in an ice-water bath, followed by centrifugation at 3500 rpm for 10 min, and the supernatant was taken afterwards. The absorbance was measured in a 1-cm cuvette at 520 nm by adding corresponding reagents in a boiling water bath for 30 min according to the proline test kit.

2.9 Determination of saponin content

The content of steroidal saponins in the rhizomes of *P. polyphylla* var. *yunnanensis* seedlings was determined by high performance liquid chromatography (HPLC) on an Agilent 4.6 × 250 mm column with the following chromatographic conditions: mobile phase acetonitrile (A): water (B) (gradient elution, 0→40 min (A:B = 30:70→60:40), 40→41 min (A:B = 60:40→80:20), 41→44 min (A:B = 80:20→80:20). The rhizomes were collected from the treated rhizomes, washed, dried to constant weight at 45 °C, and crushed. The sample was weighed precisely according to the method of Chinese Pharmacopoeia and placed in a 50 mL volumetric flask with 0.5 g of crushed sample (passed through No. 3 sieve, 50 mesh), added methanol to 20 mL, weighed at this point, soaked for 30 min, extracted by ultrasonication for 30 min, cooled at room temperature, then methanol was used to make up the lost weight, shaken well, and the extract was filtered through a 0.45 μm microporous membrane. The extract was filtered through a 0.45 μm microporous membrane. 700 uL was taken into a brown injection bottle and injected into the machine.

2.10 Determination of genes and transcriptome

Seven genes related to the steroidal saponin synthesis pathway of *P. polyphylla* var. *yunnanensis* were selected for fluorescent quantitative PCR analysis based on previous experiments. The seven related genes were: 3-hydroxy-3-methylglutaryl coenzyme A synthase (HMGS), vanilloid diphosphate synthase (GPPS), farnesyl pyrophosphate synthase (FPPS), squalene synthase (SS), squalene cyclooxygenase 1 (SE1), cycloazidyl synthase (CAS), and squalene cyclooxygenase 2 (SE2). The transcriptome assays were performed on selected rhizome fractions of *P. polyphylla* var. *yunnanensis* and sent to Shanghai Meiji Biological Company for determination. The transcripts were assembled de novo using Trinity software with default parameters. The overlapping groups were assembled into unigenes based on paired-end information and subsequently annotated against the National Center for Biotechnology Information (NCBI) database using the BLAST program, and homology searches were performed using BLAST against the following protein databases: NCBI non-redundant (nr), Kyoto Encyclopedia of Genes and Genomes (KEGG) and GO (Gene Ontology) [32]. The best comparison results were selected for single gene annotation. Sequences of unigenes belonging to cytochrome P450 and UDP-glycosyltransferase (UGT) were identified from the transcriptome, and unigenes > 1000 bp in length were screened for phylogenetic analysis. Phylogenetic tree mapping was performed using MEGA7, and some of the UGT and P450 from other plants were selected, and then some of the unigenes sequences of UGT and P450 whose functions had been identified and those of UGT and P450 screened from the transcriptome of *P. polyphylla* var. *yunnanensis* were selected for phylogenetic analysis.

2.11 Data analysis

The obtained experimental data were statistically analyzed by Excel 2013 software; SPSS 20.0 (SPSS, Chicago, USA) analysis software was used for statis-

tical analysis, and one-way ANOVA (one-way analysis of variance) was used for the analysis of significance of differences; comparison of means between treatments was performed using Duncan's multiple comparison method for analysis of significance of differences; and Prism software and Origin2019b software were used for graphing.

3. Results

3.1 AMF colonization rate

Under different N conditions, the roots of *P. polyphylla* var. *yunnanensis* inoculated with AMF treatment were all infiltrated by mycelium, and all with mycelium or spore structures, while the treatments without inoculation had no mycorrhizal structures (**Figure 1**). As seen in the colonization rate, the colonization rate of Ge decreased significantly under the highest concentration of N treatment, but the difference was not significant at low and medium concentrations, while the colonization rate of Po remained consistent with the N concentration gradient (**Figure 2**) ($p > 0.01$).

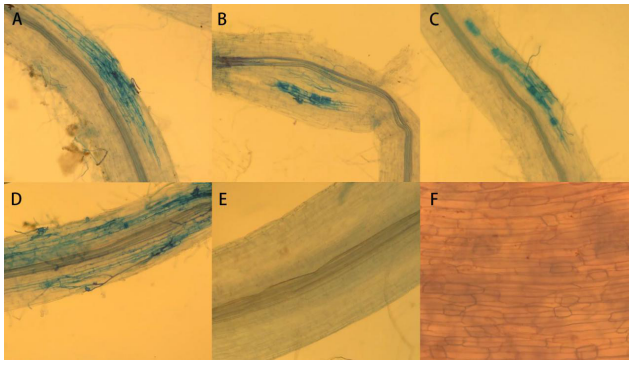

Figure 1. Mycorrhizal structure of the root system of *Pp*.

Note:

A: Mycorrhizal structure of mycorrhizal infestation by Ge under N3 treatment,

B: Mycorrhizal structure of mycorrhizal infestation by Po under N1 treatment,

C: Mycorrhizal structure of mycorrhizal infestation by Ge under N2 treatment,

D: Mycorrhizal structure of mycorrhizal infestation by Ge under N1 treatment,

E: Non-mycorrhizal structure of mycorrhizal infestation under N1 treatment,

F: Non-mycorrhizal structure of mycorrhizal infestation under N2 treatment.

3.2 Agronomic traits of *P. polyphylla* var. *yunnanensis*

After 90 days of nitrogen treatment, the agronomic trait indexes of *P. polyphylla* var. *yunnanensis* were measured. The differences in leaf length and leaf width of plants under most treatments were not significant, with leaf length under the N1Ge treatment being higher than the other treatments, while leaf length under N3Po was lower. Plant height under the N1 treatment without AMF inoculation showed lower values, while plant height under the other treatments did not differ significantly, and plant stem and root weights also showed this trend (**Table 1**).

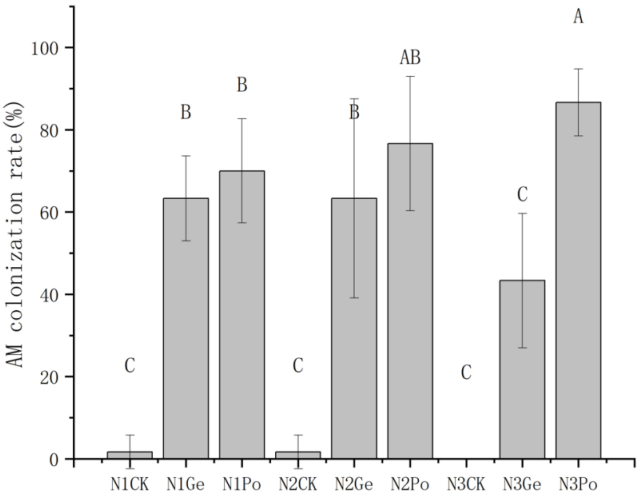

Figure 2. Root colonization rate of *Pp.* under different nitrogen treatments ($p > 0.01$).

3.3 Chlorophyll content

By applying different nitrogen to *P. polyphylla* var. *yunnanensis*, it was found that inoculation with Ge favored the accumulation of chlorophyll a, b, and carotenoids at low nitrogen concentrations, while inoculation with Po increased chlorophyll in the plants less than Ge (**Figure 3**). In the medium N treatment, both AMFs significantly increased chlorophyll a, b and carotenoid contents of the plants (**Figures 3-6**). In the high N treatment, inoculation with Po reduced the chlorophyll a and carotenoid content of the plants, with no significant difference for chlorophyll b, whereas inoculation with Ge reduced only the carotenoid content, but the total chlorophyll content was the same as in plants without AMF (**Figure 3D**).

Table 1. Effects of different nitrogen treatments on the morphological indexes of *P. polyphylla* var. *Yunnanensis.*

Treatment	Leaf length (cm)	Leaf width (cm)	Plant height (cm)	Stem weight (g)	Root weight (g)	Root length (cm)
N1CK	5.275 ± 0.57AB	3.16 ± 0.30 ns	14.65 ± 0.88B	1.0796 ± 0.05B	0.96205 ± 0.16B	9.53 ± 1.42 ns
N1Ge	5.545 ± 0.64A	3.1 ± 0.33 ns	15.66 ± 1.26A	1.1162 ± 0.04AB	1.1329 ± 0.17A	10.055 ± 0.83 ns
N1Po	5.47 ± 0.55AB	3.085 ± 0.26 ns	16.215 ± 0.67A	1.1499 ± 0.05A	1.06785 ± 0.18AB	9.175 ± 1.47 ns
N2CK	5.38 ± 0.47AB	3.045 ± 0.27 ns	16.03 ± 1.15A	1.11125 ± 0.08AB	1.03375 ± 0.17AB	9.66 ± 1.72 ns
N2Ge	5.475 ± 0.61AB	3.005 ± 0.30 ns	16.315 ± 1.08A	1.1467 ± 0.07A	1.0854 ± 0.12A	10.01 ± 1.79 ns
N2Po	5.535 ± 0.46A	3.005 ± 0.32 ns	16.205 ± 0.82A	1.12865 ± 0.06AB	1.10405 ± 0.21A	9.43 ± 1.79 ns
N3CK	5.535 ± 0.46A	3.035 ± 0.33ns	16.05 ± 0.74A	1.1392 ± 0.06AB	1.058 ± 0.18AB	9.775 ± 1.76 ns
N3Ge	5.415 ± 0.53AB	3.17 ± 0.33 ns	15.93 ± 0.90A	1.1293 ± 0.08AB	1.02415 ± 0.11AB	9.64 ± 1.78 ns
N3Po	5.12 ± 0.71B	2.96 ± 0.33 ns	15.81 ± 0.95A	1.11885 ± 0.08AB	1.07005 ± 0.16AB	10.1 ± 1.67ns

The data in the table are the mean ± standard error (n = 3). Different lowercase letters after the data in the same column indicate significant differences in the level of variation under different treatments ($p < 0.01$).

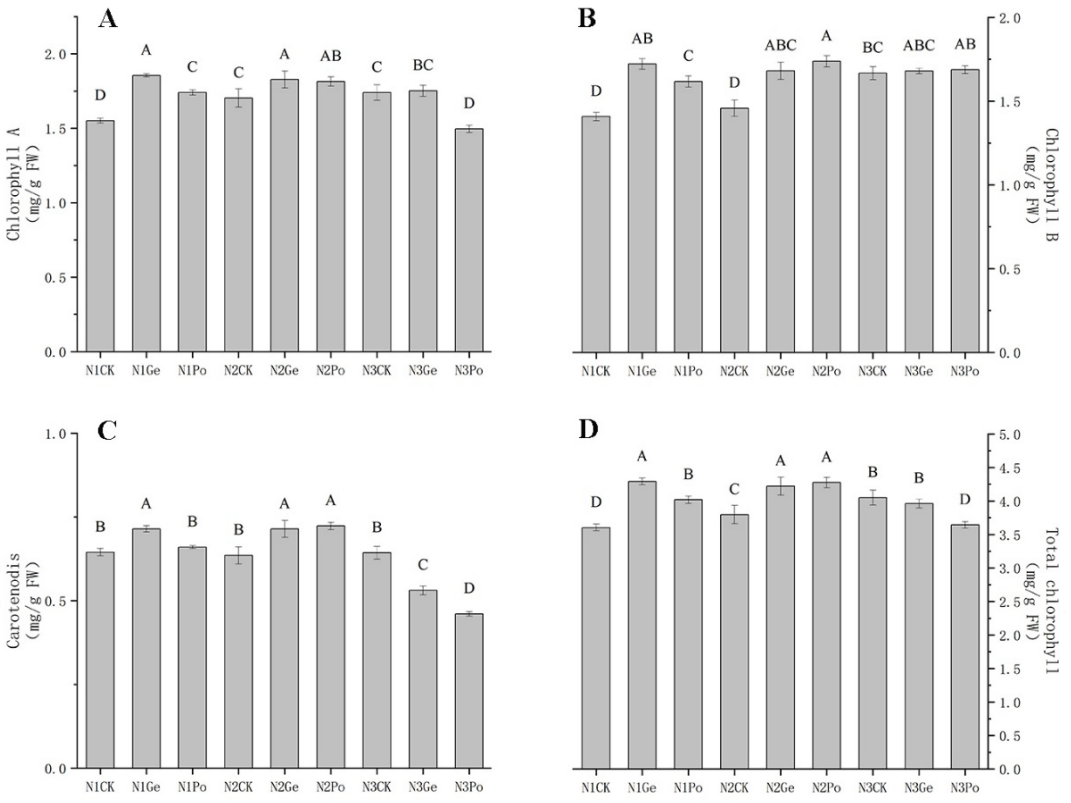

Figure 3. Effect of different nitrogen treatments on the chlorophyll content of *Pp*.

Note: A: chlorophyll a, B: chlorophyll b, C: carotenoids, D: total chlorophyll.

3.4 The contents of ABA, IAA and Pro in *P. polyphylla* var. *yunnanensis*

In this experiment, the IAA content of the roots of *P. polyphylla* var. *yunnanensis* showed an increasing trend with the increase of N concentration (**Figure 4**). In both low and medium N treatments, both AMFs increased the IAA content of plant roots up to 36.82 ng/g in N2Ge treatment, while in high N concentration, the IAA content of N3Ge was 37.39 ng/g, which was significantly higher than that of N3CK and N3Po. The accumulation trends of proline content and IAA content of *P. polyphylla var. yunnanensis* graveolens in different N treatments were similar (**Figure 5B**), with low and medium N levels, both AMF increased the Pro content of plants, but under high N treatment, the Pro content of N3CK and N3Po was significantly higher than that of N3Ge, and the highest Pro content was 20.87 ng/g and 21.5433 ng/g for N3CK and N3Po, respectively and relative to the difference between high and medium N, the AMF on plant IAA and Pro The effect of AMF on plant IAA and Pro varied most significantly from low N to medium N. In contrast, the trend of ABA accumulation in *P. polyphylla* var. *yunnanensis* was opposite to that of IAA and Pro. Under low and medium N treatments, AMF plants reduced the ABA content of *P. polyphylla* var. *yunnanensis* roots (**Figure 5A**), and the lowest ABA content of 29.54 ng/g was found in N3Ge under high N treatment, which was significantly lower than that of N3CK and N3Po.

3.5 Elemental content of the plant and soil

By applying different concentrations of nitrogen, it was found that the quick-acting N content of the soil showed a significant increase, showing a similar trend to the nitrogen gradient (**Table 2**). And under the N3 treatment, the concentration of fast-acting N was found to be higher in the AMF-inoculated soil than in the non-AMF-inoculated soil, but the increase was less than that of the different N treatments. The results of effective phosphorus showed that AMF inoculation promoted the accumulation of effective phosphorus in the soil under low N concentration. And the content of fast-acting potassium in the soil was also higher than that in the soil before nitrogen application, but the difference was not significant between different N treatments.

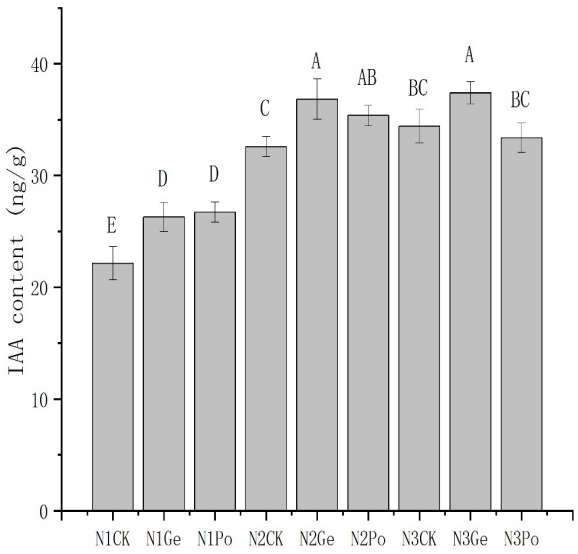

Figure 4. Effect of different nitrogen treatments on the IAA of *P. polyphylla* var. *yunnanensis*.

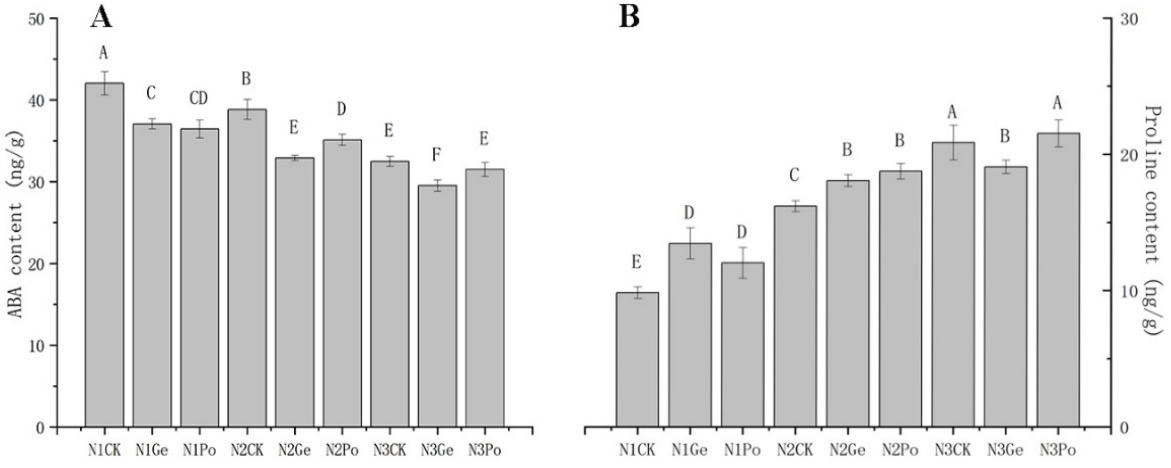

Figure 5. Effect of different nitrogen treatments on ABA and Pro of *P. polyphylla* var. *yunnanensis*.

Note: A: ABA, B: Pro.

Table 2. Effect of different nitrogen treatments on soil NPK content.

Treatment	Organic matter g/kg	Effective phosphorus mg/kg	Fast-acting potassium mg/kg	Quick-acting nitrogen mg/kg
N0(before applying N)	535.26 ± 60.92 ns	67.25 ± 1.34B	551.19 ± 34.35C	252.26 ± 4.89E
N1CK	549.13 ± 27.62 ns	66.62 ± 1.64B	630.89 ± 12.38A	298.69 ± 3.87D
N1Ge	544.46 ± 15.11 ns	71.51 ± 1.12A	632.81 ± 14.38A	296.82 ± 2.91D
N1Po	533.09 ± 11.52 ns	72.79 ± 3.15A	613.47 ± 11.74AB	300.50 ± 3.14D
N2CK	566.09 ± 9.38 ns	66.14 ± 1.38B	581.71 ± 15.97BC	359.93 ± 4.07C
N2Ge	541.25 ± 11.56 ns	64.97 ± 1.07B	602.25 ± 14.71AB	354.11 ± 6.54C
N2Po	555.80 ± 7.99 ns	64.85 ± 2.11B	611.98 ± 13.50AB	359.70 ± 5.45C
N3CK	545.93 ± 2.56 ns	65.89 ± 1.07B	600.63 ± 19.34AB	414.73 ± 1.57B
N3Ge	547.17 ± 12.82 ns	66.69 ± 0.73B	606.03 ± 11.69AB	426.51 ± 3.24A
N3Po	566.36 ± 6.82 ns	65.10 ± 0.64B	594.14 ± 5.21AB	427.01 ± 2.31A
N	F = 0.322574	F = 30.244988**	F = 3.709461*	F = 169.771011**
AMF	F = 2.675380	F = 2.950613ns	F = 0.991322 ns	F = 0.166143 ns
N*AMF	F = 1.192012	F = 4.982080**	F = 0.753217 ns	F = 1.177272 ns

The data in the table are the mean ± standard error (n = 3). Different lowercase letters after the data in the same column indicate significant differences in the level of variation under different treatments ($p < 0.01$).

CNPK measurements on the above-ground parts of nitrogen-treated *P. polyphylla* var. *yunnanensis* revealed that the C content of plants inoculated with AMF was significantly increased under low N treatment (**Table 3**), and the C% of N1Ge and N2Po increased by 3% and 2%, respectively, compared to N1CK, while this trend was reflected in the P, K, and N contents, with the greatest increase being in the P content under low N conditions. Under medium N treatment, both AMFs increased the C content of the plants, but the difference in P content was not significant and the increase in their K and N content was found only in plants inoculated with Ge. Po inoculation had no significant effect on the NPK content of the above-ground parts of the plants under medium N concentration. The C, N, P and K contents of the plants inoculated with AMF did not improve under high N treatment, and especially the C, K and N contents of N3Po showed a decreasing trend. the highest C, K and N contents were found in the N3CK treatment, while the highest P contents were found in the N1Ge-treated plants.

Measurements of C, N, P, and K in the nitrogen-treated subterranean parts of *P. polyphylla* var. *yunnanensis* revealed that both AMFs increased the C, N, P, and K contents of the subterranean parts of *P. polyphylla* var. *yunnanensis* in the low-nitrogen treatment (**Table 4**). In the medium nitrogen treatment, inoculation with Ge still ensured an increase in C, N, P, and K of the plants, but Po symbiosis with the plants only increased the C and N content of the plants. Under the high N treatment, the C and N contents of N3CK, N3Ge and N3Po were not significantly different, while the P contents of N3Ge and N3Po were significantly lower than those of N3CK, and those of N3Po were higher than those of N3CK and N3Ge. In the underground part of the assay, the P contents of AMF plants were all higher than those of other treatments at N1 concentration, while N1Po had the highest K content and N1Ge as well as N2Po had the highest N content.

3.6 Saponin content of *P. polyphylla* var. *yunnanensis*

In this experiment, the content of saponins I, II, VI, VII, D, and H was examined in *P. polyphylla* var. *yunnanensis* after 90 d of treatment with different concentrations of nitrogen. And saponin VI was not detected in any of the treatments. In the detection of saponin I (**Figure 6A**), the highest saponin I content was found in N1Ge and N1Po, which reached 0.18% and 0.167%, respectively, while the saponin I content of N1CK was only 0.047%. In the medium nitrogen treatment, Po significantly increased the saponin I content of the plants,

Table 3. Effects of different nitrogen treatments on the NPK content of above-ground parts of *P. polyphylla* var. *yunnanensis*.

Stem				
Treatment	**C%**	**P%**	**K%**	**N%**
N1CK	32.35 ± 0.49E	0.0653 ± 0.00054C	4.1036 ± 0.18029E	0.9547 ± 0.01341E
N1Ge	35.23 ± 0.63BC	0.0790 ± 0.00152A	5.3951 ± 0.0934C	1.1274 ± 0.00976C
N1Po	34.20 ± 0.61CD	0.0716 ± 0.00384B	5.0317 ± 0.13248CD	1.1099 ± 0.00878C
N2CK	33.03 ± 0.80DE	0.0721 ± 0.00295B	4.0904 ± 0.09526E	1.0755 ± 0.00891D
N2Ge	36.39 ± 0.50AB	0.0678 ± 0.00366BC	4.8664 ± 0.24111D	1.1158 ± 0.01523C
N2Po	36.40 ± 0.67AB	0.0680 ± 0.00158BC	4.1506 ± 0.21127E	1.0680 ± 0.01003D
N3CK	37.36 ± 0.37A	0.0668 ± 0.00071BC	6.8121 ± 0.21127A	1.2251 ± 0.01077A
N3Ge	36.22 ± 0.47AB	0.0682 ± 0.0019BC	5.9878 ± 0.26285B	1.2056 ± 0.02079AB
N3Po	34.14 ± 0.16CD	0.0689 ± 0.00079BC	4.2568 ± 0.09027E	1.1902 ± 0.01283B
N	F = 23.928812**	F = 7.348639**	F = 128.242518**	F = 73.197138**
AMF	F = 19.056139**	F = 2.989605ns	F = 67.923281**	F = 9.360673 **
N*AMF	F = 27.547554**	F = 5.783699**	F = 89.785862 **	F = 12.432372 **

The data in the table are the mean ± standard error (n = 3). Different lowercase letters after the data in the same column indicate significant differences in the level of variation under different treatments ($p < 0.01$).

but Ge decreased the saponin I content, while the plants not inoculated with AMF were significantly higher than the low nitrogen treatment. Under high N treatment, the saponin I content of plants not inoculated with AMF was significantly higher than that of medium N treatment, but no saponin I was detected in N3Ge, while the content of N3Po was not significantly different from that of N3CK. The results of saponin II assay showed that AMF significantly increased the accumulation of saponin II in *P. polyphylla* var. *yunnanensis* under low N treatment (**Figure 6B**), and in the medium N treatment, the saponin II content of N2CK was significantly higher than that of N1CK, but still significantly lower than that of N2Ge and N2Po, where N2Ge had the highest content of 0.713%, which was significantly higher than that of N2Po. In the high N treatment, the saponin II content of N3CK was also higher than N2CK, but not significantly different from N3Po. The lowest saponin II content of 0.481% was detected in N3Ge at high N concentration, which was significantly lower than the other treatments of N3. Only four groups of treatments in this experiment detected saponin D content (**Figure 6D**), which were N2CK > N3Po > N1Po > N1CK in descending order, 0.0641%, 0.0411%, 0.0172% and 0.0110%, respectively. The saponin H content of P. polyphylla var. yunnanensis without AMF inoculation increased with increasing N (**Figure 6E**), and under low N treatment, Ge and Po significantly increased the accumulation of saponin H. In the medium N treatment, the accumulation of saponin H was in the order of N2Ge > N2Po > N2CK with 0.13%, 0.08% and 0.04%, respectively, with significant differences among the three, and under high N treatment, N3CK and N3Po showed no significant difference in saponin H content, while no saponin H was detected in N3Ge under high N treatment. The content of non-AMF *P. polyphylla* var. *yunnanensis* saponin VII was significantly lower under the low N treatment than the medium and high N treatments (**Figure 6E**), Ge increased the saponin VII content of *P. polyphylla* var. *yunnanensis* under all three N treatments, especially under the medium N concentration, where saponin VII reached 0.433%, Po was able to increase the saponin VII content under the medium and low N treatments, but was not significantly different from non-AMF inoculated plants under the high N treatment. Overall, in the low and medium nitrogen treatments, inoculation with AMF helped to increase the total saponin content of *P. polyphylla* var. *yunnanensis*, and Ge was significantly more helpful than Po for total saponin accumulation, while when *P. polyphylla* var. *yunnanensis* was under high nitrogen treatment (**Figure 6F**), Po did not significantly improve the accumulation of total saponin in *P. polyphylla* var. *yunnanensis*, and the symbiosis of Ge with *P. polyphylla* var. *yunnanensis* reduced the total saponin content of the plants instead.

Table 4. Effects of different nitrogen treatments on the NPK content of the underground fraction of *P. polyphylla* var. *yunnanensis.*

Roots				
Treatment	**C%**	**P%**	**K%**	**N%**
N1CK	30.9716 ± 0.14946D	0.0632 ± 0.00095D	3.7397 ± 0.09179D	1.0071 ± 0.03796E
N1Ge	38.3554 ± 0.56021A	0.0795 ± 0.00168A	4.0259 ± 0.05849B	1.5314 ± 0.02330A
N1Po	36.6945 ± 0.33912B	0.0787 ± 0.00206A	4.1838 ± 0.02211A	1.4936 ± 0.01543AB
N2CK	33.11927 ± 0.53777C	0.0688 ± 0.00077C	3.7828 ± 0.06047CD	1.3230 ± 0.02394D
N2Ge	38.2088 ± 0.74297A	0.0747 ± 0.00101B	4.0909 ± 0.02555AB	1.4962 ± 0.00959AB
N2Po	37.7540 ± 0.81660AB	0.0708 ± 0.00117C	3.6792 ± 0.03545D	1.5508 ± 0.03056A
N3CK	37.3892 ± 0.45074AB	0.0685 ± 0.00112C	3.8742 ± 0.03398C	1.4205 ± 0.01857C
N3Ge	37.3140 ± 0.67672AB	0.0643 ± 0.00095D	3.8813 ± 0.06786C	1.4636 ± 0.02790BC
N3Po	37.6074 ± 0.35413AB	0.0644 ± 0.00054D	4.0177 ± 0.03687B	1.4576 ± 0.01555BC
N	F = 14.664061**	F = 68.609142**	F = 12.645827**	F = 3.511144 ns
AMF	F = 67.804434**	F = 27.104054**	F = 35.510770**	F = 26.893784 **
N*AMF	F = 19.015849**	F = 39.669369**	F = 44.406771**	F = 7.810122*

The data in the table are the mean ± standard error (n = 3). Different lowercase letters after the data in the same column indicate significant differences in the level of variation under different treatments ($p < 0.01$).

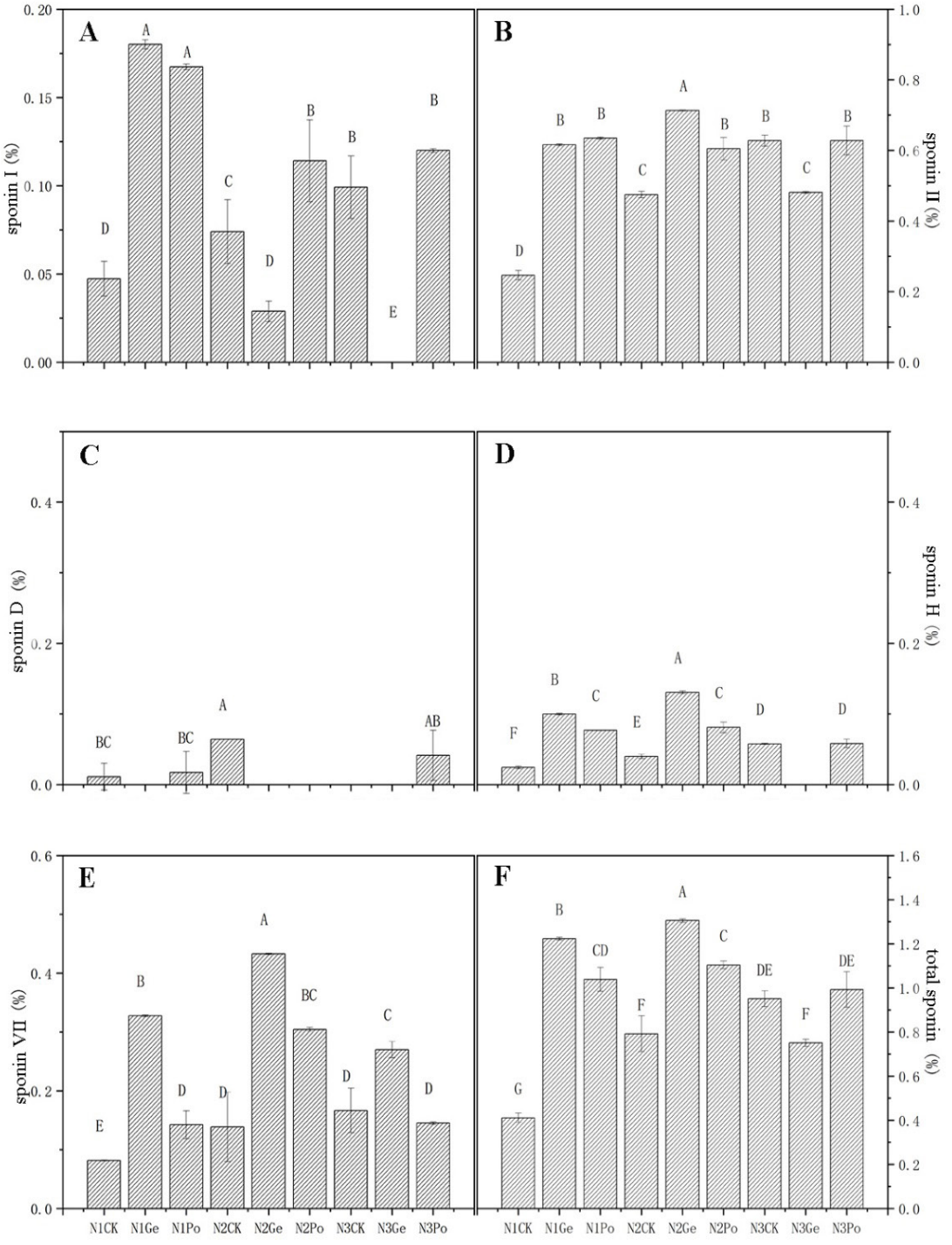

Figure 6. Effect of different nitrogen treatments on saponins of *Pp.*

Note: A: saponin I, B: saponin II, C: saponin D, D: saponin H, E: saponin VII, F: total saponin.

3.7 Saponin synthesis-related genes

Real-time fluorescence quantification of internal reference genes (β-actin) and target genes (HMGS, GPPS, FPPS, SS, SE1, CAS, SE2) was performed for the relevant genes on the steroid saponin synthesis pathway. The expression results were calculated and the specific results are shown in **Figure 7**. In this experiment, AMF increased the expression of HMGS in plants at low N concentration, but its expression was lower than that of N3CK plants at high N concentration, and in plants not inoculated with AMF, the elevated N content promoted the expression of HMGS. The expression of SE1 was significantly higher in AMF plants than in non-AM plants at low N concentration, but lower than in non-AM plants at medium N concentration, and at high N concentration, an increase in SE1 was observed only under Po treatment. AMF also increased the expression of CAS in the plants at low and medium N concentrations, but this trend did not differ significantly, and CAS expression was higher in the Po and CK treatments than in the Ge treatment at high N. There was no significant difference in SE2 expression among treatments at low and medium nitrogen concentrations, but SE2 expression was higher in each treatment at medium nitrogen concentration than at low nitrogen concentration, while high nitrogen decreased SE2 expression. An increase in SS expression was observed only in AM plants at low N concentration and decreased with increasing N. The treatments with higher GGPS expression were N1Ge, N2CK and N2Po, while the differences between the other treatments were not significant.

3.8 Transcriptome analysis

The transcriptome analysis of *P. polyphylla* var. *yunnanensis* with different nitrogen treatments revealed that the Q30 (%) of each treatment was more than 80%, and no significant deviation was found in the base content distribution. 242520 unigene were obtained by the assembly, of which 46.28% were annotated. Through the functional query analysis of the transcriptome of *P. polyphylla* var. *yunnanensis* between different nitrogen treatments, it was found from GO annotation that among the biological process categories, the unigenes annotated by metabolic

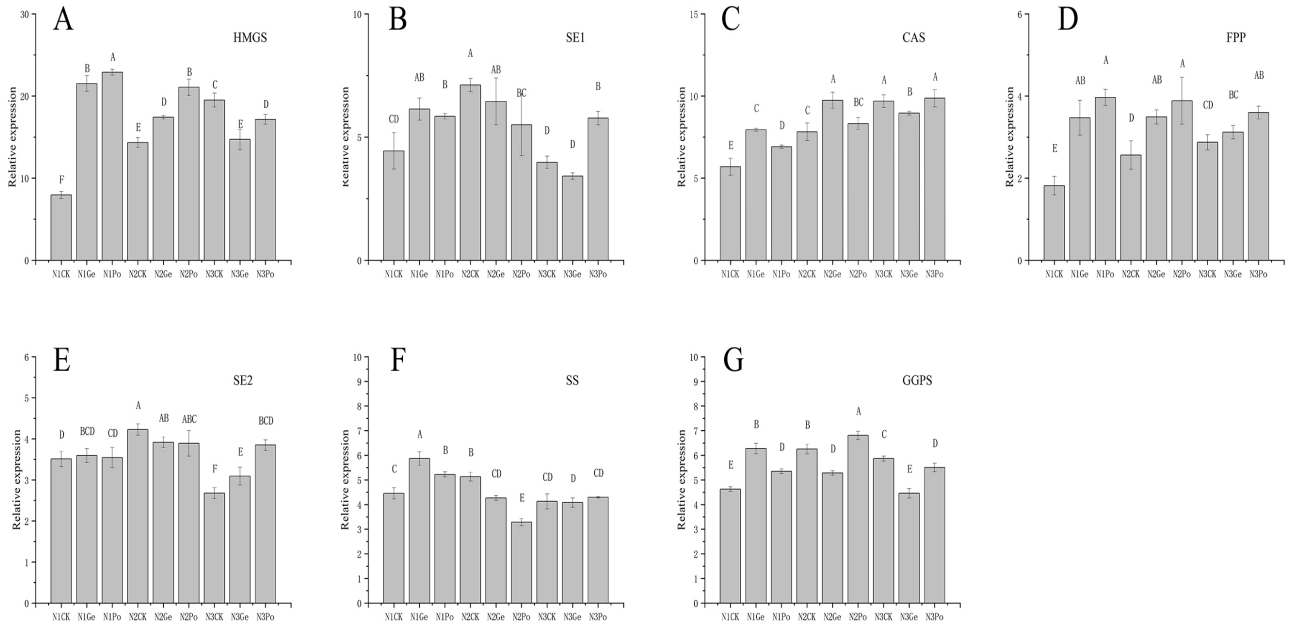

Figure 7. Effect of different nitrogen treatments on saponins of *P. polyphylla* var. *yunnanensis.*

Note: A: *HMGS*, B: *SE1*, C: *CAS*, D: *FPP*, E: *SE2*, F: *SS*, G: *GGPS.*

processes were second only to cellular processes and higher than bioregulation, among the cellular component categories, the cellular and organelle parts were annotated with the most unigenes, and among the molecular function categories, they were mainly focused on catalytic and binding functions (**Figure 8**). The metabolic pathways were found to be the most enriched in unigenes by KEGG analysis, with the most being the metabolism of carbohydrates (5509 unigenes), while the secondary metabolite pathways were enriched with 1484 unigenes **(Figure 9**). The identification of P450 and UGT-related genes was performed by KEGG, GO and NR annotation, and 30 P450 and 297 UGT genes were identified. Cds greater than 1000 bp were screened for subsequent analysis, and 16 eligible P450 unigenes and 75 UGT unigenes were obtained.

Phylogenetic trees were constructed by comparing P450s genes with genes from *Arabidopsis thaliana* (L.) Heynh., *Panax ginseng* C. A. Meyer, *Lycopersicon esculentum* Miller and *Isatis tinctoria* Linnaeus using ML method, where DN14416_c0_g2, DN29717_c0_g1 and DN820_c0_g1 were mainly concentrated in Ath CYP86 clade (Ath CYP94D2), while DN7630_c0_g1 was close to Ath CYP72 clade, DN66132_c0_g1 was close to PpCYP90G4 (**Figure 10A**), and nine unigenes were enriched in Ath CYP51G clade, namely DN342541_c0_g1, DN32483_c0_g1, DN473834_c0_g1, DN47915_c0_g1, DN36083_c0_g1, DN317186_c1_g1, DN119469_c1_g1, DN119469_c1_g3, and DN484778_c0_g1 **(Figure 10A**).

A phylogenetic tree was constructed by constructing a phylogenetic tree of UGTs genes and selected some genes known to be related to steroid, flavonoid and triterpenoid synthesis and UGTs of *Arabidopsis thaliana* (L.) Heynh. Some of the genes were clustered around the triterpene synthesis-related genes (OAGT, UGT73), and seven unigenes tended to be enriched with the Ath UGT73 family and steroid synthesis-related UGTs (**Figure 10B**), namely DN58096_c1_g3, DN43198_c1_g1, DN452515_c0_g1, DN428098_c0_g1, DN217552_c0_g1, DN7369_c0_g3, and DN49172_c1_g1.

CYP450 proteins are the largest family of plant proteins that catalyze most of the oxidative processes in plant secondary metabolism. Glycosyltransferases (UGTs) are another large multigene family in plants. Usually, glycosylation is the final step in the biosynthesis of secondary metabolites, and glycoconjugation enhances stability and water solubility. Eleven P450s and seven UGTs were analyzed by constructing a phylogeny, which was clustered. Under low nitrogen conditions, Ge increased the expression of plants DN32483, DN66132 and DN473834, while Po increased the expression of DN119469, DN484778, DN7630 and DN436083, and under medium nitrogen conditions, non-AM plants showed an increase in DN7630 but a decrease in DN484778 expression, while Po increased the expression of DN111387 and DN287723, and Ge did not increase the expression of P450 under medium nitrogen conditions. Under high nitrogen conditions, non-AM plants increased the expression of genes DN47915, DN119469, and DN342541, while Ge significantly decreased the expression of DN7630 and Po increased the expression of DN317186 (**Figure 11A**). Analysis of UGTs revealed that the screened UGTs were down-regulated in two AM plants under high nitrogen conditions, while three UGTs, DN217552, DN49172, and DN58096, were up-regulated in non-AM plants. N1CK increased the expression of DN43198 and N1Po increased the expression of DN7369 and DN42515 under low nitrogen conditions. Under medium nitrogen conditions, only N2Ge up-regulated DN428098 (**Figure 11B**).

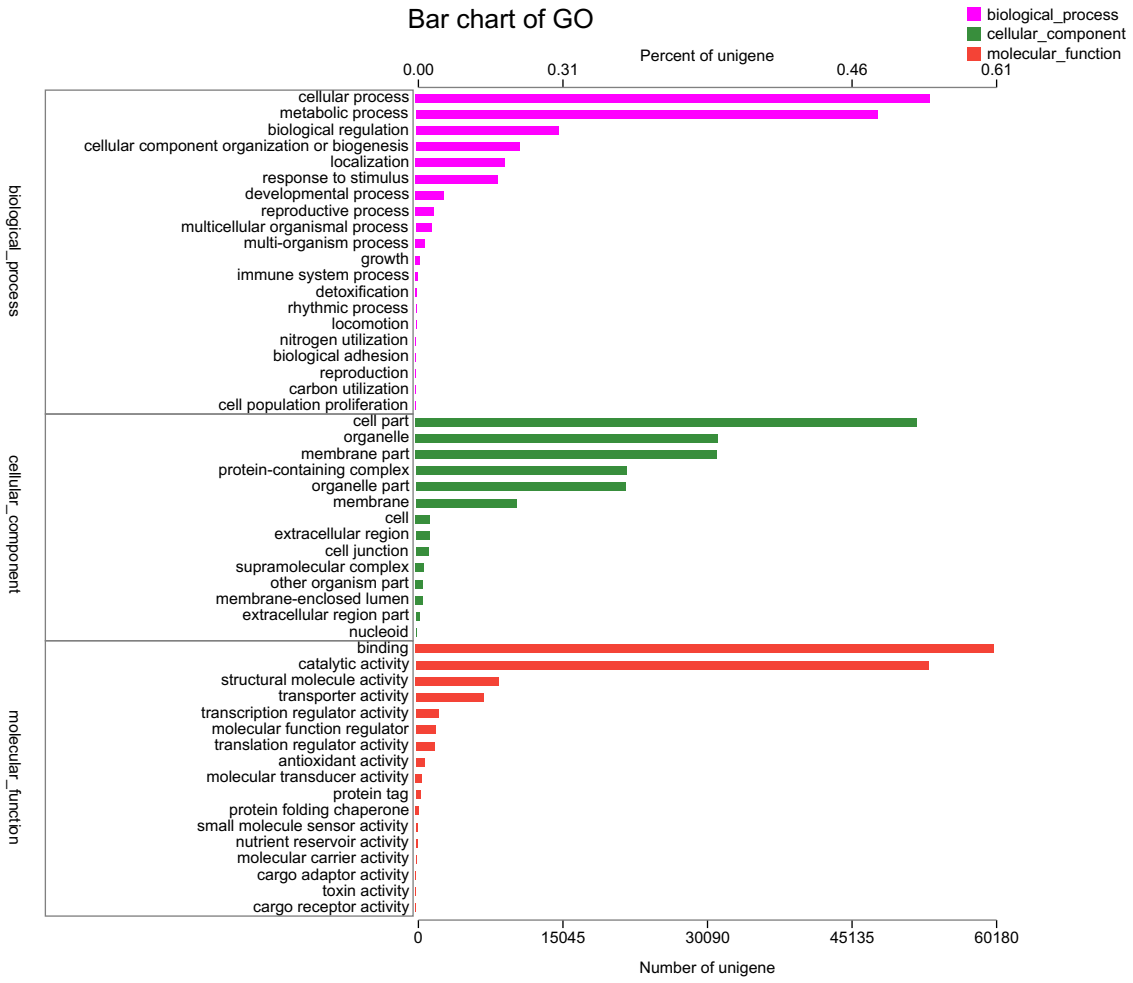

Figure 8. GO annotation of the transcriptome of *P. polyphylla* var. *yunnanensis*.

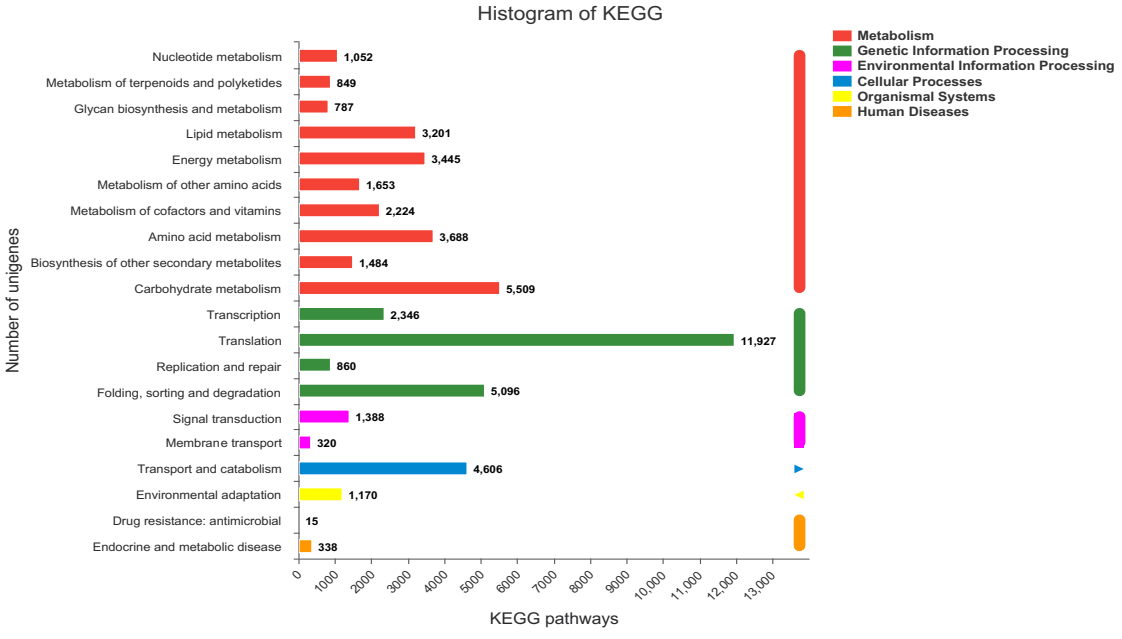

Figure 9. KEGG annotation of the transcriptome of *P. polyphylla* var. *yunnanensis*.

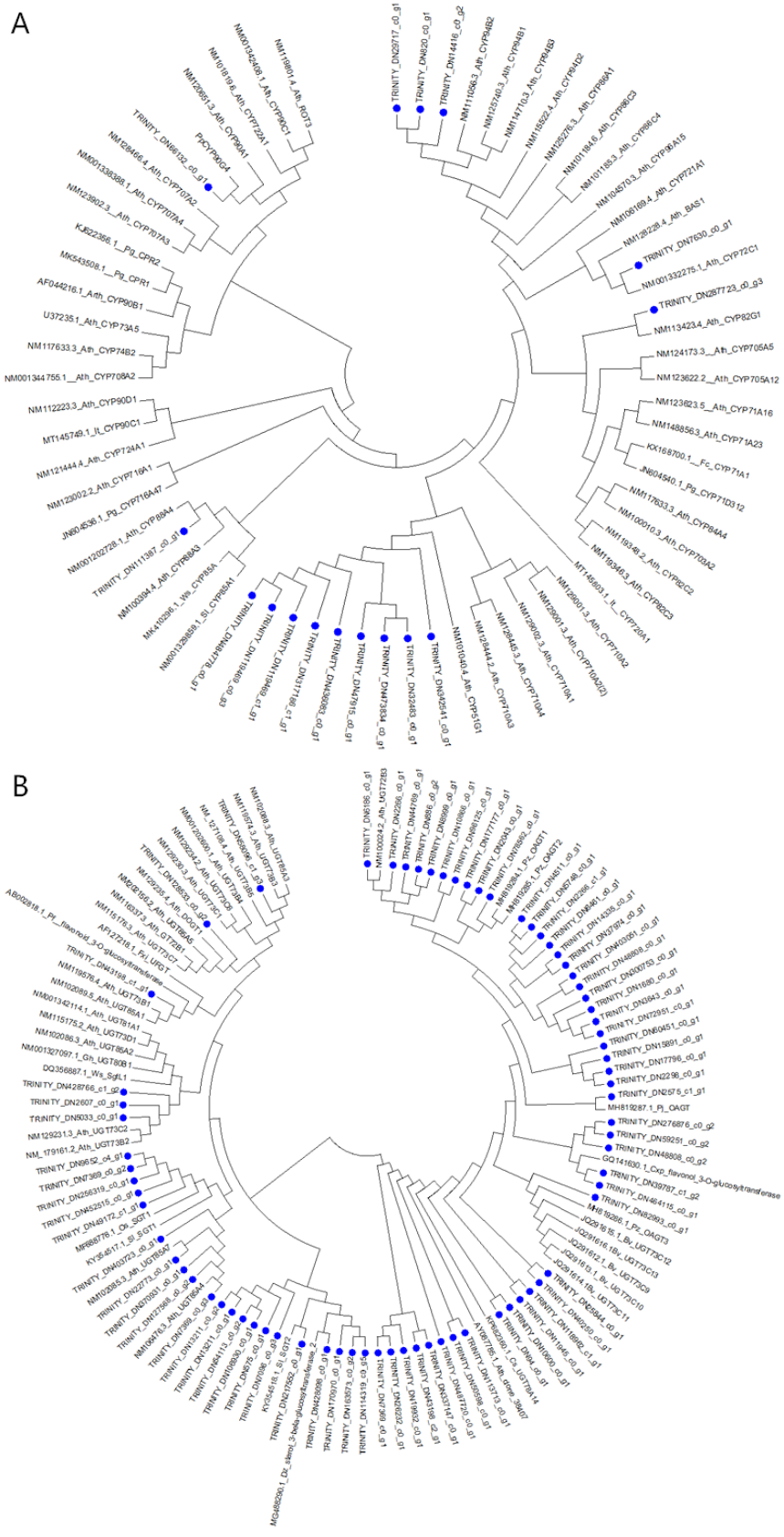

Figure 10. Phylogenetic analysis of unigenes (blue) screened from the transcriptome of *P. polyphylla* var. *yunnanensis*.

Note: A: Phylogenetic analysis of P450s, B: Phylogenetic analysis of UGT.

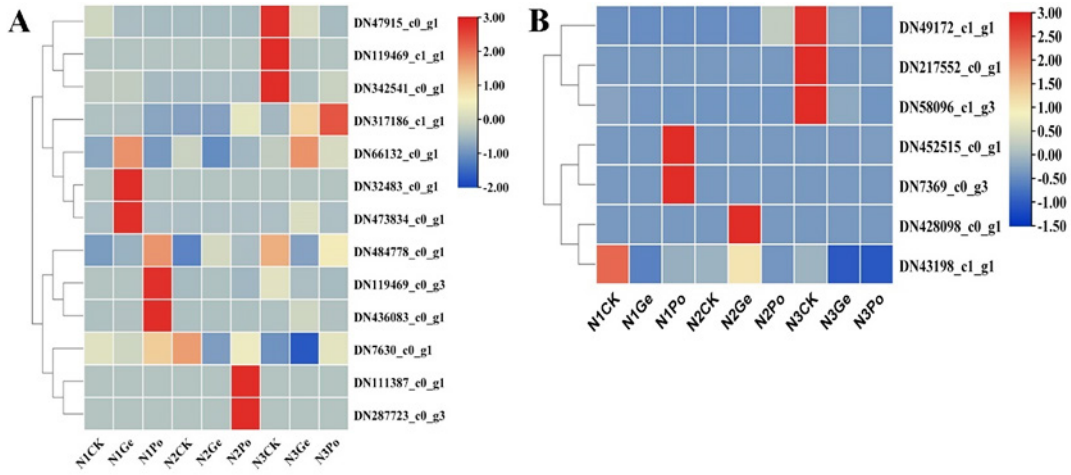

Figure 11. Clustering of transcriptome gene expression profiles under different nitrogen treatments of *P. polyphylla* var. *yunnanensis*.

Note: A: Clustering of UGT gene expression profiles, B: Clustering of P450 gene expression profiles.

4. Discussion

4.1 High nitrogen reduces the colonization rate of AMF

The symbiosis between terrestrial plants and AMF is common, and the two achieve mutual benefits by exchanging nutrients, and usually, plants prefer to form this symbiosis in an adverse environment. In nitrogen experiments, it was found that Ge and Po had very different symbiotic strategies, and with increasing N concentration, Ge showed a decreasing trend in colonization rate at high N concentration, while Po showed an increasing trend in colonization rate. Nitrogen nutrients are the second only to phosphorus nutrients as a determinant of AMF symbiosis [33], and many studies have shown that too much N may lead to a decrease in AMF symbiosis rate [34], which is due to the fact that plants in high. This is consistent with Ge's strategy in this experiment, while the increase in Po colonization rate indicates that plants are more inclined to symbiosis with *P. polyphylla* var. *yunnanensis* regardless of whether they are under environmental stresses such as drought or nutrient-rich environments, and some studies have shown that tomato plants are more inclined to symbiosis with AMF in high nutrient environments [35], which is consistent with Po's symbiosis strategy is consistent. AMFs of different populations may be able to adjust their symbiotic strategies with plants through their own unique growth and developmental patterns to obtain more suitable survival conditions.

4.2 AMF promotes the growth of plants

Most studies have demonstrated that by helping plants to obtain more nutrients AMF can help plants to increase their biomass and promote plant growth and development [36]. In the present, AMF increased plant root weight, stem weight, and plant height, but had less effect on the increase in root length, perhaps because plants prioritize nutrient supply to aboveground parts after inoculation with AMF, which was found to increase plant biomass in a previous study [37], which is similar to the results of the present experiment. In addition, AMF increased the accumulation of IAA in plants, especially under medium to high N treatment, the IAA content of AM plants was significantly higher than that of non-AM plants, indicating that AMF may help more in plant growth under N sufficiency conditions, which is contrary to the trend of AMF colonization rate, which may be due to the fact that the optimal strategy of plant-AMF symbiosis does not follow the range of symbiosis, but the efficiency of symbiosis [38]. With the increase of nitrogen concentration, the ABA content of *P. polyphylla* var. *yunnanensis* repens decreased significantly, and the hormone ABA has

a significant effect on AMF infestation [39], which may be one of the reasons for the decrease of AMF colonization rate. Usually, when plants are subjected to drought or salt stress, the ABA content in the plant will be significantly increased and ABA, as a signaling molecule, can regulate the stomatal conductance of the plant to cope with the water changes occurring in the plant, and the inoculation of AMF led to a significant decrease in the ABA content in *P. polyphylla* var. *yunnanensis*, which can indicate that AMF prevents the change of osmotic pressure brought about by the increase of soil species N content by changing the ABA content in the plant. It can be suggested that AMF can prevent water imbalance in plants by changing the ABA content in plants in response to the increase of soil N content. The study showed that the relationship between Pro and AMF is diverse, and in this experiment, the Pro content of plants inoculated with AMF showed an increasing trend with the increase of N concentration, and Pro is an important indicator of osmotic stress in plants, which can help plants regulate osmotic balance. The change of Pro content can be regarded as a protective measure taken by plants to regulate the osmotic balance. The increase of Pro content by AMF was mainly concentrated in plants treated with medium N concentration, while there was no significant difference in the change of Pro content by AMF under high N treatment, which proved that inoculation of AMF can help plants change the metabolic changes in their bodies and cope with different natural environments.

The determination of soil physicochemical properties showed that the application of N did increase the content of fast-acting N in the soil. In the detection of NPKC in plants, it was found that compared to non-AM plants, the C and N contents of the root parts of AMF plants were significantly increased, especially at N2 concentrations where their enhancement was most obvious, which is also consistent with the trend of its colonization rate, and with the increase of soil N concentration, the uptake of nutrients by *P. polyphylla* var. *yunnanensis* was also significantly increased, but the change of its content by AMF was relatively small. AMF can help plants to absorb various N elements as well as nutrients [40,41], AMF has also been shown to increase the expression of plant phosphate transporter proteins and nitrogen transporter proteins in previous mycorrhizal experiments and this result is consistent with the present experiment [42,43], but when N application was increased, the improvement of plant nutrients by AMF was significantly reduced, and in the N3 treatment, the C, P, and N contents of non-AM plants were higher than those of AM plants, indicating that excessive nutrient addition reduces the help of AMF to plants. In addition, the trend of AMF inoculation on the nutrient accumulation in the above- and below-ground parts of the plants differed. In the above-ground part of the *P. polyphylla* var. *yunnanensis* assay, it was found that the treatments with the highest plant nutrient contents were basically in N3, while in the below-ground part of the assay, the highest C contents were N1Ge and N2Ge, the highest P contents were N1Ge and N1Po, the highest K content was N1Po, and the highest N content was It can be seen that although N application increased the overall nutrient content of the above-ground part of the plant, for the below-ground part, AMF plants were still more dominant than non-AM plants, and the plant roots are the main nutrient uptake site of the plant [40] and can influence the nutrient transport and transfer in the plant, and at the same N concentration, the nutrient content of the below-ground part of AM plants was significantly higher than that of non-AM plants, while at the same N concentration, the nutrient content of the below-ground part of AM plants was significantly higher than that of non-AM plants, while the above-ground part was not significantly different from that of non-AM plants, indicating that AM plants have higher nutrient uptake than non-AM plants and their nutrient regulation is more flexible among different tissues.

4.3 AMF promotes the accumulation of saponins

AMF symbiosis with plants can promote the growth and development of plants, while the addi-

tion of N-substance is also the main way to increase the yield of crops. Usually, the most important indicator of a crop is its yield, but the most important substance of a medicinal plant is its medicinal component. Studies have shown that AMF is effective in increasing the accumulation of secondary metabolites in plants [44] and also in increasing the synthesis of terpenoids in plants [45]. In this experiment, the content of *P. polyphylla* var. *yunnanensis* I appeared significantly elevated after inoculation with AMF, with N1Ge and N1Po being the treatments with the greatest elevation, while in the N2 and N3 treatments, Ge inoculation instead reduced the content of *P. polyphylla* var. *yunnanensis* I, with a trend in the opposite direction to the trend of N vegetation concentration, while Po, although it also showed a reduction, still had a higher saponin I content than non-AM plants. In saponin II, Ge and Po increased the content of saponin II under N1 and N2, but Ge decreased the content of saponin II under N3 treatment. The content of saponin D was detected only in N1CK, N1Po, N2CK and N3Po, with lower levels under N1 treatment and relatively higher levels under N2 and N3. The increase in N content also increased the content of saponin H, and Ge and Po increased it the most, but there was no difference in the effect of the two AMFs on saponin content at high N concentrations, a trend similar to that of *P. polyphylla* var. *yunnanensis* saponin VII changes were similar. From this experiment, it is clear that the symbiosis of *P. polyphylla* var. *yunnanensis* with AMF at low N concentration can promote the accumulation of its saponin content, mainly in saponin I, II, VII and H. It shows that the promotion of secondary metabolite accumulation by AMF is selective [46]. Under low and medium nitrogen conditions, plants relied more on the AMF pathway for nutrient uptake, and through increased nutrient accumulation, the content of precursors for saponin synthesis was increased, thus improving the synthesis of total saponins. With the increase of N concentration, AM *P. polyphylla* var. *yunnanensis* saponin also possessed higher saponin content at medium N concentration, but when the soil N concentration increased to high N, the advantage brought by AMF inoculation was not significant and even decreased, and the accumulation trend of saponin in *P. polyphylla* var. *yunnanensis* saponin was not uniform for both AMFs when they were in high N soil. It can be shown that AMF under low and medium nitrogen on *P. polyphylla* var. *yunnanensis* saponin content accumulation helps more, in the nitrogen test, the nutrient content of the underground part of AM *P. polyphylla* var. *yunnanensis* is significantly higher than non-AM plants, and the highest content of the same in low and medium nitrogen concentration treatment, this trend is similar to the saponin accumulation trend of *P. polyphylla* var. *yunnanensis* saponin, which may be due to AMF can not only help the plant to absorb more mineral nutrients but also help plants to better regulate nutrient transfer transport and in this way increased the synthesis of saponins in *P. polyphylla* var. *yunnanensis*, which is similar to some studies [47]. At high N concentrations, the root nutrient and saponin contents of the plants were much less enhanced than those of non-AM plants at low N concentrations, although they were higher than those of AM plants. For medicinal plants, their yield is far more important than their biomass increase, and further experiments are needed to determine which N content is more appropriate for AM *P. polyphylla* var. *yunnanensis* to accumulate saponin components in symbiosis between AMF and *P. polyphylla* var. *yunnanensis*. In the present study, we also found that saponin VI was not detected in both AMF plants and under all three nitrogen level treatments, suggesting that AMF is specific for the alteration of secondary metabolites, which may be related to AMF itself. During plant growth, plants preferentially increase their biomass [48].In contrast, secondary metabolites are usually not directly involved in plant growth and development and only help plants to improve ecological adaptations, which may be one of the reasons why sustained increases in N do not always improve saponins. AMF alters the nutrient balance in plants by increasing nutrient uptake capacity, and AM plants have higher C:N compared to non-AMF plants, which allows more nutrients to be used for the synthesis of secondary

metabolites [18].

4.4 AMF promotes the expression of genes related to saponin synthesis

Studies have shown that overexpression of key genes on the steroid saponin synthesis pathway, HMGS, GGPS, FPPS, SS, CAS and SE2, promotes the accumulation of bioactive components and improves saponins in host plants [47], and in this experiment, it can be found that AMF increased the expression of HMGS, a key enzyme on the steroid saponin synthesis pathway, in the plants at low and medium N concentrations, indicating that AMF plants promoted the synthesis of saponin in the heavy floor by absorbing more nutrient elements, but its expression was lower than that of CK plants at high N concentrations, which may be related to the decrease in AM colonization rate, and although the expression of HMGS also appeared elevated at this N concentration, its increase was less than that of AM plants, which is also consistent with the trend of saponin accumulation in the plants in the experiment. Secondly, AMF also increased the expression of SE1 and CAS under low nitrogen concentration, indicating that AMF played a role in promoting saponin synthesis to some extent. To some extent, AMF is able to achieve changes in plant saponin content by regulating relevant genes on the steroid saponin synthesis pathway. In non-AMF plants, increased nitrogen concentration also promoted the expression of HMGS, CAS, and FPP. HMGS acts as the main rate-limiting enzyme gene and the resulting cascade reaction is able to increase the saponin content of the plant [49].

4.5 Transcriptome analysis

Transcriptome sequencing is a cost-effective method that is currently used extensively to uncover genomic information from different non-model medicinal plants that do not have a reference genome [50]. In this study, we used different nitrogen and AMF treatments of *P. polyphylla* var. *yunnanensis* and then analyzed its transcriptome data to uncover the P450 and UGT genes involved in the *P. polyphylla* var. *yunnanensis* saponin biosynthesis pathway. Steroid saponins are mainly synthesized from cholesterol via oxidation at the C-16, C-22 and C-26 positions [51], where P450 enzymes play an important role in the catalysis of these transformations. CYP90G4 and CYP51G have been shown to aid in the synthesis of steroid saponins in Dendrobium plants [52,53], and DN66132_c0_g1 is close to PpCYP90G4 and has nine unigenes enriched in the Ath CYP51G family, suggesting their possible involvement in steroid saponin synthesis. In addition to P450s, UGTs are also involved in the final modification of saponins, where the glycosylation of C-26 is catalyzed by UGTs, and it was shown that genes in the UGT73 family are able to glycosylate the C-26 position of saponin elements [26]. It suggests that seven unigenes concentrated in the UGT73 family may play a catalytic role in the glycosylation of *P. polyphylla* var. *yunnanensis* saponin. Cluster analysis showed that both Ge and Po promoted the expression of different P450s and UGTs in low and medium nitrogen treatments, whereas, in non-AM plants, significant up-regulation of P450s and UGTs was found only in N3 treatment, a pattern also similar to that of saponin accumulation. Both AMFs had no up-regulation on plant P450s and UGTs at high N concentrations, which may also be one of the reasons for the low total saponins in AM plants in high N treatments. HMGS, CAS, and FPP increased their expression with nitrogen addition, while the expression of SE1, SE2, and SS showed down-regulation under high nitrogen treatment, but in non-AM plants, the saponin content reached its maximum under high nitrogen treatment, indicating that oxidative glycosylation by the upstream rate-limiting gene HMGS and the downstream P450 and UGT are key factors in saponin synthesis pathway, and the up-regulation of P450 and UGT could offset the negative effects of the decreased expression of SE1, SE2, and SS to some extent. In addition, the P450 gene 43198 appeared to be down-regulated in AM plants under high nitrogen treatment (**Figure 11B**), which may be one of the reasons for the decrease in saponin content, and the synthesis of steroidal saponins generally oc-

curs through the MVA pathway during plant growth metabolism [54], in turn, free sterols are also a major component in controlling cell membrane fluidity and permeability [55]. In high nitrogen environments, plants do not need to rely too much on AMF for nutrient uptake, which may lead to the need for more sterol substances for membrane permeability regulation in response to excessive nitrogen in the environment, and the precursor substances for steroid saponin synthesis are then decreased, which may also be one of the reasons for the down-regulation of P450.

5. Conclusions

In order to investigate the effect of AMF on saponin synthesis of *P. polyphylla* var. *yunnanensis* under nitrogen addition, this experiment used *P. polyphylla* var. *yunnanensis* as the study material and initially investigated the effect of AMF on saponin synthesis of *P. polyphylla* var. *yunnanensis* under nitrogen addition by measuring the growth, chlorophyll, hormones, nutrients, saponin content and gene expression on the saponin synthesis pathway of *P. polyphylla* var. *yunnanensis*. Nitrogen addition was able to increase the saponin content of *P. polyphylla* var. *yunnanensis* to some extent, but AMF plants increased the saponin content of *P. polyphylla* var. *yunnanensis* more significantly, and inoculation with AMF also promoted the expression of genes related to the saponin synthesis pathway, HMGS, SE1 and CAS. Thus, the accumulation of saponin in the plants was increased. And probably by altering the expression of saponin synthesis-related P450 and UGT, thus increasing the saponin content of AMF plants.

Author Contributions

Shubiao Qian, was responsible for the whole experiment, raw data collection, collation and analysis, and original manuscript writing. Huang Can assisted in the experiment. Xiaoxian Li, Xiahong He, Shuhui Zi, Congfang Xi, Rui Shi, and Tao Liu and others are responsible for guiding the experiment and article revision.

Conflict of Interest

The authors declare that they have no conflict of interests concerning the current research publication.

Data Availability Statement

The original read registration numbers are PRJNA864763, located in the NCBI SRA database, https://www.ncbi.nlm.nih.gov/bioproject/PRJNA864763

Funding

This work was supported by the National Natural Science Foundation of China (Grant No. 31860075).

Acknowledgment

I would like to thank my supervisor, Tao Liu, and my brother, Can Huang, for their great help, as well as all the teachers, experts, and siblings. I am grateful to Yunnan Agricultural University for nurturing me and to the Southwest Biodiversity Laboratory for providing the platform. Also, this work was supported by the Key R&D Program of Yunnan Province, China (Grant No. 202103AC100003; 202101AS070228); the Major Special Project of the Ministry of Science and Technology (2021YFD1000202; 2021YFD1601003); and the National Natural Science Foundation of China (Grant No. 31860075), thank you.

References

[1] Guo, J.H., Liu, X.J., Zhang, Y., et al., 2010. Significant acidification in major Chinese croplands. Science. 327(5968), 1008-1010. DOI: https://doi.org/10.1126/science.1182570

[2] Raza, S., Miao, N., Wang, P., et al., 2020. Dramatic loss of inorganic carbon by nitrogen-induced soil acidification in Chinese croplands. Global Change Biology. 26(6), 3738-3751. DOI: https://doi.org/10.1111/gcb.15101

[3] Ramirez, K.S., Craine, J.M., Fierer, N., 2012. Consistent effects of nitrogen amendments on soil microbial communities and processes across

biomes. Global Change Biology. 18(6), 1918-1927.
DOI: https://doi.org/10.1111/j.1365-2486.2012.02639.x

[4] Walters, D.R., Bingham, I.J., 2007. Influence of nutrition on disease development caused by fungal pathogens: Implications for plant disease control. Annals of Applied Biology. 151(3), 307-324.
DOI: https://doi.org/10.1111/j.1744-7348.2007.00176.x

[5] Hestrin, R., Hammer, E.C., Mueller, C.W., et al., 2019. Synergies between mycorrhizal fungi and soil microbial communities increase plant nitrogen acquisition. Communications Biology. 2(1), 233.
DOI: https://doi.org/10.1038/s42003-019-0481-8

[6] Müller, L.M., Harrison, M.J., 2019. Phytohormones, miRNAs, and peptide signals integrate plant phosphorus status with arbuscular mycorrhizal symbiosis. Current Opinion in Plant Biology. 50, 132-139.
DOI: https://doi.org/10.1016/j.pbi.2019.05.004

[7] Smith, S.E., Smith, F.A., Jakobsen, I., 2004. Functional diversity in arbuscular mycorrhizal (AM) symbioses: The contribution of the mycorrhizal P uptake pathway is not correlated with mycorrhizal responses in growth or total P uptake. New Phytologist. 162(2), 511-524.
DOI: https://doi.org/10.1111/j.1469-8137.2004.01039.x

[8] Johansen, A., Jakobsen, I., Jensen, E.S., 1993. Hyphal transport by a vesicular-arbuscular mycorrhizal fungus of N applied to the soil as ammonium or nitrate. Biology and Fertility of Soils. 16, 66-70.
DOI: https://doi.org/10.1007/bf00336518

[9] Hodge, A., Campbell, C.D., Fitter, A.H., 2001. An arbuscular mycorrhizal fungus accelerates decomposition and acquires nitrogen directly from organic material. Nature. 413(6853), 297-299.
DOI: https://doi.org/10.1038/35095041

[10] Koegel, S., Ait Lahmidi, N., Arnould, C., et al., 2013. The family of ammonium transporters (AMT) in s orghum bicolor: Two AMT members are induced locally, but not systemically in roots colonized by arbuscular mycorrhizal fungi. New Phytologist. 198(3), 853-865.
DOI: https://doi.org/10.1111/nph.12199

[11] Chen, A., Gu, M., Wang, S., et al., 2018. Transport properties and regulatory roles of nitrogen in arbuscular mycorrhizal symbiosis. Seminars in Cell & Developmental Biology. 74, 80-88.
DOI: https://doi.org/10.1016/j.semcdb.2017.06.015

[12] Bona, E., Lingua, G., Manassero, P., et al., 2015. AM fungi and PGP pseudomonads increase flowering, fruit production, and vitamin content in strawberry grown at low nitrogen and phosphorus levels. Mycorrhiza. 25, 181-193.
DOI: https://doi.org/10.1007/s00572-014-0599-y

[13] Bills, G.F., Gloer, J.B., 2017. Biologically active secondary metabolites from the fungi. The Fungal Kingdom. 4(6), 1087-1119.
DOI: https://doi.org/10.1128/microbiolspec.FUNK-0009-2016

[14] Boby, V.U., Bagyaraj, D.J., 2003. Biological control of root-rot of Coleus forskohlii Briq. using microbial inoculants. World Journal of Microbiology and Biotechnology. 19(2), 175-180.
DOI: https://doi.org/10.1023/A:1023238908028

[15] Yu, Y., Yu, T., Wang, Y., et al., 2010. Effect of inoculation time on camptothecin content in arbuscular mycorrhizal Camptotheca acuminata seedlings. Chinese Journal of Plant Ecology. 34(6), 687.
DOI: https://doi.org/10.3724/SP.J.1142.2010.40521

[16] Mandal, A., Mandal, S., Park, M.H., 2014. Genome-wide analyses and functional classification of proline repeat-rich proteins: Potential role of eIF5A in eukaryotic evolution. PloS One. 9(11), e111800.
DOI: https://doi.org/10.1371/journal.pone.0111800

[17] Mandal, S., Upadhyay, S., Singh, V.P., et al., 2015. Enhanced production of steviol glycosides in mycorrhizal plants: A concerted effect of arbuscular mycorrhizal symbiosis on transcription of biosynthetic genes. Plant Physiology and

Biochemistry. 89, 100-106.
DOI: https://doi.org/10.1016/j.plaphy.2015.02.010

[18] Xie, W., Hao, Z., Zhou, X., et al., 2018. Arbuscular mycorrhiza facilitates the accumulation of glycyrrhizin and liquiritin in Glycyrrhiza uralensis under drought stress. Mycorrhiza. 28, 285-300.
DOI: https://doi.org/10.1007/s00572-018-0827-y

[19] Chaudhary, V., Kapoor, R., Bhatnagar, A.K., 2008. Effectiveness of two arbuscular mycorrhizal fungi on concentrations of essential oil and artemisinin in three accessions of Artemisia annua L. Applied Soil Ecology. 40(1), 174-181.
DOI: https://doi.org/10.1016/j.apsoil.2008.04.003

[20] Zeng, Y., Guo, L.P., Chen, B.D., et al., 2013. Arbuscular mycorrhizal symbiosis and active ingredients of medicinal plants: Current research status and prospectives. Mycorrhiza. 23, 253-265.
DOI: https://doi.org/10.1007/s00572-013-0484-0

[21] Weng, W., Yan, J., Zhou, M., et al., 2022. Roles of arbuscular mycorrhizal fungi as a biocontrol agent in the control of plant diseases. Microorganisms. 10(7), 1266.
DOI: https://doi.org/10.3390/microorganisms10071266

[22] Tsiokanos, E., Cartabia, A., Tsafantakis, N., et al., 2022. The metabolic profile of Anchusa officinalis L. differs according to its associated arbuscular mycorrhizal fungi. Metabolites. 12(7), 573.
DOI: https://doi.org/10.3390/metabo12070573

[23] Toussaint, J.P., Smith, F.A., Smith, S.E., 2007. Arbuscular mycorrhizal fungi can induce the production of phytochemicals in sweet basil irrespective of phosphorus nutrition. Mycorrhiza. 17(4), 291-297.
DOI: https://doi.org/10.1007/s00572-006-0104-3

[24] Zhao, Y., Cartabia, A., Lalaymia, I., et al., 2022. Arbuscular mycorrhizal fungi and production of secondary metabolites in medicinal plants. Mycorrhiza. 32(3-4), 221-256.
DOI: https://doi.org/10.1007/s00572-022-01079-0

[25] Wu, X., Wang, L., Wang, H., et al., 2012. Steroidal saponins from *Paris polyphylla* var. *yunnanensis*. Phytochemistry. 81, 133-143.
DOI: https://doi.org/10.1016/j.phytochem.2012.05.034

[26] Upadhyay, S., Jeena, G.S., Shukla, R.K., 2018. Recent advances in steroidal saponins biosynthesis and in vitro production. Planta. 248(3), 519-544.
DOI: https://doi.org/10.1007/s00425-018-2911-0

[27] Gao, X., Zhang, X., Chen, W., et al., 2020. Transcriptome analysis of *Paris polyphylla* var. *yunnanensis* illuminates the biosynthesis and accumulation of steroidal saponins in rhizomes and leaves. Phytochemistry. 178, 112460.
DOI: https://doi.org/10.1016/j.phytochem.2020.112460

[28] Trouvelot, A., Kough, J.L., Gianinazzi-Pearson, V. (editors), 1985. Mesure du taux de mycorhization VA d'un système radiculaire. Recherche de méthode d'estimation ayant une signification fonctionnelle. Physiological and genetical aspects of mycorrhizae: Proceedings of the 1st european symposium on mycorrhizae (French) [Measurement of the VA mycorrhization rate of a root system. Physiological and genetical aspects of mycorrhizae: Proceedings of the 1st european symposium on mycorrhizae]. European symposium on mycorrhizae (1; Dijon 1985-07-01); 1985 1-5 July; Dijon. Paris:INRA, Paris. p. 217-221.

[29] Sartory, D.P., Grobbelaar, J.U., 1984. Extraction of chlorophyll a from freshwater phytoplankton for spectrophotometric analysis. Hydrobiologia. 114, 177-187.
DOI: https://doi.org/10.1007/BF00031869

[30] Li, T., Sun, Y., Ruan, Y., et al., 2016. Potential role of D-myo-inositol-3-phosphate synthase and 14-3-3 genes in the crosstalk between Zea mays and Rhizophagus intraradices under drought stress. Mycorrhiza. 26, 879-893.
DOI: https://doi.org/10.1007/s00572-016-0723-2

[31] Bates, L.S., Waldren, R.A., Teare, I.D., 1973. Rapid determination of free proline for water-stress studies. Plant and Soil. 39, 205-207.
DOI: https://doi.org/10.1007/bf00018060

[32] Conesa, A., Götz, S., García-Gómez, J.M., et al., 2005. Blast2GO: A universal tool for annotation, visualization and analysis in functional genomics research. Bioinformatics. 21(18), 3674-3676. DOI: https://doi.org/10.1093/bioinformatics/bti610

[33] Lanfranco, L., Fiorilli, V., Gutjahr, C., 2018. Partner communication and role of nutrients in the arbuscular mycorrhizal symbiosis. New Phytologist. 220(4), 1031-1046. DOI: https://doi.org/10.1111/nph.15230

[34] Zhou, Z., Wang, C., Zheng, M., et al., 2017. Patterns and mechanisms of responses by soil microbial communities to nitrogen addition. Soil Biology and Biochemistry. 115, 433-441. DOI: https://doi.org/10.1016/j.soilbio.2017.09.015

[35] Wang, L., Chen, X., Du, Y., et al., 2022. Nutrients regulate the effects of arbuscular mycorrhizal fungi on the growth and reproduction of cherry tomato. Frontiers in Microbiology. 13, 843010. DOI: https://doi.org/10.3389/fmicb.2022.843010

[36] Zhang, S., Lehmann, A., Zheng, W., et al., 2019. Arbuscular mycorrhizal fungi increase grain yields: A meta-analysis. New Phytologist. 222(1), 543-555. DOI: https://doi.org/10.1111/nph.15570

[37] Ma, N., Yokoyama, K., Marumoto, T., 2007. Effect of peat on mycorrhizal colonization and effectiveness of the arbuscular mycorrhizal fungus Gigaspora margarita. Soil Science and Plant Nutrition. 53(6), 744-752. DOI: https://doi.org/10.1111/j.1747-0765.2007.00204.x

[38] Clark, R.Á., Zeto, S.K., 2000. Mineral acquisition by arbuscular mycorrhizal plants. Journal of Plant Nutrition. 23(7), 867-902. DOI: https://doi.org/10.1080/01904160009382068

[39] Foo, E., Ross, J.J., Jones, W.T., et al., 2013. Plant hormones in arbuscular mycorrhizal symbioses: An emerging role for gibberellins. Annals of Botany. 111(5), 769-779. DOI: https://doi.org/10.1093/aob/mct041

[40] Averill, C., Bhatnagar, J.M., Dietze, M.C., et al., 2019. Global imprint of mycorrhizal fungi on whole-plant nutrient economics. Proceedings of the National Academy of Sciences. 116(46), 23163-23168. DOI: https://doi.org/10.1073/pnas.1906655116

[41] Wang, W., Shi, J., Xie, Q., et al., 2017. Nutrient exchange and regulation in arbuscular mycorrhizal symbiosis. Molecular Plant. 10(9), 1147-1158. DOI: https://doi.org/10.1016/j.molp.2017.07.012

[42] Kobae, Y., Tamura, Y., Takai, S., et al., 2010. Localized expression of arbuscular mycorrhiza-inducible ammonium transporters in soybean. Plant and Cell Physiology. 51(9), 1411-1415. DOI: https://doi.org/10.1093/pcp/pcq099

[43] Wang, S., Chen, A., Xie, K., et al., 2020. Functional analysis of the OsNPF4. 5 nitrate transporter reveals a conserved mycorrhizal pathway of nitrogen acquisition in plants. Proceedings of the National Academy of Sciences. 117(28), 16649-16659. DOI: https://doi.org/10.1073/pnas.2000926117

[44] Dang, H., Zhang, T., Wang, Z., et al., 2021. Succession of endophytic fungi and arbuscular mycorrhizal fungi associated with the growth of plant and their correlation with secondary metabolites in the roots of plants. BMC Plant Biology. 21, 1-16. DOI: https://doi.org/10.1186/s12870-021-02942-6

[45] Sharma, E., Anand, G., Kapoor, R., 2017. Terpenoids in plant and arbuscular mycorrhiza-reinforced defence against herbivorous insects. Annals of Botany. 119(5), 791-801. DOI: https://doi.org/10.1093/aob/mcw263

[46] Cartabia, A., Tsiokanos, E., Tsafantakis, N., et al., 2021. The arbuscular mycorrhizal fungus Rhizophagus irregularis MUCL 41833 modulates metabolites production of Anchusa officinalis L. under semi-hydroponic cultivation. Frontiers in Plant Science. 12, 724352. DOI: https://doi.org/10.3389/fpls.2021.724352

[47] Pedone-Bonfim, M.V.L., da Silva, D.K.A., da Silva-Batista, A.R., et al., 2018. Mycorrhizal inoculation as an alternative for the sustainable production of Mimosa tenuiflora seedlings with improved growth and secondary compounds

content. Fungal Biology. 122(9), 918-927.
DOI: https://doi.org/10.1016/j.funbio.2018.05.009

[48] McCarthy, M.C., Enquist, B.J., 2007. Consistency between an allometric approach and optimal partitioning theory in global patterns of plant biomass allocation. Functional Ecology. 21(4), 713-720.
DOI: https://doi.org/10.1111/j.1365-2435.2007.01276.x

[49] Enfissi, E.M., Fraser, P.D., Lois, L.M., et al., 2005. Metabolic engineering of the mevalonate and non-mevalonate isopentenyl diphosphate-forming pathways for the production of health-promoting isoprenoids in tomato. Plant Biotechnology Journal. 3(1), 17-27.
DOI: https://doi.org/10.1111/j.1467-7652.2004.00091.x

[50] Gupta, P., Goel, R., Agarwal, A.V., et al., 2015. Comparative transcriptome analysis of different chemotypes elucidates withanolide biosynthesis pathway from medicinal plant Withania somnifera. Scientific Reports. 5(1), 18611.
DOI: https://doi.org/10.1038/srep18611

[51] Thimmappa, R., Geisler, K., Louveau, T., et al., 2014. Triterpene biosynthesis in plants. Annual Review of Plant Biology. 65, 225-257.
DOI: https://doi.org/10.1146/annurev-arplant-050312-120229

[52] Christ, B., Xu, C., Xu, M., et al., 2019. Repeated evolution of cytochrome P450-mediated spiroketal steroid biosynthesis in plants. Nature Communications. 10(1), 3206.
DOI: https://doi.org/10.1038/s41467-019-11286-7

[53] Bak, S., Kahn, R.A., Olsen, C.E., et al., 1997. Cloning and expression in Escherichia coli of the obtusifoliol 14α-demethylase of Sorghum bicolor (L.) Moench, a cytochrome P450 orthologous to the sterol 14α-demethylases (CYP51) from fungi and mammals. The Plant Journal. 11(2), 191-201.
DOI: https://doi.org/10.1046/j.1365-313x.1997.11020191.x

[54] Liao, P., Chen, X.J., Wang, M.F., et al., 2018. Improved fruit α-tocopherol, carotenoid, squalene and phytosterol contents through manipulation of *Brassica juncea* 3-HYDROXY-3-METHYLGLUTARYL-COA SYNTHASE1 in transgenic tomato. Plant Biotechnology Journal. 16(3), 784-796.
DOI: https://doi.org/10.1111/pbi.12828

[55] Piironen, V., Lindsay, D.G., Miettinen, T.A., et al., 2000. Plant sterols: Biosynthesis, biological function and their importance to human nutrition. Journal of the Science of Food and Agriculture. 80(7), 939-966.
DOI: https://doi.org/10.1002/(SICI)1097-0010(20000515)80:7<939::AID-JSFA644>3.0.CO;2-C

BILINGUAL PUBLISHING GROUP

Journal of Botanical Research

https://journals.bilpubgroup.com/index.php/jbr

ARTICLE

Species Distribution and Patterns in a Forest-savannah Ecotone: Environmental Change and Conservation Concerns

Nwabueze Ikenna Igu

Department of Geography and Meteorology, Nnamdi Azikiwe University, PMB 5025, Awka, Nigeria

ABSTRACT

Understanding the dynamics and patterns of biodiversity in transition forests is vital in promoting conservation and addressing environmental change issues. This work focused on elucidating the diversity, structure, and carbon potentials of a forest-savannah ecosystem. To achieve this, 8 forest plots that measured 50 m × 50 m each was set up in a forest-savannah landscape and used to identify and measure tree species ≥ 10 cm diameter at breast height (DBH measured at 130 cm). Species importance value was used to summarize the biodiversity patterns and the aboveground carbon estimates were elicited with the allometric equation. 43 species within 22 families were enumerated and the diversity was generally low (ranging from 1.82-2.5). Species such as *Daniellia oliveri* (Rolfe) Hutch. & Dalziel, *Pyrostria guinnensis* Comm. ex A. Juss, *Dialium guineense* Willd. and *Margariteria discoidea* (Baill.) G.L Webster were the dominant species, and had the highest importance values of 113.06, 55.13, 28.16 and 16.95, respectively, while *Allophlus africanus* P. Beauv., *Annona senegalensis* Pers., *Anthonatha macrophylla* P. Beauv., *Ficus capensis* Thumb. and *Lecaniodiscus cupanioides* Planch had the least importance values of 0.16 each. Carbon estimates ranged from 16.43172-42.9298 t/Ha. Most frequent species with higher basal areas no doubt contributed much to the carbon estimates, but did not have higher capacities in storing carbon. Managing the ecosystem with more carbon-dense species was seen as a suitable strategy for addressing environmental change in the ecosystem and region.

Keywords: Biodiversity; Carbon potentials; Climate change; Ecosystem conservation; Land use change

*CORRESPONDING AUTHOR:

Nwabueze Ikenna Igu, Department of Geography and Meteorology, Nnamdi Azikiwe University, PMB 5025, Awka, Nigeria; Email: nik.igu@unizik.edu.ng

ARTICLE INFO

Received: 22 March 2023 | Revised: 8 May 2023 | Accepted: 15 May 2023 | Published Online: 8 June 2023

DOI: https://doi.org/10.30564/jbr.v5i3.5588

CITATION

Igu, N.I., 2023. Species Distribution and Patterns in a Forest-savannah Ecotone: Environmental Change and Conservation Concerns. Journal of Botanical Research. 5(3): 27-35. DOI: https://doi.org/10.30564/jbr.v5i3.5588

1. Introduction

Tropical forest ecosystems play vital roles in addressing environmental change issues and are repositories of biodiversity. Though they occupy less than 10% of terrestrial surface land, they host much of global biodiversity, store 40-50 percent of terrestrial vegetation carbon and contribute more than one-third of primary productivity [1,2]. Traversing different latitudinal gradients, tropical ecosystems are found across different continents: America, Africa and Asia, and have varied biogeography, disturbance history and extents. The ecosystem is characterized by species-rich and diverse plant communities with its distributional patterns remaining a central question in ecology [3]. Efforts to unravel such patterns abound and have spanned a long period of time; with testimonials of such seen in the development of theories, models and hypotheses surrounding tropical ecology, biogeography and more recently its biogeochemical cycles. Distribution patterns across the ecosystem are inherently varied according to niche processes (more evidently on larger scales) and neutral processes on smaller scales [4]. Hence, the ecosystem is seen to be substantially varied in species richness, density and primary productivity across biomes and geographical delimitations.

Rainforests are particularly high in biodiversity; compared with other tropical ecosystems and known to occur in large proportions in regions such as the Amazon, Congo basin, and the Indo-Malayan Archipelago. Features of the rainforest are much known since the works of Richards [5], however, specific details on its surrounding zones are less known and much generalized. Notably among these are the transition forests that border the rainforest ecosystem; being where ecological communities of the rainforest and the adjoining ecosystem coincide. Such landscapes are found across the whole of the tropics where rainforests occur and notably along ecological gradients. With such gradients being created due to shifts in environmental factors, ecotones thus have the potentials of being hosts to populations that are adapted to both ecosystems on each side and species that accommodate changing environments.

Understanding biodiversity patterns across ecosystems is vital for ecological management and conservation and provides insights as key indicators to inherent environmental factors that define regions and ecosystems. Across Nigeria, baselines on the biodiversity of ecosystems are much documented by earlier inventories [6]. However, there is yet much dearth of knowledge regarding its transition to the savannah ecosystem particularly in South East Nigeria. Rainforest transition with savannah in south east Nigeria covers about a quarter of the eastern states. It is found in the north of the rainforest zone and is the transitional zone between grassland of northern Nigeria and the rainforest south [7]. Land use change is growing in magnitude across the region and is affecting the ecosystem greatly. In a bid to provide baseline insights on the ecotone and document the inherent botanical features of the ecosystem, this study was conducted. This work specifically focused on the diversity, structure, and carbon potentials of the ecosystem and thus, its conservation and climate change mitigation prospects.

2. Materials and methods

2.1 Study area

The area for the research is a part of South East Nigeria (**Figure 1**). The climate is characterized by a humid tropical, tropical wet and dry, and marked with rainy and dry seasons. It has a high annual rainfall which ranges from 1,400 mm in the North to 2,500 mm in the South, and a mean monthly temperature of 27.6 °C. The geology of the region comprises the ancient Cretaceous delta, with the Nkporo shale, the Mamu formation, the Ajali sandstone and the Nsukka formation as its main deposits [8]. The natural vegetations in this region are mainly the rainforest—savannah ecotone ecosystem. The zone experiences about 3 dry months in its northern zone and 1-2 dry months in the south, making it much more humid and with sufficient rainfall. Forest inventory was done in Awlaw in Oji River local government area of Enugu State. This location is characterized by an undulating and rugged terrain with an

extensive and relatively undisturbed ecosystem.

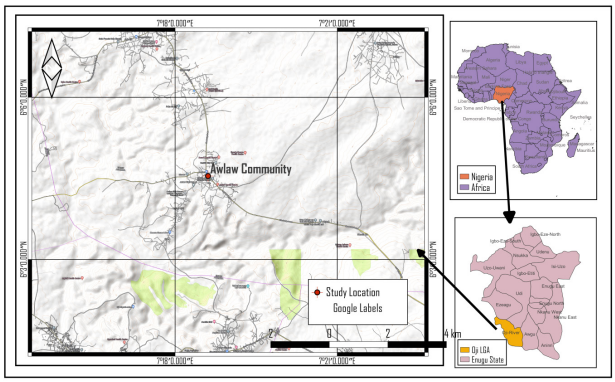

Figure 1. Map of the study area with the local government, Nigeria and Africa inset.

2.2 Data collection and analysis

To be able to determine the biodiversity and its patterns across the ecosystem, 8 forest plots were set up randomly across the forest locations. Each of the plots measured 50 m × 50 m and had intervals of not less than a hectare between the plots in each location. Tree species ≥ 10 cm diameter at breast height (DBH measured at 130 cm) were identified. DBH or girth tape was used to measure the tree stems while a rangefinder was used to measure the heights. Species found within all the plots were identified, measured and documented. Species identification followed the taxonomy of Nigerian plants [9] and The Plant List [10].

The species importance index was used to characterize the forest locations and verify the patterns of abundance of the species. This was calculated as follows:

Species importance values (SIV) = Relative density + Relative frequency + Relative dominance [11], where:

$$\text{Relative Density} = 100 \times \frac{\text{Number of stems of a species}}{\text{Total number of stems}} \quad (1)$$

$$\text{Relative frequency} = 100 \times \frac{\text{Frequency of a species}}{\text{Sum of all species}} \quad (2)$$

$$\text{Relative dominance} = 100 \times \frac{\text{Total basal area of a species}}{\text{Total basal area of all}} \quad (3)$$

The basal area was calculated as follows:

$$\text{BA} = \left(\frac{dbh}{2}\right)^2 \times \pi \quad (4)$$

where BA is the basal area (m^2); dbh is the diameter at breast height (cm) and π as pie (3.142).

The diversity of the ecosystem was ascertained following Kent and Coker [12]:

Shannon-Wiener index:

$$H' = -\sum_{i=1}^{s} pi \ln pi \quad (5)$$

where H^1 is the Shannon-Weiner index, s is the total number of species, pi is the proportion of individuals in the ith species, and ln is the natural logarithm.

Above ground carbon (AGC) was estimated with a pan-tropical equation [13]:

$$AGB = 0.0673 \times (pD^2H)^{0.976} \quad (6)$$

where AGB is the above ground biomass; ρ is the wood specific gravity (WSG; $g \cdot cm^{-3}$); D is the diameter at breast height (DBH; cm) and H is the height (m). Forest structural classes were categorized as small (< 20 cm dbh), medium (21-40 cm dbh), large (41-60 cm dbh) and largest (> 60 cm dbh). Pearson correlation was used to verify the correlation between the amount of carbon, basal area and number of stems.

3. Results

The ecosystem is composed of 43 species within 22 families. Distinct species ranged from 11-22 and the number of stems within each of the plots ranged from 46-110 individual stems (**Table 1**). Diversity was generally low (ranging from 1.82-2.5) and was not determined by the number of stems (**Table 1**).

As expected in a forest ecosystem, the structural patterns varied between the small (< 20 cm dbh), medium (21-40 cm dbh), large (41-60 cm dbh) and largest (> 60 cm dbh) stem sizes (**Figure 2**). Medium stem sizes (21-40 cm dbh) had the highest number of tree stems and were followed by the large stem, largest stem and small stems, respectively (**Figure 2**). The highest total basal area of 51452994.56 was from *Daniellia oliveri* (Rolfe) Hutch. & Dalziel and were followed by *Pyrostria guinnensis* Comm. ex A. Juss (with 20090882.585 total basal areas) and *Dialium guineense* Willd. (with a total basal area of 8876584.76265).

The dominant species within the ecosystem were

Daniellia oliveri (Rolfe) Hutch. & Dalziel, *Pyrostria guinnensis* Comm. ex A.Juss, *Dialium guineense* Willd. and *Margariteria discoidea* (Baill.) G.L Webster, with 50.06%, 19.67%, 8.69% and 4.22% dominance, respectively (**Table 2**). Similarly, the same species were seen to record in the same order, the highest important values of 112.76, 55.28, 28.22 and 16.98 values, respectively, while *Allophlus africanus* P.Beauv., *Annona senegalensis* Pers., *Anthonatha macrophylla* P. Beauv., and *Ficus capensis* Thumb., had the least importance values of 0.0008, 0.0012, 0.0012 and 0.0020, respectively (**Table 2**). *Pyrostria guinnensis* Comm. ex A. Juss was the species with the highest frequency of occurrence (15.92%), while 12 different species had the least frequency of occurrence (0.164204%; **Table 2**).

Table 1. Species diversity, richness and stem distribution.

Plot number	No. of species	Shannon diversity	No of stems
1	22	2.5892	79
2	14	2.01666	64
3	12	2.17817	46
4	14	1.99636	72
5	17	2.35784	75
6	18	2.32089	90
7	11	1.97324	72
8	12	1.82118	110

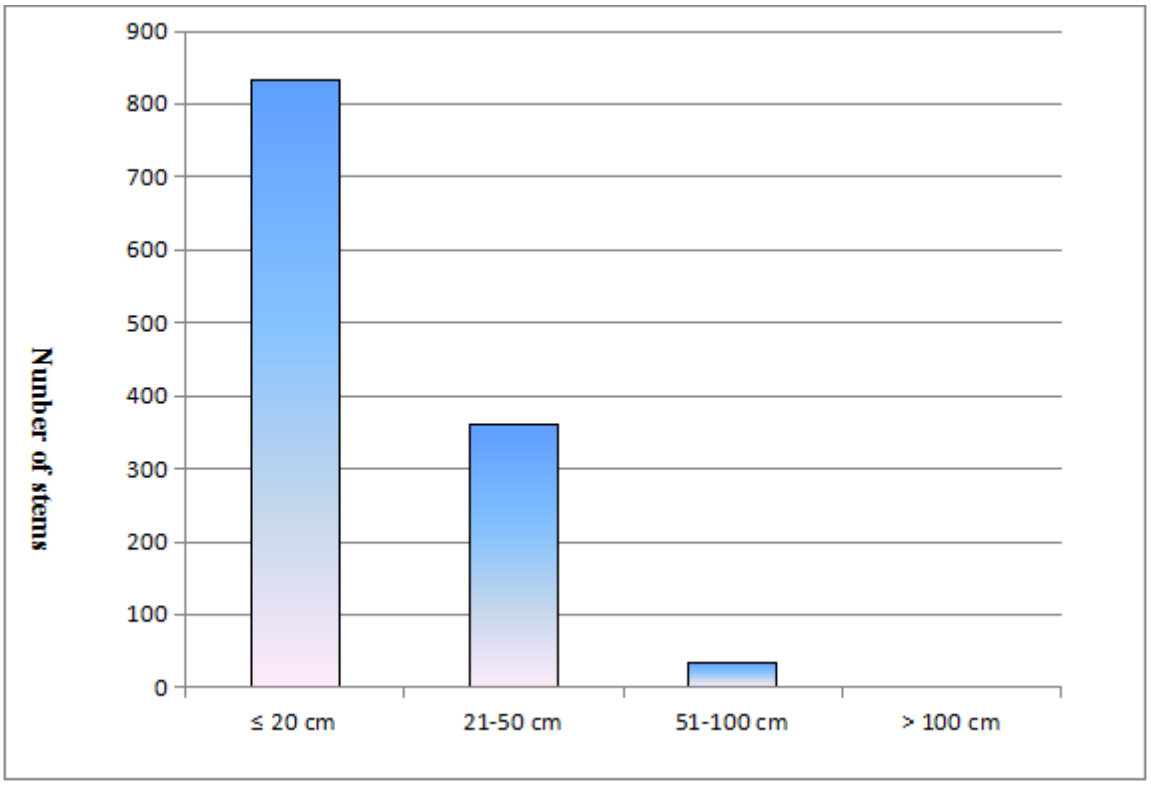

Figure 2. Stem sizes of the different individual stems in the ecosystem.

Table 2. Species importance values (SIV).

Species	Relative frequency	Relative density	Relative dominance	SIV
Afzelia africana (Sm. Ex pers.)	1.149425	0.187622	0.187622	1.524668
Albezia zygia (DC.)	0.492611	0.046715	0.046715	0.58604
AlbIzia adianthifolia (Shumach.) W.Wight	0.328407	0.015724	0.015724	0.359855
Allophlus africanus P.Beauv.	0.164204	0.000888	0.000888	0.16598
Annona senegalensis Pers.	0.164204	0.00123	0.00123	0.166663
Anthocleista djalonensis A. Chev.	1.970443	0.732412	0.732412	3.435267
Anthocleista vogelii (Planch.)	0.328407	0.014432	0.014432	0.357271
Anthonatha macrophylla P. Beauv.	0.164204	0.00123	0.00123	0.166663
Bridelia ferruginea Benth	0.328407	0.003876	0.003876	0.336159
Ceiba pentandra L.	0.164204	0.005297	0.005297	0.174797
Cola millenii (K. Schum.)	0.492611	0.009644	0.009644	0.5119
Daniellia oliveri (Rolfe) Hutch. & Dalziel	12.64368	50.06055	50.06055	112.7648
Dialium guineense Willd.	10.83744	8.694261	8.694261	28.22596
Ekerberga senegalensis A. Juss	0.985222	0.192207	0.192207	1.369636
Entandrophragma angolense (Welw.)	0.328407	0.012994	0.012994	0.354395
Ficus capensis Thumb.	0.164204	0.002079	0.002079	0.168361
Funtumia elastica (P. preuss)	1.642036	0.209512	0.209512	2.061061
Gmelina arborea Roxb.	0.164204	0.012008	0.012008	0.18822
Hymenocardia acida Tul.	1.642036	0.159175	0.159175	1.960385
Khaya senegalensis (Desr.) A. Juss	0.164204	0.039964	0.039964	0.244132
Lannea welwitsschii (Hien) Engl.	6.568144	2.764013	2.764013	12.09617
Lecaniodiscus cupanioides Planch.	0.164204	0.002497	0.002497	0.169198
Lophira lanceolata Tiegh. Ex Keay	6.075534	3.958401	3.958401	13.99234
Margariteria discoidea (Baill.) G.L Webster	8.538588	4.224488	4.224488	16.98756
Milicia excelsa Welw.	0.164204	0.00609	0.00609	0.176385
Milletttia thonngii (Shumach & Thonn.) Baker	0.492611	0.002586	0.002586	0.497783
Musanga cecropoides R.Br.	0.164204	0.007382	0.007382	0.178968
Napoleona imperialis P.Beauv.	3.284072	0.54899	0.54899	4.382052
Nauclea latifolia Smith	0.492611	0.010344	0.010344	0.513298
Parkia biglobosa (Jacq.) G.Don	3.284072	1.598756	1.598756	6.481584
Pentaclethra macrophylla Benth.	1.477833	0.31004	0.31004	2.097913
Periscopsis elata (Harms) van Meeuwen	0.492611	0.002079	0.002079	0.496768
Pseudocedrela kotschyi (Schweinf) Harms	5.090312	2.938613	2.938613	10.96754
Pterocarpus osun Craib	0.985222	0.051574	0.051574	1.08837
Pyrostria guinnensis Comm. ex A.Juss	15.92775	19.67825	19.67825	55.28425
Rauvolfia vomitoria Afzel.	0.164204	0.003051	0.003051	0.170305
Spathodea campanulata (P. Beauv.)	0.821018	0.039262	0.039262	0.899543
Spondias mombin (L.)	0.656814	0.052378	0.052378	0.761571
Sterculia tragacantha Lindl.	2.627258	0.552916	0.552916	3.733089
Terminalia avicennoides Guill. & Perr.	5.91133	2.496663	2.496663	10.90466
Terminalia glaucescens Planch.	0.985222	0.091521	0.091521	1.168263
Treculia africana Decene	0.164204	0.030753	0.030753	0.22571
Vitex doniana	1.149425	0.227537	0.227537	1.604499
	100	100	100	300

The carbon storage in the biomass across the plots ranged from 16.43172-42.9298 t/Ha (**Figure 3**).

Species within the ecosystem were dominated by three families: Fabaceae, Euphorbiaceae and Moraceae which had 9, 3 and 3 species, respectively (**Table 3**).

Carbon estimates across the plots correlated with the total basal area and a number of stems across the ecosystem.

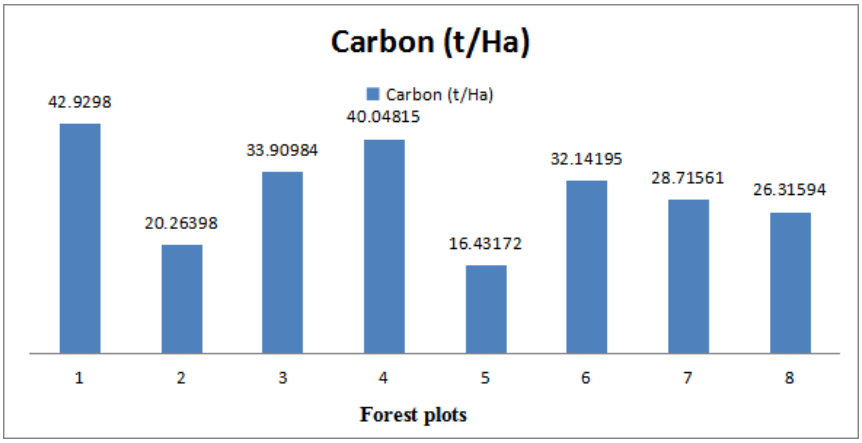

Figure 3. Distribution of aboveground carbon across the plots.

Table 3. Distribution of families and their species.

Family	Number of species
Anacardiaceae	2
Annonaceae	1
Apocynaceae	2
Bignoniaceae	1
Combretaceae	2
Euphorbiaceae	3
Fabaceae	9
Gentianaceae	1
Lamiaceae	1
Lecythidaceae	1
Leguminosae	2
Loganiaceae	1
Maliaceae	2
Malvaceae	1
Meliaceae	2
Moraceae	3
Ochinaceae	1
Rubiaceae	2
Sapindaceae	2
Streculiaceae	2
Urticaceae	1
Verbenaceae	1

4. Discussion

Tree species composition of the ecosystem was made up of 43 species (**Table 2**) that differed in occurrence/presence across the ecosystem (**Table 1**). This is however lower than what is recorded for other tropical forests in Africa [14]. This is equally much lower than the records from the Neotropics [15]. Such low occurrence was mainly because the region is within forest-savannah ecotone and not exclusively a rainforest, which will expectedly record a higher number of tree species as is characteristic of tropical forests. The abundance of trees in such ecotones is equally dependent on how far the ecosystem entered into the savannah (grassland). The extent or the depth of edge a vegetation type extends into the other ecosystem has much influence on the vegetation [16,17]. Such is due to inherent features such as microclimate conditions and fire vulnerabilities of (the major zone that dominates) the transition zone. Tree dominance was concentrated on *Daniellia oliveri* (Rolfe) Hutch. & Dalziel, *Pyrostria guinnensis* Comm. ex A.Juss, and *Dialium guineense* Willd.; which had more than half (78.42%) of the dominance in the region. Such dominance is however not characteristic of such transition zone alone, but are also patterns of dominance and monodominance that

are similar to rainforest ecosystems [18]. The dominance of species in ecosystem borders directly on the successes species achieves in an environment [19]. Such is mainly characterized by the frequency/abundance of such species in a community. On the other hand, few families were seen to have many of the species in the ecosystem (**Table 3**); with Fabaceae being the most dominant (with the highest number of species). Fabaceae family is among the families with the largest number of species in the world [20,21]. It is equally reported to be very diverse and dominant in other ecosystems and regions, including the dry forests in the Neotropics [22,23].

The forest structure showed tree stems for each of the categories (**Figure 2**), with a greater number of tree stems concentrated in the lowest stem category than others. Ample number of stems was found within the middle class/juvenile stems and sufficient for good recruitment and replacement. Fewer tree stems were large and showed that the ecosystem though mature, is not however a climax vegetation; being greatly affected by disturbance regimes. Ecosystems undergo natural disturbances periodically and in most situations, recover from them within short time scales; depending on their intensity. Disturbances are equally important natural phenomenon of forest ecosystem dynamics and largely modulate the structure and functioning of forest ecosystems [24]. While such patterns are inherent in ecosystems and benefit them, landscapes (such as the ecotones with savannah) that may not have much resilience that exists in some others (such as the rainforest) are however more adversely affected by such occurrences. On the other hand, it may equally affect their biological diversity and other roles such as their capacity to provide ecosystem services; such as adequate timber supply and carbon storage. Ensuring that disturbances in ecosystems, especially anthropogenic associated disturbances are greatly minimized in the rainforest-savannah ecotones as well as other forest landscapes are much needed to inhibit the debilitating impacts on the forest structure and the ecosystem function and service provision in totality.

The aboveground carbon of the ecosystem ranged from 16.43172-42.9298 t/Ha across the ecosystem (**Figure 3**). Species composition is much varied across and within ecosystems, and largely influences their ability to provide varied functions. Carbon estimates correlated with basal area and a number of stems in the ecosystem. With R values of 0.71 and 0.55 (**Table 4**), it showed that there were other variables that contributed to the estimate. Plots that had higher basal areas and a number of stems did not consistently record higher estimates of carbon (**Table 5**) either. Such variations in carbon estimate of the plots were mainly due to differences in tree structure, density and composition across the plots. While these biodiversity variables are expected to vary at the plot level due to inherent local factors and disturbance ranges, the role the (plots) ecosystem plays in carbon storage is worthy of note. Species with higher frequencies of occurrence and dominance (**Table 2**) had cumulative higher basal areas, and densities, and hence, contributed to much of the carbon stores. However, many of such species did not necessarily have higher (WSG) capacities to store carbon as distinct species and showed how weak the landscape could be as regards climate change mitigation. *Daniellia oliveri* (Rolfe) Hutch. & Dalziel recorded the highest dominance of 50.06% and a low WSG (0.493 g/cm^3) while *Anthonatha macrophylla* P. Beauv. had the highest WSG (0.842 g/cm^3) and the second least dominance of 0.0012%; occurring only once alongside other 12 species (**Table 2**). This meant that the main species in the ecosystem do not necessarily have much capacity to store carbon, and could only store some ample amount due to its structural features (which could be prone to disturbance like any other landscape). Managing the ecosystem adequately to ensure higher carbon storage is a necessity for mitigating environmental change concerns. Such strategies would be best actualized by utilizing target species such as *Anthonatha macrophylla* P. Beauv. which can thrive in the ecosystem and possesses higher carbon capture potentials in reforestation and ecosystem restoration.

Table 4. Correlation between carbon estimates, basal area and number of stems.

		Total basal area	Total amount of carbon	Number of stems
TBA	Pearson Correlation	1	0.155	0.250
	Sig. (2-tailed)		0.714	0.551
	N	8	8	8
CARBON	Pearson Correlation	0.155	1	–0.066
	Sig. (2-tailed)	0.714		0.877
	N	8	8	8
STEMS	Pearson Correlation	0.250	–0.066	1
	Sig. (2-tailed)	0.551	0.877	
	N	8	8	8

TBA = Total basal area, STEMS = Number of stems.

Table 5. Distribution of basal area, carbon and number of stems across the plots.

Plot number	Total basal area	Carbon (t/Ha)	No of stems
1	1649359	42.9298	79
2	2833696	20.26398	64
3	3512737	33.90984	46
4	3494514	40.04815	72
5	1551143	16.43172	75
6	4213784	32.14195	90
7	2976830	28.71561	72
8	3977356	26.31594	110

5. Conclusions

Forest-savannah ecotone is not as diverse as tropical rainforests due to its transition to the savannah. They recorded ample carbon estimates but were characterized by many species that were not as carbon dense as the few ones. Managing the ecosystem with the more carbon-dense species was advocated as measure that could help the ecosystem ensure better climate change mitigation.

Conflict of Interest

There is no conflict of interest.

References

[1] Pan,. Y., Birdsey, R.A., Fang, A., et al., 2011. A large and persistent carbon sink in the world's forests. Science. 333, 988-993.

[2] Erb, K.H., Kastner, T., Plutzar, C., et al., 2018. Unexpectedly large impact of forest management and grazing on global vegetation biomass. Nature. 553(7686), 73-76.

[3] Gaviria, J., Turner, B.L., Engelbrecht, B.M.J., 2017. Drivers of tree species distribution across a tropical rainfall gradient. Ecosphere. 8(2), e01712.
DOI: https://doi.org/10.1002/ecs2.1712

[4] Chase, J.M., 2014. Spatial scale resolves the niche versus neutral theory debate. Journal of Vegetation Science. 25(2), 319-322.

[5] Richards, P.W., 1952. The tropical rain forest: An ecological study. Cambridge University Press: Cambridge. pp. 450.

[6] Keay, R.W., 1959. An outline of the Nigerian vegetation. Federal Department of Forest Research. Federal Ministry of Information: Lagos.

[7] Igbozurike, M.U., 1975. Vegetation types. Nigeria in maps: Eastern States. Ethiope Publishing House: Benin. pp. 30-31.

[8] Ofomata, G.E.K., 1975. Vegetation types and soils. Nigeria in maps: Eastern states. Ethiope Publishing House: Benin. pp. 30-45.

[9] Keay, R.W.J., 1989. Trees of Nigeria. Clarendon Press: Oxford.

[10] Plant List Version 1.1 [Internet]. The Plant List; 2013. Available from: http://www.theplantlist.org/

[11] Cottam, G., Curtis, J.T., 1956. The use of distance measurements in phytosociological sampling. Ecology. 37(3), 451-460.

[12] Kent, M., Coker, P., 1992. Vegetation description analysis. Wiley: Chichester.

[13] Chave, J., Réjou-Méchain, M., Burquez, A., et al., 2015. Improved allometric models to estimate the aboveground biomass of tropical trees. Global Change Biology. 20(10), 3177-3190. DOI: https://doi.org/10.1111/gcb.12629

[14] Ndah., N.R., Andrew, E.E., Bechem, E., 2013. Species composition, diversity and distribution in a disturbed Takamanda Rainforest, South West, Cameroon. African Journal of Plant Science. 7(12), 577-585. DOI: https://doi.org/10.5897/AJPS2013.1107

[15] Gentry, A.H., 1988. Changes in plant community diversity and floristic composition on environmental and geographical gradients. Annals of the Missouri Botanical Garden. 75, 1-34. DOI: https://doi.org/10.2307/2399464

[16] Hoffmann, W.A., Jaconis, S.Y., Mckinley, K.L., et al., 2012. Fuels or microclimate? Understanding the drivers of fire feedbacks at savanna-forest boundaries. Austral Ecology. 37(6), 634-643.

[17] Ibanez, T., Hély, C., Gaucherel, C., 2013. Sharp transitions in microclimatic conditions between savanna and forest in New Caledonia: Insights into the vulnerability of forest edges to fire. Austral Ecology. 38(6), 680-687.

[18] Lewis, S.L., Sonké, B., Sunderland, T., et al., 2013. Aboveground biomass and structure of 260 African tropical forests. Philosophical Transactions of the Royal Society B. 368, 20120295.

[19] Terra, M.N.S., do Prado-Júnior, J.A., de Souza, C.R., et al., 2021. Tree species dominance in neotropical savanna aboveground biomass and productivity. Forest Ecology and Management. 496, 119430.

[20] Chase, M.W., Christenhusz, M.J.M., Fay, M.F., et al., 2016. An update of the Angiosperm Phylogeny Group classification for the orders and families of flowering plants: APG IV. Botanical Journal of the Linnean Society. 181(1), 1-20.

[21] Baptista, M.S.P., Assunção, V.A., Bueno, M.L., et al., 2020. Species representativeness of Fabaceae in restrictive soils explains the difference in structure of two types of Chaco vegetation. Acta Botanica Brasilica. 34(3), 559-569.

[22] Gentry, A.H., 1995. Diversity and floristic composition of Neotropical dry forests. Seasonally dry tropical forests. Cambridge University Press: Cambridge, UK. pp. 146-194.

[23] Lima, J.R., Tozzi, A.M., Mansano, V.F., 2015. A checklist of woody Leguminosae in the South American Corridor of Dry Vegetation. Phytotaxa. 207(1), 1-38.

[24] Thom, D., Seidl, R., 2016. Natural disturbance impacts on ecosystem services and biodiversity in temperate and boreal forests. Biological Reviews. 91(3), 760-781.

BILINGUAL PUBLISHING GROUP

Journal of Botanical Research

https://journals.bilpubgroup.com/index.php/jbr

ARTICLE

Diversity of Flower Opening Time and Duration in Rice (*Oryza sativa* ssp. *indica*) Landraces of South and Southeast Asia in Different Cultivation Seasons

***Debal Deb*[1*], *Niranjan V Joshi*[1,2], *Debdulal Bhattacharya*[1], *Mahendra Nauri*[1], *Rakesh Ganguly*[1]**

[1] *Basudha, Centre for Interdisciplinary Studies, Kolkata, 700068, India*

[2] *Energy and Wetlands Research Group, CES TE 15, Indian Institute of Science, Bangalore, 560012, India*

ABSTRACT

Different cultivars of rice (*Oryza sativa*) open at different times of the day, and the overlap of anthesis time in rice between the neighbouring cultivars is of crucial importance to the degree of cross pollination in rice. Nevertheless, none of the past experiments with cross pollination between different rice cultivars ever reported the respective flower opening time (FOT) and flower exposure duration (FED) of the parent cultivars, until recently. The authors present here the first record of FOT and FED of 1114 *indica* rice landraces of South and Southeast Asia, growing during summer and winter seasons in three consecutive years. The authors also present an analysis of the influences of the growing season on the anthesis behaviour, and present the first records of the FOT and FED variability on sunny and cloudy days of a large number of landraces. The data show that rice florets tend to open earlier in the morning (that is, take a shorter time to anthesis after sunrise) on sunny days than on cloudy days, and also significantly later during long day seasons (spring and summer) than during short day season (winter); and that FED is inversely related to both FOT and the length of duration from sunrise to first flower opening. The wide ranges of FOT (8:50 a.m. to 12:40 p.m.) and FED (15 to 194 minutes) also suggest the ample time window for receiving pollen from neighbouring cultivars with different FOT, enhancing the chances of cross pollination between hundreds of rice landraces with FOT and FED overlaps.

Keywords: Anthesis; Flower opening time; *Indica* landraces; Pollination; Rice; Season

*CORRESPONDING AUTHOR:

Debal Deb, Basudha, Centre for Interdisciplinary Studies, Kolkata, 700068, India; Email: debdebal@gmail.com

ARTICLE INFO

Received: 11 March 2023 | Revised: 13 June 2023 | Accepted: 15 June 2023 | Published Online: 25 June 2023

DOI: https://doi.org/10.30564/jbr.v5i3.5724

CITATION

Deb, D., Joshi, N.V., Bhattacharya, D., et al., 2023. Diversity of Flower Opening Time and Duration in Rice (*Oryza sativa* ssp. *indica*) Landraces of South and Southeast Asia in Different Cultivation Seasons. Journal of Botanical Research. 5(3): 36-48. DOI: https://doi.org/10.30564/jbr.v5i3.5724

1. Introduction

The flower opening time (FOT) and the duration of the flowers remaining open (= flower exposure duration, FED) are crucially important for the success of pollination and fertilization in rice (*Oryza sativa* L.) plants. Although rice is widely known to be predominantly self-pollinating, our recent study [1] showed that cross-pollination can occur at a high frequency between cultivars with a large temporal overlap of FED. In cross pollination experiments, published since the early last century, the FOT and FED of the cultivars were never recorded. It seems likely that the FED of the pairs of cultivars chosen in those experiments were non-overlapping, resulting in their reporting of extremely low (0 to 2%) frequency of cross-pollination between different rice cultivars [1]. The knowledge of FOT and FED is of crucial importance, both for the purpose of preventing cross-pollination between neighbouring cultivars, and to ensure cross-pollination success in hybridization experiments. Indeed, if the florets of the ovary parent (OP) close even a second before the FOT of the pollen parent (PP), the FED overlap between the two parents is zero, and consequently, there would be no cross pollination. In spite of the crucial importance of FOT and FED overlap between the OP and the PP, none of the reports of cross pollination experiments, published since Beachell et al. [2] till Somaratne et al. [3], surprisingly mention any of these three important parameters: FOT, flower closing time (FCT), and FED of the cultivar pairs selected in the respective experiments.

The earliest record of FOT in cultivated rice was made by Stok [4], informing that in Java, flowers of many rice cultivars opened between 0900 h and 1000 h, while some opened between 1200 h to 1300 h. Pope [5] reported that in the US, rice florets fully opened at 1014 h, and closed at 1300 h. A more recent study [6] reports that the beginning of the FOT of Nanjing 11 in temperate Japan was at ca. 0900, and the FOT of IR64 in the Philippine tropics began at ca. 1100.

There is a paucity of FOT and FED data for *O. sativa* ssp. *indica* landraces, of which the first record of FOT is found in Sharngapani [7], who noted that *aus* rice varieties (flowering in April-May) open at ca. 0700 h, while the winter rice cultivars, flowering in September-October, opened at ca. 0900 h. A large number (n = 289) of Asian cultivars, including some landraces from South and Southeast Asia, are reported to open their florets between 2.35 h and 5.08 h after sunrise during the dry hot season, compared to 3.05 h and 5.50 h after sunrise during the wet colder season in southern India [8]. However, the exact time of FOT is not available from their data. A later examination [9] of FOT and FCT of both *indica* and *japonica* cultivars, totalling 93, including 17 South Asian cultivars (12 from India, 2 from Nepal and 1 each from Bangladesh, Bhutan and Sri Lanka) revealed that the FOT of the *indica* cultivars, all grown in Japan, ranges between 0953 h and 1116 h.

A brief range of FOT data, gathered from published literature (summarised in **Table 1**) indicates that flowers of *indica* varieties tend to open earlier than *Japonica* varieties in similar latitudes. However, The FOT of a cultivar native to lower latitudes (e.g. southern India) is apt to be delayed in northern latitudes (e.g. in the US and Japan), due to lower temperatures and shorter day length. Anthesis of winter rice cultivars of South Asia would begin too late at the cold northern latitudes, "because frost will set in before harvest" [10]. This corroborates an earlier report [11] that a majority of flowers of 12 rice cultivars of Asian origin opened between 1200 h and 1400 h in California, while only 0.53% of the florets of these cultivars opened between 1600 h and 1700 h. While these reports indicate a wide diversity of FOT in rice cultivars in different geographical locations, the corresponding data of flower closing time (FCT) and the duration of the rice florets remaining open (FED) are not available. Here we contribute to expanding the database of FOT, FCT and FED of landraces, and constitute the first comprehensive report of FOT and FED of 1114 *indica* landraces cultivated in South and Southeast Asia.

Table 1. Published records of the earliest and last FOT (local time) for rice cultivars from different countries.

Country of origin	*Indica*		*Japonica*		Reference
	Earliest FOT	Last FOT	Earliest FOT	Last FOT	
China	09:01	10:47	11:44	12:02	[9]
Bangladesh	10:47	-			[9]
Japan			08:00 to 09:00	16:00 to 17:00	[11]
	10:08	11:42	10:19	12:35	[9]
India	07:00	12:00			[7]
	09:53	11:16			[9]
Indonesia	09:00	13:00			[4]
	10:44	12:00	11:01	-	[9]
Myanmar	07:00	09:00			[12]
	10:38	11:31			[9]
Nepal	10:51	11:30			[9]
Philippines			09:00	11:30	[13]
	09:55	11:15			[9]
USA			10:00 to 12:00	14:00 to 16:00	[11]
			10:10	11:42	[9]

2. Materials and methods

2.1 Study site and materials

A total of 1140 landraces were grown for this study on the Basudha conservation farm (http://cintdis.org/basudha), located in Bissam Cuttack block, Rayagada district of southern Odisha (19°42'32.0" N, 83°28'8.4" E). However, owing to the lack of adequate resources and field hands, we were able to document the complete flowering data of 1114 landraces, which comprise the materials for this study. All these landraces, originally collected from different districts of Bangladesh, India, Myanmar, Nepal, Pakistan and Sri Lanka, in addition to 18 landraces from Southeast Asia and 2 from East Asia (**Table 2**), were subjected to phenol reaction test and endosperm translucence examination for amylose [14,15], based on which we detected the presence of only five *Japonica*-type landraces (0.45%) in our sample, amongst whom one was accessed from Italy, 1 from South Korea, 1 from Myanmar and 2 from India. We added the Korean and Italian cultivars as references for characters of the South Asian *japonica* landraces.

2.2 Study period and seasons of cultivation

All landraces were sown during the *aman* season (sown in June, harvested from September to February of 2020 with 969 landraces, followed by 31 landraces during *boro* (sown in January, harvested during mid-summer during May-June) of 2021, 117 landraces during *aman* of 2021, 49 landraces during boro of 2022, and 5 landraces during *aus* season (sown in March, harvested in late summer to Autumn in June-July) of 2022, and 389 landraces during *aman* of 2022 (See **Table 3** and **Table 4**). During each growing season, all the rice seeds were sown within 6 days in nursery beds for germination. After germination, 14 to 16-day-old seedlings of each landrace were transplanted in an 8 × 8 matrix, at 16/m^2 density, in a 4 m^2 farm plot, where the soil had been prepared following standard organic method, with no synthetic agrochemical inputs. We followed the steps described below, to record the flower opening time (FOT) and closing time (FCT) in each discrete varietal plot:

Among the *aman* 2020 landraces (harvested in winter 2020), 29 were sown successively during *boro* 2021, and 22 *aman* 2021 landraces were sown

in succeeding *boro* 2022. Further, 8 landraces were repeated between *boro* and *aman* of 2021, and 73 landraces between *boro* and *aman* of 2022. **Table 4** summarises the sowing schedules. A total of 58 landraces were harvested in summer (*boro* and *aus*) seasons of 2021 to 2022, whereas a total of 1111 *aman* varieties were harvested in winter from 2020 to 2022.

Table 2. Countries of origin of the 1114 landraces cultivated in different seasons.

Country	**No. of landraces**		
	Aman (winter harvest)	*Boro* and *aus* (summer harvest)	All seasons
Bangladesh	39	1	39
India	1017	54	1020
Myanmar	3	0	3
Nepal	2	0	2
Pakistan	1	1	1
Sri Lanka	30	1	30
Philippines	15	0	15
Thailand	2	0	2
South Korea	1	0	1
Italy	1	1	1
Total	**1111**	**58**	**1114**

Table 3. Life history stages of the *aman*, *boro* and *aus* landraces.

Season	**No. of landraces examined**	**Sowing dates**	**Transplanting dates**	**Flowering dates**	**Harvesting dates**
Aman 2020	969	15 Jun-30 Jun	6 Jul-16 Jul	8 Aug-22 Jan	2 Sep-5 Feb
Boro 2021	31	20 Jan-23 Jan	5 Feb-12 Feb	2 Apr-5 May	30 May-3 Jun
Aman 2021	117	28 Jun-4 Jul	15 Jul-19 Jul	1 Sep-22 Oct	17 Sep-2 Jan
Boro 2022	47	20 Jan-23 Jan	6 Feb-11 Feb	4 Apr-6 May	2 Jun-8 Jun
Aus 2022	5	3 Mar	3 Apr	27 May-21 Jun	25 Jun-9 Jul
Aman 2022	391	21 Jun-31 Jun	10 Jul-18 Jul	31 Aug-27 Nov	13 Sep-8 Jan

Table 4. Schedule of sowing of 1114 landraces from winter 2020 to winter 2022. Numbers above the diagonal are the number of varieties repeat-sown in different cultivation seasons.

Cultivation season	***Aman* 2020**	***Boro* 2021**	***Aman* 2021**	***Boro* & *Aus* 2022**	***Aman* 2022**
Aman 2020	**969**	30	108	48	258
Boro 2021		**31**	8	23	18
Aman 2021			**117**	22	5
Boro & Aus 2022				**50**	22
Aman 2022					**390**

2.3 Procedure of data recording

A total of 1114 landraces were sown, among which 717 landraces were cultivated only once over the entire study period of 3 years (2020 to 2022). To record the variations of flower opening time and duration in different seasons and in different light conditions, 397 landraces were repeatedly cultivated in different seasons. Some of the landraces, which were attacked by pests in the nursery were also grown in replicated plots during the same season and in the same year. The procedure of recording the time and duration of anthesis of each landrace is as follows:

a) As flowering typically begins one day after heading [16,17], we prepared for recording the time of anthesis soon after recording the heading date and time. We recorded the time of opening of the first (apical) floret in the first emerged panicle in each landrace population (consisting of 64 plants), and recorded the time of each event, before moving on to another plot that was also expected to open on the same date.

b) We often missed the FOT of several cultivars that simultaneously flowered on the same day at the same time. Over three years (2020-2022) of the study, we were able to record the FOT and FCT of a total of 1114 rice landraces.

c) After recording the FOT of each varietal population, we re-visited the same plot regularly to record the FOT and FCT of the last florets of the same panicle. The length of time between the FOT of the first floret and the FCT of the last florets in a panicle indicates the exposure duration (FED) of a variety's florets.

d) If the florets of the first emerged panicle opened and/or closed on a cloudy day, we also recorded both the FOT and FCT of other florets on another panicle of the same cultivar on a subsequent sunny day. This was not possible for every cultivar, so the number of observations of FOT and FCT on sunny and cloudy days was not equal.

e) The length of sunrise-to-anthesis duration (SAD) was estimated from the local sunrise time on each day of anthesis. The exact sunrise time at Bissamcuttack Block was obtained from https://www.timeanddate.com/sun/@10775335 and https://isubqo.com/prayer-time/india/odisha/bishama-katek.

The FOT and FED of all the cultivars were recorded, generating a total of 1660 data points (including data on flowering on sunny and cloudy days of the cropping seasons of 2020, 2021, and 2022). All these data are available on Harvard Dataverse [18], which is the first comprehensive database of the range of FOT, FED, and the length of time after sunrise until the anthesis of 1114 *indica* rice landraces.

2.4 Statistical analyses

All analyses were made on a desktop using Open Office Calc program on Linux-Max. The distribution of data was examined using Shapiro-Francia *W'* and Anderson-Darling *W* tests, which are more sensitive and powerful than other tests of normality [19,20]. When the normality assumption was not supported, we employed the Mann-Whitney *U* test to test the significance of the difference between means. We chose $p < 0.01$ for the level of significance as well as confidence intervals for all $df > 50$.

3. Results and discussion

We present here the first description of the range of FOT of 1114 *indica* rice landraces and the variability of flower opening behaviour of a portion of these landraces on both sunny and cloudy days from September 2020 to February 2022. For the convenience of usage, we shall henceforth describe the colder long day seasons of flowering as "winter" and hotter long day seasons as "summer", although some calendar months may not strictly correspond to these shorthand terms.

3.1 Frequency distribution of FOT during summer and winter

The *aman* type landraces are characterized by their flowering during the progressively shortening day length in colder months (September to January). In all three years (2020, 2021 and 2022), the peak of anthesis of these landraces occurred in early October.

The flowering of a majority of *boro* and *aus* landraces peaked in the middle of April (**Figure 1**). As the sunrise hour changes with the season, the length of time from a sunrise hour to FOT varies with the cultivation seasons. The sunrise to anthesis duration (SAD) for *aman* rices (of 2020, 2021 and 2022 combined) flowering in winter and that of the *boro* and *aus* landraces flowering in summer (of 2021 and 2022 combined) are shown in **Figure 2**. During summer, anthesis frequency reaches a peak between 290 min and 300 min after sunrise, whereas during winter months, the frequency is the highest between 260 min and 270 min after sunrise. Thus, SAD with > 270 min after sunrise are more frequent in landraces flowering in summer than in landraces flowering in winter. Our finding corroborates some earlier reports [9,13], but does not agree with some other studies [7,12] reporting FOT occurring earlier than 0800 h.

3.2 The relationships between FOT and FED

It appears that FED is inversely related to FOTd (FOT, expressed in a decimal hour) for both winters ($p < 0.05$) and summers ($p < 0.0001$) flowering (**Figure 3**). FOTd and SAD seem to strongly induce the shortening of FED on both cloudy and sunny days in both summer and winter (**Figure 4A**). The inverse relationship of FED with both SAD (**Figure 4A**) and with FOT (**Figure 3**) is warranted by the tight direct relationship of FOT and SAD during winter as well as summer, on both sunny and cloudy days (**Figure 3B**). This strong relationship between FOTd and SAD entails that longer SAD strictly corresponds to later FOT. As the FOT hour is always coterminous with the length of SAD, an association of FOTd with any other parameter is *ipso facto* coterminous with that of SAD.

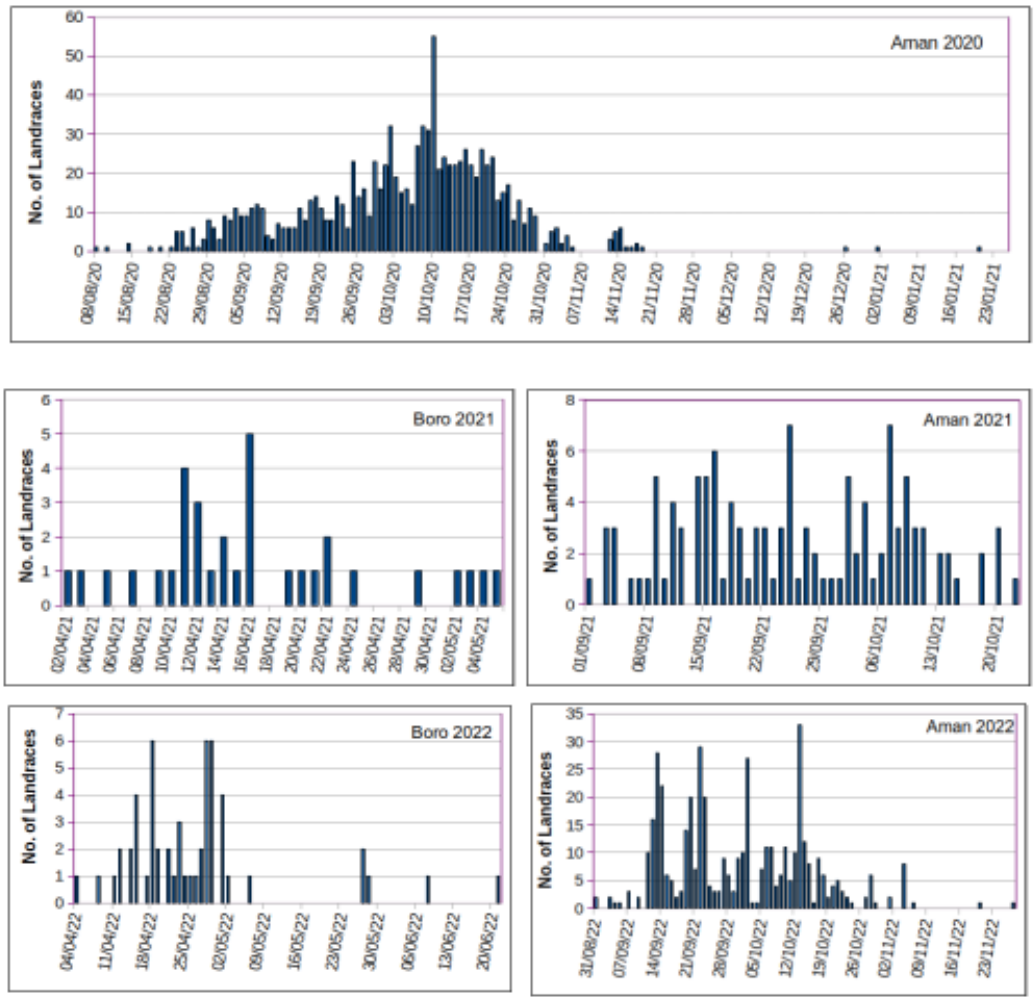

Figure 1. Frequency distribution of FOT of landraces flowering in *aman* and *boro* seasons from 2020 to 2022.

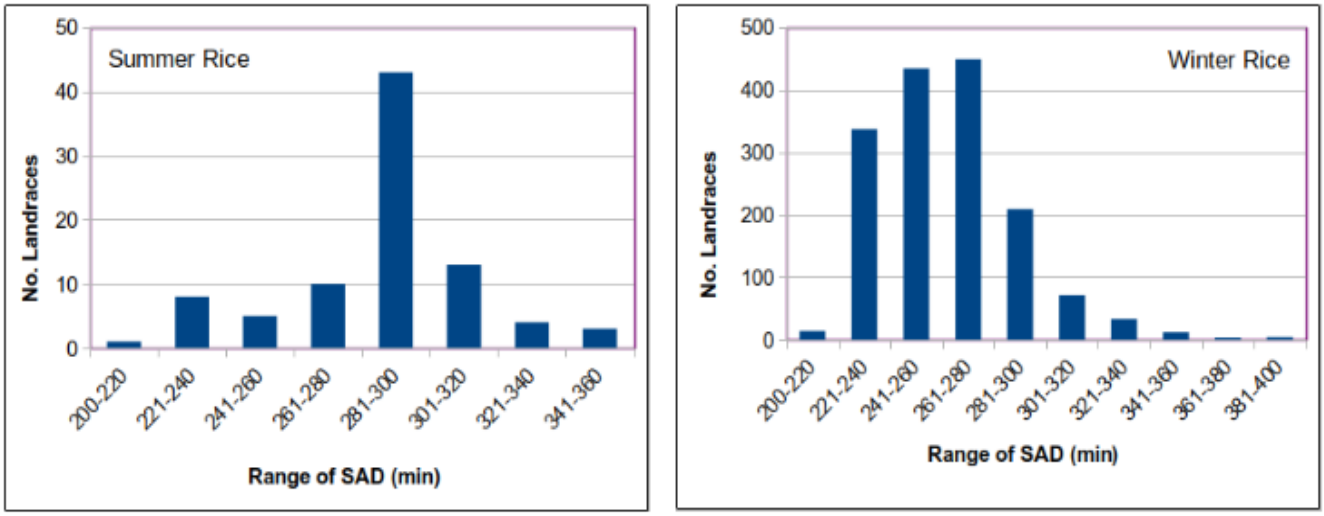

Figure 2. Frequency distribution of SAD of landraces flowering during winter and summer from 2020 to 2022 (combined).

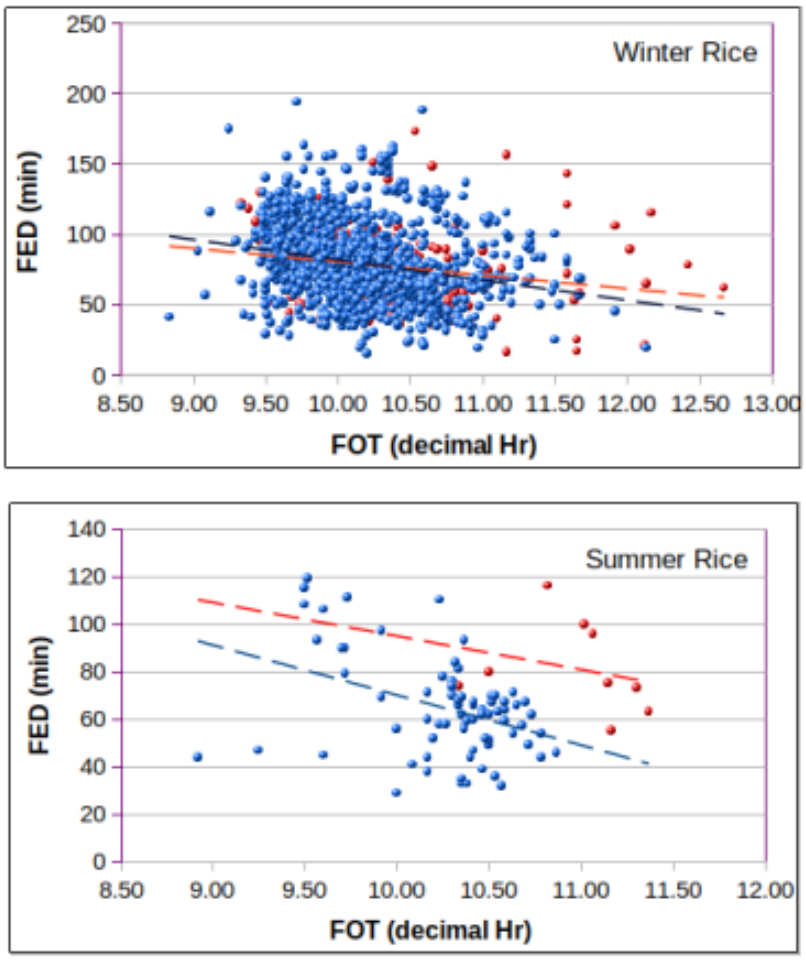

Figure 3. Regression of FED on FOT in decimal time (FOTd) for winter landraces (top panel) on sunny (blue) and cloudy days (red), with regression slope $b = -13.16$ ($R^2 = 0.051$) and -8.87 ($R^2 = 0.04$), respectively, and for summer landraces (bottom) on sunny (blue) and cloudy days (red), with regression slope $b = -21.02$ ($R^2 = 0.156$) and -14.09 ($R^2 = 0.067$), respectively.

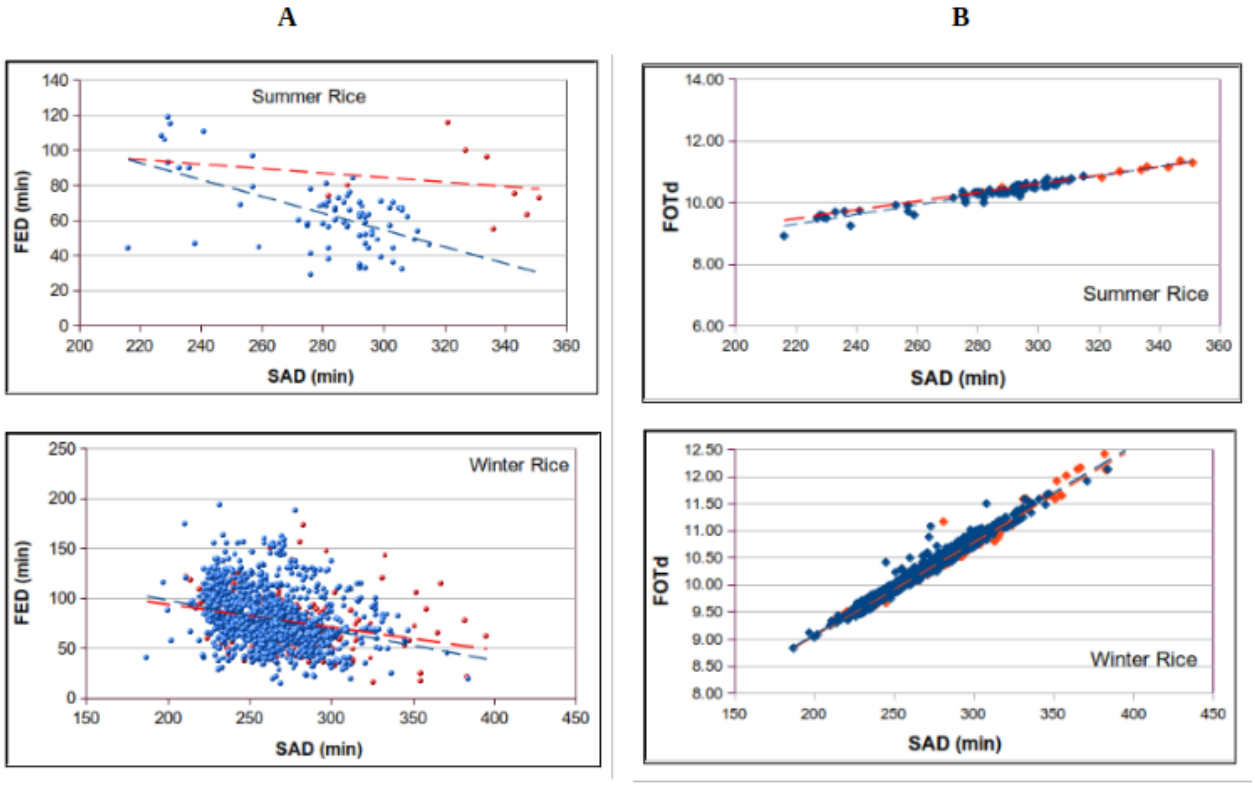

Figure 4. (A) Regression of (A) FED on SAD of summer rice landraces (top panel) on sunny (blue) and cloudy days (red), with regression slope $b = –0.48$ ($R^2 = 0.304$) and –0.127 ($R^2 = 0.027$), respectively, and of winter rice landraces (bottom panel) on sunny (blue) and cloudy days (red), with regression slope $b = –0.303$ ($R^2 = 0.086$) and –0.202 ($R^2 = 0.066$), respectively. (B) Regression of FOT (decimal hr) on SAD in summer (top) on sunny (blue) and cloudy days, with slope $b = 0.02$ ($R^2 = 0.904$) and 0.01 ($R^2 = 0.97$), respectively, and of winter rice landraces (bottom) on sunny (blue) and cloudy days (red), with slope $b = 0.02$ ($R^2 = 0.97$) and 0.02 ($R^2 = 0.97$), respectively.

3.3 The relationship of local sunrise time with FOT, FED and SAD

Several landraces opened their first florets on the same day and at about the same FOT. During colder months of *aman* season, the FOT is directly related to the sunrise time ($p < 0.00001$) on both sunny and cloudy days. In contrast, an earlier FOT and shorter SAD correspond to both early and late sunrise time on sunny days during summer. This is shown by a strong non-linear relationship during summer, best described by a second degree polynomial, on sunny days (**Figures 5A and 5B**), for which the adjusted R^2 was much greater than R^2 of linear regression. On cloudy summer days, the slope of regression for FOT was scarcely different from zero, while the SAD was strongly inversely related to sunrise hour during summer (that is, lengthens with receding sunrise hours). However, during short day colder seasons, SAD becomes directly related to sunrise hours, for both sunny and cloudy days (**Figure 5B**), repeating the pattern observed for the regression of FOT on sunrise hour (**Figure 5A**).

3.4 The influence of seasons on the FOT, FED and SAD of the same landraces

As the length of daylight hours changes with seasons, the FOT of a landrace is expected to change with seasonality. We compared the FOT of a total of 84 landraces, which were repeat-sown in both summer and winter over different years. The range of difference in time between FOT during summer and that between winter was 0 to 84 min, with a mean of 27.8 minutes (**Figure 6**). The difference between FOT during summer and winter was < 20 min in

55% of these landraces, while the difference was < 10 min for only 20 (= 24%) landraces.

A comparison of FOTd of the 84 landraces between *aman* and *boro* seasons from 2020 to 2022 (including the repeats mentioned in **Table 4**) reveals that the range of FOT is much wider during winter than during summer (**Figure 7A**), and that FOT tends to be delayed (**Figure 7B**), and correspondingly, SAD tends to lengthen (**Figure 8B**) when the sun rises progressively earlier in hotter months until Summer Solstice. Because the distributions of the FOTd, FED and SAD during both *Aman* and *Boro* seasons do not support the assumption of normality (**Table 5**), we conducted Mann-Whitney *U* test, instead of *t*-test for the difference between the means of FOTd during winter and summer. In general, rice florets tend to open later on hot summer days than during winter: The difference between means of the FOTd in two seasons (**Figure 7A**) was highly significant (Mann-Whitney $U = 1726.5$, $z = 5.71$, $p < 0.0001$), the difference being predominantly caused by delayed FOT during summer in over 70% of the same landraces (**Figure 7B**).

In 81% of the same landraces grown in both seasons, the mean SAD was significantly (Mann-Whitney $U = 1165.5$, $z = 7.49$, $p < 0.00001$) longer during summer than during winter (**Figure 8B**). Conversely, the FED was significantly (Mann-Whitney $U = 2267.5$, $z = 3.997$, $p < 0.0001$) longer during winter than during summer in 70% of these same landraces (**Figure 8A**). This mutually contrary seasonal effect on FED and SAD is consonant with the strong inverse relationship between FED and SAD (**Figure 4**).

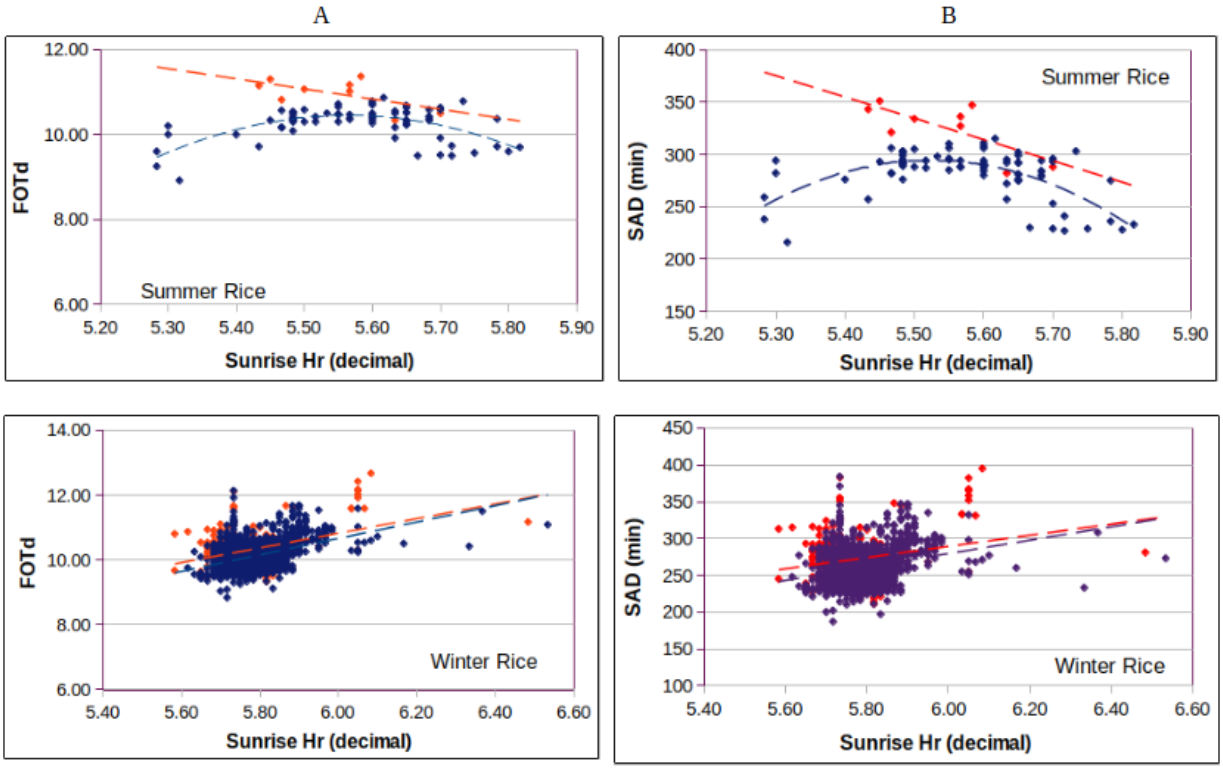

Figure 5. (A) Relationship of FOT (decimal hr) with local sunrise time in summer (top panel) on sunny days (blue), with second degree polynomial (*adjusted* $R^2 = 0.40$), and on cloudy days (red), with linear slope $b = -2.38$ ($R^2 = 0.36$), respectively; and of winter landraces (bottom) on sunny (blue) and cloudy days (red), with regression slope $b = 2.53$ ($R^2 = 0.18$) and $b = 2.26$ ($R^2 = 0.14$), respectively. (B) Relationship of SAD with sunrise time (decimal hr) in summer (top panel) on sunny days (blue) with second degree polynomial slope (*adjusted* $R^2 = 0.41$) and on cloudy days (red), with linear regression slope $b = -203.1$ ($R^2 = 0.53$), respectively; and in winter (bottom) on sunny (Blue) and cloudy days (red), with regression slope $b = 91.62$ ($R^2 = 0.07$) and $b = 75.84$ ($R^2 = 0.05$), respectively.

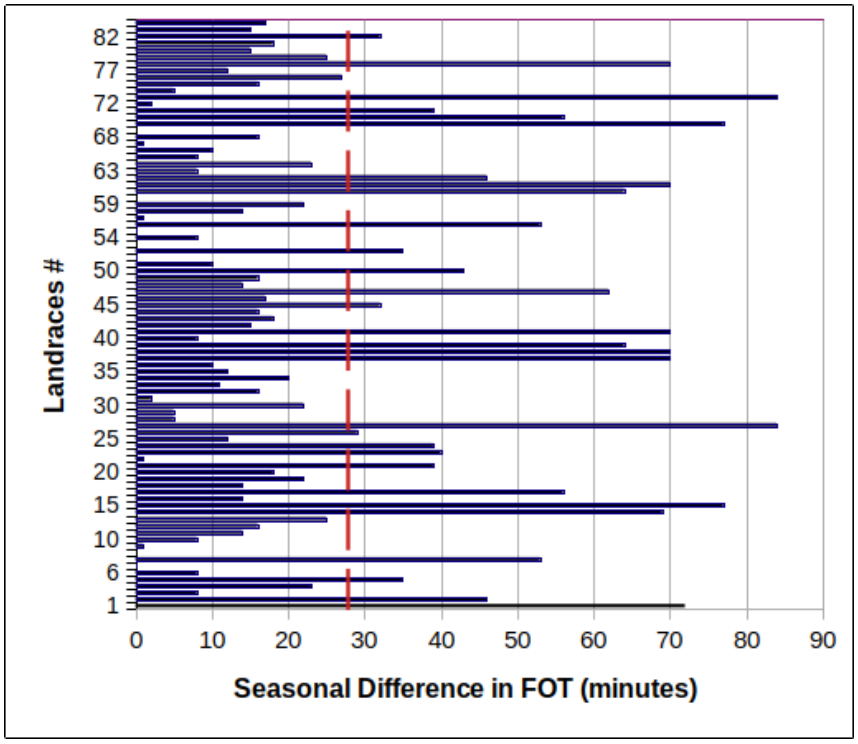

Figure 6. The difference of FOTs (in minutes) of 84 landraces between *Boro* and *Aman* seasons in different years. The red broken line is the mean difference.

Table 5. Test of normality of distribution of FOTd, FED and SAD of 84 landraces grown during two seasons.

	Shapiro-Francia W'	***p***	**Anderson-Darling W**	***p***
FOTd *Aman*	0.0394	0	1.0063	0.0112
FOTd *Boro*	0.0194	0	0.6485	0.0876
FED *Aman*	0.0099	0	0.9294	0.0175
FED *Boro*	0.0030	0	2.2225	0.00001
SAD *Aman*	0.0307	0	0.9407	0.01642
SAD *Boro*	0.0026	0	0.9167	0.0188

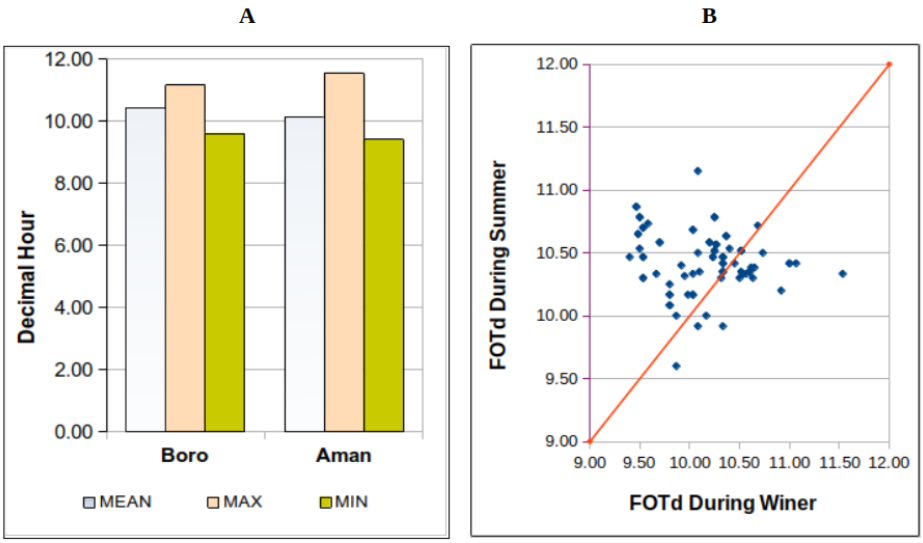

Figure 7. (A) The range and mean of FOTd of 84 landraces flowering during boro and aman seasons. (B) A comparison of FOTd of the same landraces flowering during winter and summer from 2020 to 2022; the red line is the isocline.

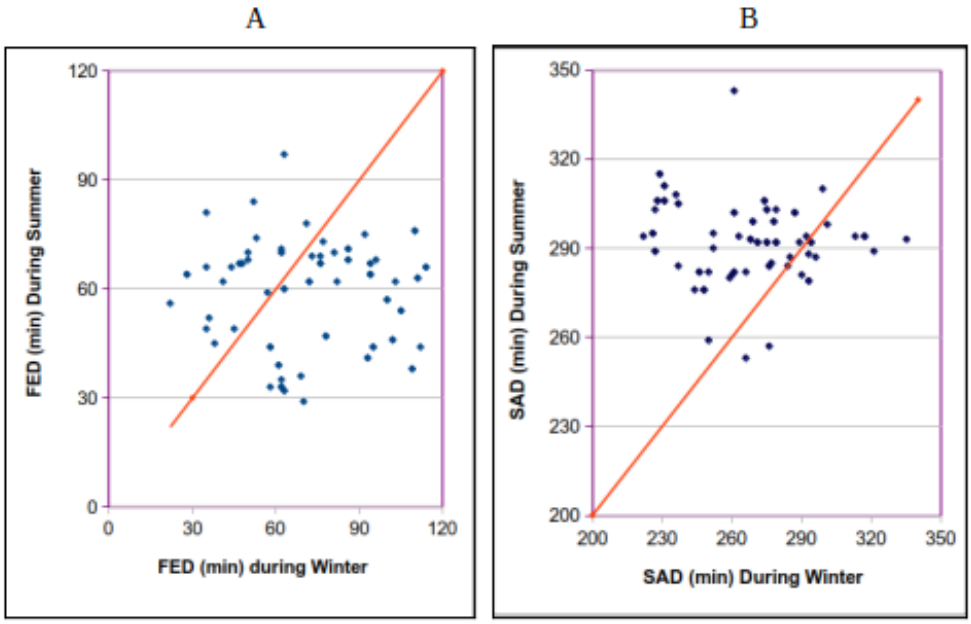

Figure 8. A comparison of (A) FED and of (B) SAD of 84 landraces flowering during winter and summer from 2020 to 2022. The red line in each panel is the isocline. Two-tailed t = 4.97 for FED and 8.005 for SAD.

4. Conclusions

Our observations of SAD and FED during summer and winter may be summarized as follows:

(a) None of the landraces examined here opens their florets earlier than 0850 h; the FOT delays on cloudy/rainy days.

(b) The SAD of *O. sativa* ssp. *indica* landraces tend to lengthen when the sun rises earlier during summer.

(c) The flowers that open late in the morning on sunny days tend to close quicker.

(d) The FED tends to shorten with longer SAD, both during summer and winter; this shortening is more prominent during summer than during winter, presumably to protect the pollen from higher midday temperatures.

(e) As the sun rises later in the morning during winter, the florets tend to open progressively earlier, and remain open longer during winter likely in wait for a longer exposure to sunlight.

As conventional farmers, as well as breeders, often may grow several cultivars on neighbouring plots on the presumption of very low cross pollination chances, a wide window of FED and a wide range of overlap between FOT and FED of the neighbouring cultivars may result in a high frequency of cross pollination. This is of crucial importance for the genetic purity of landraces with special morphological and agronomic traits. As long as the neighbouring pairs have a considerable overlap of FOT and FED, high cross pollination frequencies are likely to be more prevalent in cultivated rice than so far reported in the literature (Moldenhauer and Gibbons 2003; OGTR 2005). In contrast, a wide (> 2 hours) temporal gap between the FOTs of the neighbouring cultivars may obviate cross pollination. It would thus be necessary to take note of the extent of FOD and FED overlaps between neighbouring cultivars on the farm during different growing seasons, in order to preclude the chances of cross pollination and maintain germline purity of each of the neighbouring landraces, as well as to ensure cross pollination success in hybridization experiments.

Author Contributions

DD conceived, designed, and supervised the study, analysed the data, and prepared the mss. DB, MN and RG recorded all the data pertaining to anthesis behavior of 1114 landraces *in situ*. NVJ supervised all statistical analyses and edited the mss.

Conflict of Interest

Authors declare no competing interests.

Data Availability Statement

The primary data of FOT and FED of all rice landraces, as well as air temperature and sunrise data are freely available on Harvard Dataverse (Deb 2022). All other data will be freely available on request.

Funding

This work received neither funding nor technical support from any institution.

Acknowledgement

We are grateful to Aniket Aga, Shaliesh Awate, Chitrangada Chowdhury, Shikha Kansagara, Raghuveer Nandam, Sahith Ravindra, and Karan Sarin for devoting their time and labour of love for weeks to the recording of flowering data.

References

[1] Deb, D., Bhattacharya, D., 2021. Unusually high frequency of cross-pollination between rice landraces Shiuli and Kharah with coincident flower-opening times. Current Science. 121(1), 121-126.
DOI: https://doi.org/10.18520/cs/v121/i1/121-126

[2] Beachell, H.M., Jodon, C.R., Adair, N.E., et al., 1938. Extent of natural crossing in rice. Journal of the American Society of Agronomy. 30, 743-653.

[3] Somaratne, L.H.M.Y.K., Abayawickrama, A.S.M.T., Wickramasinghe, I.P., et al., 2012. Estimating out-crossing rate of Bg 379-2 using morphological markers and confirmation by molecular markers. Rice Science. 19(2), 166-168.
DOI: https://doi.org/10.1016/S1672-6308(12)60036-5

[4] van der Stok, J.E., 1910. Onderzorkingen omtrent rijst en tweede gewassen (Dutch) [Experiments with rice and secondary crops]. G. Kolff. Co.: Batavia.

[5] Pope, M.N., 1916. The mode of pollination in some farm crops. Journal of the American Society of Agronomy. 8(4), 209-227.

[6] Hirabayashi, H., Sasaki, K., Kambe, T., et al., 2015. *qEMF3*, a novel QTL for the early-morning flowering trait from wild rice, *Oryza officinalis*, to mitigate heat stress damage at flowering in rice, *O. sativa*. Journal of Experimental Botany. 66(5), 1227-1236.
DOI: https://doi.org/10.1093/jxb/eru474

[7] Sharngapani, S.G., 1928. A few observations of paddy (*Oryza sativa*) crossing. Agriculture Journal of India. 19, 48-50.

[8] Bheemanahalli, R., Sahishraj, R.T., Manoharan, M., et al., 2017. Is early morning flowering an effective trait to minimize heat stress damage during flowering in rice? Field Crops Research. 203, 238-242.
DOI: http://doi.org/10.1016/j.fcr.2016.11.011

[9] Kobayasi, K, Masui, H., Atsuta, Y., et al. (editors), 2009. Flower opening time in rice—cultivar difference and effect of weather factors. Proceedings of the MARCO Symposium; 2009 Oct 5-7; Tsukuba, Japan. Available from: https://www.naro.affrc.go.jp/archive/niaes/marco/marco2009/english/program/W2-12_Kobayasi_Kazuhiro_P.pdf

[10] Vergara, B.S., Chang, T.T., 1985. The flowering response of the rice plant to photoperiod, 4th ed. International Rice Research Institute: Los Baños, Philippines. pp. 16.

[11] Jones, J.W., 1924. Observations on the time of blooming of rice flowers. Journal of the American Society of Agronomy. 16 (10), 665-670.

[12] Thompstone, E., 1915. Some observations on Upper Burma paddy (grown under irrigation). The Agricultural Journal of India. 10, 26-53.

[13] Torres, J.P., 1923. Some notes on rice hybridization work. Philippine Agricultural Review. 16, 46-48.

[14] Chang, T.T., Bardenas, E.A., 1965. The Morphology and Varietal Characteristics of the Rice Plant [Internet]. International Rice Research In-

stitute: Los Baños, Philippines. Available from: http://books.irri.org/9711040085_content.pdf

[15] Bioversity International, International Rice Research Institute (IRRI), The Africa Rice Center (WARDA), 2007. Descriptors for wild and cultivated rice *(Oryza spp.*). Bioversity International: Rome. pp. 63.

[16] Moldenhauer, K.A.K., Gibbons, J.H., 2003. Rice morphology and development. Rice: Origin, history, technology and production. Wiley: Hoboken, NJ. pp. 103-127.

[17] OGTR, 2005. The Biology and Ecology of Rice (*Oryza sativa* L.) in Australia [Internet]. Office of the Gene Technology Regulator: Woden, Australia. Available from: https://www.ogtr.gov.au/sites/default/files/files/2021-07/the_biology_of_rice.pdf

[18] Deb, D., 2022. Rice Flower Opening Time and Flower Opening Duration Data [Internet]. DOI: https://doi.org/10.7910/DVN/KYW1UC

[19] Mbah, A.K., Paothong, A., 2014. Shapiro-Francia test compared to other normality test using expected p-value. Journal of Statistical Computation & Simulation. 85(15), 3002-3016. DOI: https://doi.org/10.1080/00949655.2014.947986

[20] Georgiev, G.Z., 2023. Normality Calculator [Internet]. Available from: https://www.gigacalculator.com/calculators/normality-test-calculator.php

BILINGUAL PUBLISHING GROUP

Journal of Botanical Research

https://journals.bilpubgroup.com/index.php/jbr

ARTICLE

Effects of Electroplating Effluents on Growth, Heavy Metals Accumulation and Concentrations in *Amaranthus viridis* Lin.

Oluwole Surukite O., Ogun Mautin L.**[*], Ewekeye Tolulope S., Tope-Akinyetun Racheal O., Asokere Simeon Y., Usamot Q.

Department of Botany, Lagos State University, Ojo, Lagos, 102101, Nigeria

ABSTRACT

Pollution in recent times has become prevalent due to industrial expansion, hence, releasing pollutants into the environment. Thus, this study aimed at investigating the effects of effluents from electroplating companies on growth, heavy metals accumulation and concentrations in *Amaranthus viridis*. Seeds of *A. viridis* were obtained from the National Institute of Horticulture, Ibadan. Loam soils were collected from Lagos State University and two samples of electroplating effluents were obtained from Oregun, Lagos. Seeds were sown, nursed, and transplanted in a uniform bucket filled with 5 kg loam soil and transplanted seedlings were treated with Effluent A (5 and 10% conc.) and Effluent B (5 and 10% conc.) and control respectively. Growth parameters such as plant height and so on were measured and plant samples harvested were analyzed for heavy metal concentrations using Atomic Absorption Spectrophotometer. Data collected were subjected to a one-way analysis of variance. Results revealed that Effluents A and B are highly acidic and above discharge limits. Also, the result revealed that 5% conc. of Effluents A and B had more effects on growth ($p < 0.05$) of *A. viridis* across the harvests than 10% conc. in relation to control. This result showed that the effluent samples affect the growth rhythms of plants. Results further revealed vigorous accumulation of the heavy metals: Zn (241.66 µg kg^{-1} ± 0.10 at third harvest in Effluent A: 10%), Cu (68.25 µg kg^{-1} ± 0.23 at first harvest in Effluent B: 5%), Cr (500 µg kg^{-1} ± 0.90 in harvests at all concentrations.) and Ni (500 µg kg^{-1} ± 0.90 at third harvest in Effluent B: 5%) and all these metals are far above the control and permissible limits of WHO/FAO recommendations. From this study, it could be concluded that electroplating effluents had adverse effects on growth and increased metals' bioaccumulation in *A. viridis*. Therefore, the treatment of effluents to enhance an eco-friendly environment should be done.

Keywords: Electroplating; Effluent; Pollution; Heavy metals; Discharge; Vegetable; *Amaranthus viridis*

*CORRESPONDING AUTHOR:

Ogun Mautin L., Department of Botany, Lagos State University, Ojo, Lagos, 102101, Nigeria; Email: mautinogun@lasu.edu.ng; mautinogun@gmail.com

ARTICLE INFO

Received: 18 May 2023 | Revised: 5 July 2023 | Accepted: 7 July 2023 | Published Online: 18 July 2023

DOI: https://doi.org/10.30564/jbr.v5i3.5730

CITATION

Oluwole, S.O., Ogun, M.L., Ewekeye, T.S., et al., 2023. Effects of Electroplating Effluents on Growth, Heavy Metals' Accumulation and Concentrations in *Amaranthus viridis* Lin. Journal of Botanical Research. 5(3): 49-59. DOI: https://doi.org/10.30564/jbr.v5i3.5730

1. Introduction

Industrial pollution has become prevalent, especially in developing nations like Nigeria. However, in recent times, concerns about the environment are widely being expressed by environmentalists and health organizations. Effluents from industries are among the major wastes causing environmental pollution [1,2].

Industries in particular make prodigious use of water as an ingredient with other raw materials to create finished products. It is also used as a transporting medium, a cleansing agent, a coolant and a source of steam for heating and power generation. The main problem, however, is that water that goes out of these industries is discharged into the waterways in a relatively polluted condition depending on its use and treatment, if at all it receives any before discharge [3-5].

The discharge of industrial, agricultural, and domestic wastes or effluents have led to the degradation of water bodies due to high concentration of heavy metals and other pollutants. Whatmuff [6] and McBride [7] reported that increased concentrations of heavy metals in soil often lead to increased crop uptake of these heavy metals. Nriagu [8] observed that we may be experiencing what he termed a silent epidemic of environmental and metal poisoning from ever-increasing amounts of metals dumped or washed into the biosphere and hydrosphere. Sources of heavy metal deposition include metalliferous mining, electroplating, galvanizing and agricultural materials such as fertilizers, pesticides, fungicides, sewage sludge, compost manure, corrosion of metal objects and domestic wastes [9,10].

The main environmental agency in Nigeria-Federal Environmental Protection Agency (FEPA) and other world-recognized agencies have drawn attention to the effluents being discharged into the wetlands and farmland near the industries and possible attendant problems on crops and vegetables being produced by small-scale farmers [11-14].

Amaranthus viridis L. is a green vegetable belonging to the family Amaranthaceae. It occurs mainly in tropical and sub-tropical countries as a semi-wild protected plant that is grown when land is cleared or weeded [15]. It is a robust annual herb with erect stem. The seeds are small and dark brown to black with shining testa. It is a popular plant known for its nutritive value containing various essential amino-acids, and little amount of crude fibre or carbohydrate [16,17].

In view of the above, the study investigates the effects of effluents from an electroplating company on *Amaranthus viridis*, a popular nutritious vegetable in West Africa. This study, thus, reports the effects of two effluent samples on the growth, accumulation, and concentration levels of heavy metals such as zinc, nickel, chromium, and copper in the plant parts (leaf, stem and root) of *Amaranthus viridis*.

2. Materials and methods

2.1 Collection of materials

Amaranthus viridis seeds were obtained from the National Institute of Horticulture (NIHORT), Ibadan, Oyo State, Nigeria. The loam soil was collected from the Botanical Garden of the Lagos State University, Ojo in Nigeria. Two different samples of electroplating effluents tagged: Sample A and B were obtained from Grizzi Nigeria Limited situated at Plot 2, Adewumi Estate, Kudirat Abiola Road, Oregun in Ikeja, Lagos State (**Figure 1**), Nigeria, manufacturer of wooden and metal electroplating or coating substances. Effluents were collected in clean containers and transported to laboratory for analysis and usage.

2.2 Soil preparation and nursery

Matured seeds of *Amaranthus viridis* were sundried and sown in seed trays (30 cm in width and 10 cm in depth) filled with loam soil and watered moderately. The seeds emerged after the third day. After 14 days of emergence, the seedlings were ready for transplant.

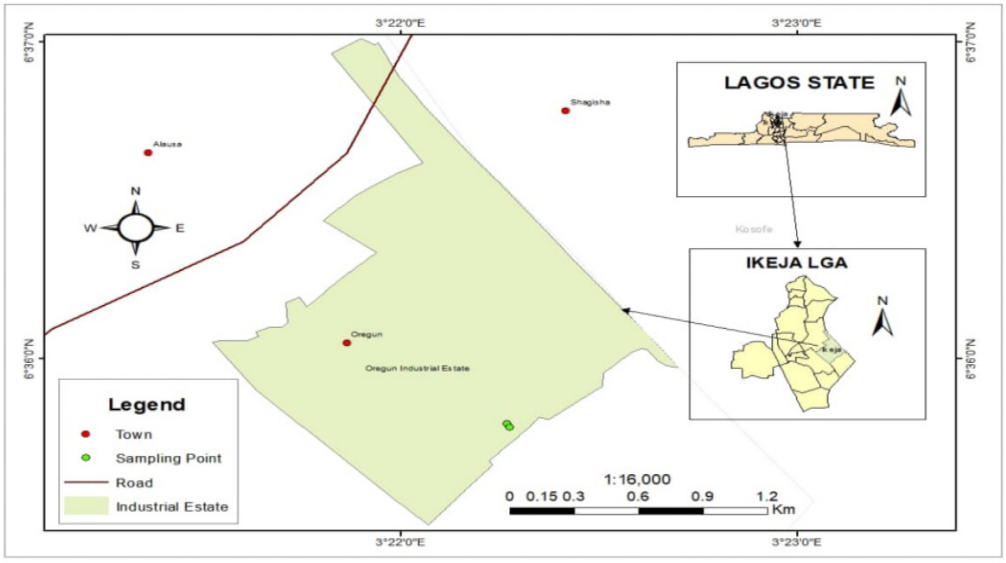

Figure 1. Map of Ikeja LGA, Lagos State showing sampling point.

2.3 Seedling transplant and growth experimental design

One hundred (100) equally perforated plastic buckets were used. Each bucket was filled with 5 kg of loam soil respectively and uniform seedlings of *Amaranthus viridis* were transplanted respectively. The seedlings were watered twice daily. After two weeks of establishment, the established seedlings were divided into five groups, namely Control, Sample A_1 Plants, Sample A_2 Plants, Sample B_1 Plants and Sample B_2 Plants respectively. Control was watered with distilled water, Sample A_1 Plants were watered with a 5% concentration of Effluent A mixed with 95% distilled water, Sample A_2 Plants were watered with a 10% concentration of Effluent A mixed with 90% distilled water, Sample B_1 Plants were watered with 5% concentration of Effluent B mixed with 95% distilled water while Sample B_2 Plants were watered with 10% concentration of Effluent B mixed 90% distilled water.

2.4 Analysis of effluent samples

Sample A contained a chromium-plating effluent which was golden yellow while Sample B contained a nickel-plating effluent which had a greenish blue colour collected separately and differently as these two metals are the major electroplates used. The samples were collected in sterilized containers and filtered out of the debris. The analysis of the effluents was carried out using standard methods for the examination of water and wastewater as reported by Rice and Bridgewater [18]. Thus, the physico-chemical analysis carried out includes pH, turbidity, acidity, total dissolved solids, suspended solids, and heavy metal content.

pH: The pH of the samples was determined using a standardized buffer solution and a pH meter model 22409 (United Kingdom).

Turbidity: The turbidities of these effluents were measured by H193703 portable microprocessor turbidity meter and readings were taken in the Formzin Turbidity unit (TU).

Acidity: This was determined using 0.02M NaOH and 0.02M KHP prepared with distilled water. The 0.02M NaOH was standardized against 0.02M KHP. The standardized NaOH was then titrated with 2 mL of each of the effluents using phenolphale as an indicator. The acidity was calculated using the formula:

$$\text{Acidity} = \frac{\text{Molarity of Base-Titre value} \times 500}{\text{Volume of effluent used}}$$

Total solids: This was determined by mixing the samples thoroughly and heating 20 mL of each of the samples to complete dryness in Petri dishes in ovens at 105 °C. The solids were calculated using the for-

mula:

$$\text{Total solids (mg/L)} = \frac{(A - B) \times 1000}{\text{Volume of the Sample}}$$

where: A is the weight of dried residue + Petri-dish; B is the weight of empty Petri-dish.

Total Dissolved Solids (TDS): This was determined using 20 mL of filtered samples and heating to complete dryness. Total dissolved solids were calculated using the formula:

$$\text{TDS} = \frac{(A - B) \times 1000}{\text{Volume of the Sample}}$$

where A represents the weight of dried residue + Petri-dish while B represents the weight of an empty petri-dish.

2.5 Harvesting and data collection

Leaves from each group [Sample A_1, Sample A_2, Sample B_1 and Sample B_2] in three replicates were harvested every two weeks for six weeks. These plants were harvested using the traditional destructive method outlined by Oluwole et al. [19]. The plants were carefully uprooted, and the root parts were rinsed with clean water. The weights of the plants were determined before separating into parts namely leaves, stems, and roots. Fresh weights of the parts were determined, thereafter the plant parts were oven dried at 80 °C for 48 hours, cooled and their dry weights were determined using electric balance. Growth analysis was carried out using a completely randomized design. Data collected were used to determine the following growth parameters—mean total dry weight (TDW), leaf weight ratio (LWR), stem weight ratio (SWR), root weight ratio (RWR) and shoot-root ratio (S: R). The plant part dry weight is calculated as a percentage of total dry weight.

2.6 Digestion of plant samples and heavy metal analysis

One gram (1 g) of dried finely grounded plant sample was weighed into Kjedahl flask and 20 mL of nitric acid was then added to it. The Kjedahl flask was placed on a hot plate for approximately 2 hours. The hot plate was then placed in the fume cupboard to avoid choking from the fumes released from the nitric acid. After the 2 hours, the digested sample was poured out into a 25 mL flask, distilled water was then added to make up to the 25 mL mark, cooled for some minutes and the digested samples of each plant part were filtered into clean plastic (60 mL) bottles and then taken for chemical analysis using Atomic Absorption Spectrophotometer (AAS) model 1233 (England).

2.7 Statistical analysis

The data obtained from the study for various plant parameters were subjected to single univariate summary statistics such as the mean and standard deviation. The analysis of variance (ANOVA) was then used to compare the variability in the selected parameters with the aid of the software SPSS 2007 version 20. Significant means were separated by the Least Significance Difference test (LSD) at the 95% probability level using Duncan Multiple Range Test.

3. Results and discussion

3.1 Physicochemical analysis of electroplating effluent samples

Table 1 shows the result of the chemical analysis of the two Effluents A and B collected. The result showed that samples A and B have high heavy metal content far above the effluent discharge limits by Federal Environmental Protection Agency [14]. However, apart from the heavy metal concentrations, the effluent samples were highly acidic (**Table 1**). The heavy metals present in sample A are nickel, chromium, zinc and copper with concentrations of 65.43 $\mu g\ L^{-1}$, 388.20 $\mu g\ L^{-1}$, 12.32 $\mu g\ L^{-1}$ and 50.17 $\mu g\ L^{-1}$ respectively with Sample B having the same metals as in Effluent A (**Table 1**) but in varying concentrations. The concentration of chromium (388.20 $\mu g\ L^{-1}$) was about six times greater than the concentration of nickel and copper, and about twenty-five times greater than the concentration of zinc. This is in no doubt responsible for the deep-golden yellow colour of this sample. Effluent B also had the highest concentration of nickel, about six times greater than the concentra-

tion of chromium and copper and about sixty times greater than the concentration of zinc. The high concentration of nickel in Effluent B is also responsible for the greenish blue colour of this sample. This was supported by Yasser et al. [2] and Monica et al. [5], when they reported that wastewater irrigation, solid waste disposal, sludge applications, vehicular exhaust and industrial activities are the major sources of soil contamination with heavy metals.

3.2 Effects of electroplating effluents on the growth of *Amaranthus viridis*

Effects of two electroplating effluents of Samples A and B collected on the growth of *A. viridis* is shown in **Table 2**. The results showed that control, Effluent A (5 and 10% conc.) and Effluent B (5% conc.) had ascending increases in mean plant fresh and dry weights of *A. viridis,* while Effluent B (10% conc.) showed descending increase in mean plant fresh and dry weights (**Table 2**). The mean plant heights of seedlings subjected to treatments showed ascending increase in plant heights, the seedlings in control had the best plant heights while those subjected to both Effluent A (5 and 10%) and Effluent B (5 and 10%) had similar poor heights. However, fresh, and dry weights and plant heights in Control ($p < 0.05$) were significantly higher than others (**Table 2**). This result showed that the height of the seedlings of *A. viridis* watered with effluent samples was hindered (**Table 2**). The leaf weight ratios of seedlings of *A. viridis* in Control, Effluent A (5% conc.) and Effluent B (10% conc.) showed ascending increase, while Effluent A (10% conc.) and Effluent B (5% conc.) revealed descending increase in mean leaf weight ratios (**Table 2**). More so, the stem weight ratios, root weight ratios and shoot-root ratios showed that seedlings in control and Effluent A (5% conc.) had a positive increase, while those in Effluent A (10% conc.) and Effluent B (5 and 10% conc.) showed a significant decrease (**Table 2**). However, leaf weight ratios and stem weight ratios at the third harvest in Control and Effluent A (10% conc.) at the first harvest were significantly higher ($p < 0.05$) than others. It was observed that the leaves of seedlings of *A. viridis* treated with Effluent A had some yellow patches on them, which were later glaring on the seedlings subjected to Effluent A (10% conc.). However, this result was supported by the work of Bahemuka and Mubofu [20] and Ikeda et al. [21] when they reported that intake of toxic metals at a chronic level through soil had adverse impacts on plants and the associated harmful effects become apparent after days of exposure. Oluwole et al. [22] also reported that bioaccumulation of several factors is responsible for the effective and efficient growth of plants. Some of the factors itemized include soil water, soil mineralization, organic and inorganic components such as metallic concentrations within the soil. Oluwole et al. [19,23] further reported that variation in the growth parameters of seedlings under different treatments is a function of both biotic and abiotic factors.

3.3 Effects of electroplating effluents on heavy metal concentrations in *Amaranthus viridis*

Effects of electroplating effluents on heavy metal concentrations in *Amaranthus viridis* is shown in **Table 3**. The results revealed that the chromium (Cr) metal was significantly ($p < 0.05$) accumulated by the vegetable from the first to the third harvests. Also, Cr concentrations were above the standard permissible limits of WHO/FAO for chromium which is 2.3 $\mu g\ kg^{-1}$ (**Table 3**). Thus, the consumption of such vegetables with high concentrations of Cr is toxic. This result was against the findings of Tasrina et al. [24] which reported lower concentrations of Cr in some vegetables contaminated with heavy metals. However, Romic and Romic [3] reported that toxicity of Cr in the body causes skin ulceration, damage to the liver, kidney, and nerve tissues. They further reported that Cr contamination is usually from the wearing down of asbestos lining, tobacco smoke and so on. Also, from the results, nickel (Ni) was not detected at all during the first harvest until the second harvest in the roots of *A. viridis* watered with Effluent A (5%

conc.) while significantly ($p < 0.05$) higher concentrations were also found in those treated with Effluent B (5 and 10% conc.) by third harvest (**Table 3**). The concentration of Ni estimated in the vegetable was above the WHO/FAO permissible limits, which invariably poses a danger to the consumers. This study was supported by Ibrahim [25], which reported the accumulation of nickel in some plants; he said nickel is disastrous to both animal and human health. He also reported that automobile exhausts are the major source of atmospheric nickel.

The results further showed that the concentrations of both zinc and copper taken by *A. viridis* treated with Effluent samples A and B. The results revealed that concentrations of Cu and Zn increased arithmetically throughout the three harvests (**Table 3**). These concentrations are more than permissible limits recommended by WHO/FAO (**Table 3**). Similar findings to the current study were also reported by Landsberger and Iskander [26] and Oluwole et al. [27] where higher and lower concentrations of zinc in vegetables cultivated along the roadsides were reported respectively. However, zinc has been reported to be an essential element in the human diet as it helps in maintaining the functioning of the immune system but its excess or toxicity could be detrimental to human health [28]. While copper toxicity has been reported to cause anaemia, changes in ossification and Wilson's disease. However, copper has been described as an important element for plants and animals [29].

More so, it could be observed from the results (**Table 3**) that there were metallic uptakes and accumulations by the plant compared to the control and excessive accumulation of these metals in the plant is evident in its growth from the first harvest to the third harvest in the study. This is an indication that effluents should be properly treated before being disposed of into the environment (land or water).

Table 1. Physicochemical analysis of electroplating effluent samples.

Parameters	**Effluents**		**Discharge limit [14]**
	A	B	
pH	4.14	4.87	6.00-9.00
Acidity (as µg L^{-1} $CaCO_3$)	25000	52000	
Alkalinity (as µg L^{-1} $CaCO_3$)	*	*	45
Turbidity NTU	0.86	4.0	
Total Dissolved Solid (mg/w)	17.82	71.67	2000
Total Solid (mg/w)	24.24	100.75	2300
Nickel (µg L^{-1})	65.43	75.70	1.00
Chromium (µg L^{-1})	388.20	10.53	1.00
Zinc (µg L^{-1})	12.32	1.40	1.00
Copper (µg L^{-1})	50.17	11.03	1.00

(*) means Not Found.

Table 2. Effects of electroplating effluent on the growth of *Amaranthus viridis*.

Treatment/Growth parameter	PFW (g)	PDW (g)	pH (cm)	LWR (% total dry weight)	SWR (% total dry weight)	RWR (% total dry weight)	SRR
Control Mean ± S.D 1st Harvest 2nd Harvest 3rd Harvest	9.01 ± 0.05^{a} 11.77 ± 1.80^{b} 14.65 ± 0.22^{d}	1.08 ± 0.10^{a} 2.00 ± 0.40^{bc} 2.46 ± 0.12^{d}	19.50 ± 0.90^{a} 25.40 ± 0.40^{bc} 30.90 ± 1.10^{d}	30.73 ± 1.04^{a} 45.66 ± 0.29^{c} 51.81 ± 0.11^{d}	32.78 ± 0.10^{a} 35.79 ± 0.30^{ab} 48.33 ± 0.81^{d}	15.41 ± 0.17^{a} 18.54 ± 0.05^{a} 20.94 ± 0.30^{ab}	3.78 ± 0.70^{cd} 4.40 ± 0.20^{d} 5.40 ± 0.18^{d}
Effluent A (5% Conc.) Mean ± S.D 1st Harvest 2nd Harvest 3rd Harvest	9.93 ± 0.50a 12.03 ± 1.00^{b} 12.06 ± 0.80^{b}	1.09 ± 0.03^{a} 1.58 ± 0.03^{b} 1.69 ± 0.08^{bc}	18.30 ± 0.10^{a} 21.15 ± 0.70^{ab} 22.50 ± 1.00^{b}	26.47 ± 0.01^{a} 34.60 ± 0.08^{ab} 39.07 ± 0.20^{b}	25.69 ± 0.02^{a} 31.27 ± 0.08^{ab} 33.79 ± 0.16^{b}	31.61 ± 0.12^{b} 35.24 ± 0.02^{c} 42.26 ± 0.15^{d}	1.37 ± 0.08^{a} 1.84 ± 0.01^{ab} 2.16 ± 0.10^{b}
Effluent A (10% Conc.) Mean ± S.D 1st Harvest 2nd Harvest 3rd Harvest	7.47 ± 1.80^{a} 8.68 ± 0.30^{a} 10. 67 ± 0.60^{b}	1.38 ± 0.05^{a} 1.31 ± 0.10^{a} 1.06 ± 0.20^{a}	18.95 ± 0.10^{a} 20.76 ± 0.40^{ab} 23.30 ± 0.80^{bc}	36.71 ± 0.13^{a} 35.23 ± 0.03^{ab} 28.36 ± 0.05^{a}	48.07 ± 0.24^{d} 35.58 ± 0.05^{b} 30.56 ± 0.02^{a}	36.04 ± 0.10^{c} 32.72 ± 0.14^{bc} 16.70 ± 0.01^{a}	3.98 ± 0.70^{cd} 2.06 ± 0.07^{b} 1.77 ± 0.30^{ab}
Effluent B (5% Conc.) Mean ± S.D 1st Harvest 2nd Harvest 3rd Harvest	9.41 ± 0.23^{a} 11.53 ± 0.16^{b} 12. 66 ± 1.30^{c}	1.23 ± 0.10^{a} 1.73 ± 0.03^{b} 1.75 ± 0.10^{b}	18.65 ± 0.50^{a} 21.25 ± 0.45^{ab} 24.40 ± 0.20^{bc}	47.28 ± 0.05^{b} 42.62 ± 0.23^{c} 35.38 ± 0.08^{a}	40.10 ± 0.09^{bc} 35.99 ± 0.10^{ab} 31.60 ± 0. 02^{a}	33.01 ± 0.02^{b} 18.38 ± 0.05^{a} 12.62 ± 0.11^{a}	3.92 ± 0.66^{cd} 3.40 ± 0.20^{b} 2.03 ± 0.04^{a}
Effluent B (10% Conc.) Mean ± S.D 1st Harvest 2nd Harvest 3rd Harvest	11.15 ± 0.40^{b} 9.30 ± 1.00^{a} 9.67 ± 0.16^{a}	1.28 ± 0.08^{a} 1.25 ± 0.20^{a} 1.20 ± 0.05^{a}	18.80 ± 0.01^{a} 21.10 ± 0.20^{ab} 23.95 ± 0.15^{bc}	28. 31 ± 0.07^{a} 43.30 ± 0.07^{c} 50.69 ± 0.16^{d}	43.43 ± 0.29^{c} 28.26 ± 0.12^{a} 24.54 ± 0.01^{a}	32.15 ± 0.001^{b} 28.25 ± 0.19^{ab} 21.04 ± 0.09^{ab}	3.76 ± 0.16^{cd} 2.54 ± 0.50^{c} 2.11 ± 0.66^{ab}

Means ± S.D in the same column that do not have similar letters are significantly different at $P < 0.05$ according to one-way Analysis of Variance (ANOVA-1); PFW = Plant Fresh Weight; PDW = Plant Dry Weight; PH = Plant Height; LWR = Leaf Weight Ratio; SWR = Stem Weight Ratio; RWR = Root Weight Ratio; SRR = Shoot-Root Ratio.

Table 3. Effects of electroplating effluents on heavy metal concentrations in *Amaranthus viridis*.

	1st Harvest				2nd Harvest				3rd Harvest			
Samples	**Zn** µg kg^{-1}	**Ni** µg kg^{-1}	**Cr** µg kg^{-1}	**Cu** µg kg^{-1}	**Zn** µg kg^{-1}	**Ni** µg kg^{-1}	**Cr** µg kg^{-1}	**Cu** µg kg^{-1}	**Zn** µg kg^{-1}	**Ni** µg kg^{-1}	**Cr** µg kg^{-1}	**Cu** µg kg^{-1}
Control **Leaves** **Stems** **Roots**	41.65 ± 0.01^{a} 38.88 ± 0.01^{a} 36.10 ± 0.01^{a}	* * *	1.00 ± 0.90^{a} 1.10 ± 0.40^{a} 1.10 ± 1.10^{a}	30.55 ± 0.05^{a} 31.73 ± 0.29^{a} 29.73 ± 0.11^{a}	55.65 ± 0.10^{b} 50.00 ± 0.30^{b} 38.88 ± 0.81^{a}	* * *	1.00 ± 0.70^{a} 1.10 ± 0.20^{a} 1.15 ± 0.18^{a}	34.55 ± 0.05^{a} 30.90 ± 0.80$_{a}$ 24.10 ± 0.22^{a}	56.65 ± 0.10^{a} 52.78 ± 0.40^{a} 44.42 ± 0.12^{a}	1.00 ± 0.01^{a} * *	1.20 ± 0.04^{a} 1.15 ± 0.29^{a} 1.15 ± 0.29^{a}	35.39 ± 0.10^{a} 31.37 ± 0.30^{a} 30.73 ± 0.01^{a}
Effluent A-5% **Leaves** **Stems** **Roots**	91.65 ± 0.50^{bd} 72.20 ± 0.22^{bc} 66.65 ± 0.80^{b}	* * *	500.00 ± 0.10^{b} 485.70 ± 0.70^{b} 357.00 ± 0.03^{b}	34.10 ± 0.01^{a} 54.55 ± 0.08^{b} 40.90 ± 0.20^{c}	88.88 ± 0.02^{c} 50.00 ± 0.08^{b} 41.65 ± 0.16^{a}	* * 168.58 ± 0.01^{a}	357.15 ± 0.01^{b} 357.15 ± 0.01^{b} 428.57 ± 0.10^{bc}	42.90 ± 0.05$_{b}$ 41.90 ± 0.05$_{b}$ 54.55 ± 0.22$_{c}$	130.55 ± 0.10^{c} 136.10 ± 0.40^{c} 86.10 ± 0.12^{b}	357.15 ± 0.90^{c} * *	357.15 ± 0.04^{bc} 428.57 ± 0.29^{c} 428.57 ± 0.29^{c}	47.73 ± 0.10^{b} 34.10 ± 0.30^{c} 47.73 ± 0.10^{a}
Effluent A-10% **Leaves** **Stems** **Roots**	47.20 ± 0.80^{a} 36.10 ± 0.30^{a} 36.10 ± 0.60^{a}	* * *	500.00 ± 0.10^{b} 485.57 ± 0.40^{b} 500.00 ± 0.80^{b}	68.18 ± 0.13^{d} 61.37 ± 0.03^{d} 68.18 ± 0.05^{d}	230.55 ± 0.2^{d} 69.43 ± 0.05^{bc} 61.10 ± 0.02^{b}	* * *	214.30 ± 0.70^{bd} 357.15 ± 0.07^{b} 357.15 ± 0.07^{b}	47.30 ± 0.05$_{bc}$ 40.90 ± 0.40$_{b}$ 34.10 ± 0.22$_{a}$	241.66 ± 0.10^{d} 55.55 ± 0.40^{a} 47.20 ± 0.12^{a}	357.15 ± 0.90^{c} 142.85 ± 0.40^{b} *	357.15 ± 0.11^{bc} 347.15 ± 0.29^{bc} 357.15 ± 0.11^{bc}	40.90 ± 0.10^{ab} 40.90 ± 0.10^{ab} 37.90 ± 0.21^{a}
Effluent B-5% **Leaves** **Stems** **Roots**	55.55 ± 0.23^{cd} 44.42 ± 0.16^{ac} 36.10 ± 1.30^{a}	* * *	500.00 ± 0.50^{b} 214.30 ± 0.45^{c} 500.00 ± 0.20^{b}	47.73 ± 0.05^{c} 68.25 ± 0.23^{d} 34.10 ± 0.08^{a}	33.32 ± 0.09^{a} 38.88 ± 0.10^{a} 36.10 ± 0.02^{a}	178.58 ± 0.02^{a} * 214.30 ± 0.11^{ab}	428.57 ± 0.02^{b} 258.70 ± 0.20^{d} 258.70 ± 0.04^{d}	54.55 ± 0.05^{c} 47.73 ± 1.80^{bc} 40.90 ± 0.22^{b}	133.30 ± 0.10^{d} 113.87 ± 0.40^{d} 61.10 ± 0.12^{b}	500.00 ± 0.90^{d} 250.00 ± 0.40^{bc} 71.43 ± 0.10^{b}	357.15 ± 0.04^{bc} 214.31 ± 0.29^{d} 357.15 ± 0.04^{bc}	61.37 ± 0.10^{d} 54.55 ± 0.30^{bc} 61.37 ± 0.10^{d}
Effluent B-10% **Leaves** **Stems** **Roots**	47.20 ± 0.40^{ac} 30.55 ± 0.50^{a} 27.78 ± 0.16^{a}	* * *	500.00 ± 0.01^{b} 258.70 ± 0.20^{c} 258.70 ± 0.15^{c}	54.55 ± 0.07^{b} 47.73 ± 0.07^{c} 47.73 ± 0.16^{c}	91.65 ± 0.29^{c} 75.00 ± 0.12^{c} 38.88 ± 0.01^{a}	107.15 ± 0.01^{c} 178.58 ± 0.19^{a} 178.58 ± 0.19^{a}	158.70 ± 0.16^{d} 158.70 ± 0.16^{d} 148.70 ± 0.06^{d}	47.73 ± 0.22^{bc} 47.73 ± 0.22^{bc} 47.73 ± 0.22^{bc}	83.32 ± 0.10^{b} 61.10 ± 0.12^{a} 61.10 ± 0.12^{a}	285.70 ± 0.90^{bc} * 142.85 ± 1.10^{b}	357.15 ± 0.04^{bc} 357.15 ± 0.04^{bc} 357.15 ± 0.04^{bc}	54.55 ± 0.10^{bc} 61.37 ± 0.30^{d} 47.73 ± 0.01^{a}
Standard Permissible Limits	60[1]	1.50[1]	2.32	40[3]	60[1]	1.50[1]	2.32	40[3]	60[1]	1.50[1]	2.32	40[3]

(*) means Metal Not Detected; [1]WHO/FAO (Codex Alimentarius Commission. Joint FAO/WHO [30]; [2]WHO (Codex Alimentarius Commission, Joint FAO/WHO [31] and codex alimentarius commission [28]; [3]WHO/FAO (FAO/WHO, codex general standard for contamination and toxin in foods [32]); Means ± S.D (µg kg^{-1}) in the same column that do not have similar letters are significantly different at $P < 0.05$ according to one-way Analysis of Variance (ANOVA-1).

4. Conclusions and recommendation

This research has shown that there were great effects of electroplating effluents on the growth and heavy metals' accumulations and concentrations in *A. viridis*. The results revealed that the effluent affects the growth rhythms of the plant. Also, it showed that plants do take up metals from the soil and surrounding media. Furthermore, it revealed that most of the effluents are either acidic or alkaline in nature, which is toxic to plants. Thus, from all indications, *A. viridis* and many other leafy vegetables may take up heavy metals from the soil through their roots to the stem and then to the leaves. This, therefore, poses a great risk to the consumers of vegetables especially those grown around discharge areas of industrial effluents. However, waste from industries especially those from electroplating companies should be treated and all heavy metals removed or reduced to the required discharge limits before they are released into the environment.

Author Contributions

Oluwole S.O. and Ogun M.L. conceived the idea, Ogun M.L., Tope-Akinyetun, R.O., Asokere S.Y., Ewekeye T.S. and Usamot Q., designed it, Ogun M.L., Asokere S.Y., and Usamot Q., executed it, Oluwole S.O, Asokere S.Y., Ewekeye T.S and Ogun M.L. interpreted the data and Ogun M.L., Ewekeye T.S., Asokere S.Y. and Tope-Akinyetun, R.O. wrote the manuscript.

Conflict of Interest

All Authors declare no conflict of interest.

Funding

This research received no external funding.

Acknowledgement

Authors appreciate all members of staff of the Department of Botany, Faculty of Science, Lagos State University, Ojo, Lagos, Ojo, Nigeria towards the success of this study.

References

[1] Fang, G.C., Chang, C.N., Chu, C.C., et al., 2003. Characterization of particulate, metallic elements of TSP, PM2.5 and PM2.5-10 aerosols at a farm sampling site in Taiwan, Taichung. Science of the Total Environment. 308(1-3), 157-166.

[2] Ibrahim, Y.H., Shakour, A.A., Abdel-Latif, N.M., et al., 2011. Assessment of heavy metal levels in the environment, Egypt. The Journal of American Science. 7(12), 148-153.

[3] Romic, M., Romic, D., 2003. Heavy metals distribution in agricultural topsoils in urban area. Environmental Geology. 43, 795-805.

[4] Pilon-Smits, E., 2005. Phytoremediation. Annual Reviews of Plant Biology. 56, 15-39.

[5] Monica, S., Karthik, L., Mythili, S., et al., 2011. Formulation of effective microbial consortia and its application for sewage treatment. Journal of Microbial Biochemistry Technology. 3, 051-055.

[6] Whatmuff, M.S., 2002. Applying biosolids to acid soils in NSW: Are guideline soil metal limits from other countries appropriate? Soil Research. 40(6), 1941-1056.

[7] McBride, M.B., 2003. Toxic metals in sewage sludge-amended soils: Has promotion of beneficial use discounted the risks? Advances in Environmental Research. 8(1), 5-19.

[8] Nriagu, J.O., 1988. A silent epidemic of environmental metal poisoning? Environmental Pollution. 50(1-2), 139-161.

[9] Alloway, B.J., Ayres, C.D., 1997. Chemical principals of environmental pollution, (2nd ed.). Blackie Academic and Professional: London.

[10] Oluwole, S.O., Makinde, S.C.O., Ogun, M.L., et al., 2020. Evaluation of heavy metal concentrations and proximate compositions of *Amaranthus spinosus* L. and *Talinum triangulare* J. and soils collected dumpsites in some selected areas in Lagos State, Nigeria. World Environment. 10(1), 16-26.

DOI: https://doi.org/10.5923/j.env.20201001.03

[11] Fatoki, O.S., 2000. Trace zinc and copper concentrations in roadside vegetation and surface soils: A measurement of local atmospheric pollution in Alice, South Africa. International Journal of Environmental Studies. 57(5), 501-513.

[12] Cobbett, C., 2003. Heavy metals and plants: Model systems and hyperaccumulators. New Phytologist. 159, 289-293.

[13] Stolt, P., Asp, H., Hultin, S., 2006. Genetic variation in wheat cadmium accumulation on soils with different cadmium concentrations. Journal of Agronomy and Crop Science. 192(3), 201-208.

[14] FEPA, 1991. Guidelines and standards for environmental pollution control in Nigeria. Federal Environmental Protection Agency: Lagos.

[15] Okigbo, B.N. (editor), 1975. Neglected plants of horticultural and nutritional importance in traditional farming systems of tropical Africa. Fourth Africa Symposium on Horticultural Crop; 1975 Aug 12-17; Kumasi, Ghana. 53, 131-150.

[16] Odjegba, V.J., Sadiq, A.O., 2000. Effects of spent engine oil on the growth parameters, chlorophyll, and protein level of *Amaranthus hybridus L*. The Environmentalist. 22, 23-28.

[17] Oluwole, S.O., Ogun, M.L., Adogba, N.P., et al., 2020. Impacts of two different locations on the growth, proximate and mineral compositions of *Celosia argentea* L. and *Amaranthus cruentus*. Research and Analysis Journal of Applied Research. 6(7), 2698-2705.

[18] Baird, R., Bridgewater, L., 2012. Standard methods for the examination of water and wastewater. American Public Health Association: Washington, DC.

[19] Oluwole, S.O., Ogun, M.L., Balogun, O.A., 2018. Effects of different watering regimes on the growth of Talinum triangulare Jacq.(Waterleaf). Journal of Research and Review in Science. 5(1), 14-23.

[20] Bahemuka, T.E., Mubofu, E.B., 1999. Heavy metals in edible green vegetables grown along the sites of the Sinza and Msimbazi rivers in Dar es Salaam, Tanzania. Food Chemistry. 66(1), 63-66.

[21] Ikeda, M., Zhang, Z.W., Shimbo, S., et al., 2000. Urban population exposure to lead and cadmium in east and south-east Asia. Science of the Total Environment. 249(1-3), 373-384.

[22] Oluwole, S.O., Ogun, M.L., Dajakpome, G.O., 2020. Mineral analysis and morphological responses on the seedling growth of Telfairia occidentalis (Ugwu) on four different soil types. International Journal of Modern Botany. 10(1), 9-14.
DOI: https://doi.org/10.5923/j.ijmb.20201001.02

[23] Oluwole, S.O., Fajana, O.O., Ogun, M.L., et al., 2019. Proximate and mineral composition analysis of the leaves of *Amaranthus cruentus* and *Ocimum gratissimum* in some selected areas in Lagos State, Nigeria. International Journal of Ecosystem. 9(1), 6-11.
DOI: https://doi.org/10.5923/j.ije.20190901.02

[24] Tasrina, R.C., Rowshon, A., Mustafizur, A.M.R., et al., 2015. Heavy metals contamination in vegetables and its growing soil. Journal of Environmental Analytical Chemistry. 2(142), 1-6.

[25] Ibrahim, Y.H., 2000. Air pollution in the Industrial area north of Cairo with special reference to its effects on plants [Ph.D. Thesis]. Egypt: Cairo University, Egypt.

[26] Landsberger, S., Iskander, F., Basunia, S., et al., 1999. Lead and copper contamination of soil from industrial activities and firing ranges. Biological Trace Element Research. 71, 387-396.

[27] Oluwole, S.O., Makinde, S.C.O., Yusuf, K.A., et al., 2013. Determination of heavy metal contaminants in leafy vegetables cultivated by the Roadside. International Journal of Engineering Research and Development. 7(3), 1-5.

[28] Inorganic Lead [Internet]. World Health Organization; 1995. Available from: https://apps.who.int/iris/handle/10665/37241

[29] Khemani, L.T., Momin, G.A., Rao, P.P., et al., 1989. Spread of acid rain over India. Atmospheric Environment. 23(4), 757-762.

[30] Safety Evaluation of Certain Food Additives

and Contaminants [Internet]. Joint FAO/WHO Expert Committee on Food Additives; 2002. Available from: https://apps.who.int/iris/handle/10665/42501

[31] FAO, 2001. Codex alimentarius commission. ALINORM 01/12A, 1-289.

[32] General Standard for Contaminants and Toxins in Food and Feed [Internet]. FAO & WHO; 1995. Available from: https://www.fao.org/fao-who-codexalimentarius/sh-proxy/en/?lnk=1&url=https%253A%252F%252Fworkspace.fao.org%252Fsites%252Fcodex%252FStandards%252FCXS%2B193-1995%252FCXS_193e.pdf

BILINGUAL PUBLISHING GROUP

Journal of Botanical Research

https://journals.bilpubgroup.com/index.php/jbr

ARTICLE

A Farmer's Approach to Detecting Photoperiod Sensitivity in Rice (*Oryza sativa* ssp. *indica*) Landraces

Debal Deb

Centre for Interdisciplinary Studies, Kolkata, 700075, India

ABSTRACT

Most indigenous rice landraces are sensitive to photoperiod during short day seasons, and this sensitivity is more pronounced in *indica* than in *japonica* landraces. Attempts to identify photoperiod sensitive (PPS) cultivars based on the life history stages of the rice plant, and several models and indices based on phenology and day length have not been precise, and in some cases yield counterfactual inferences. Following the empirical method of traditional Asian rice farmers, the author has developed a robust index, based on the sowing and flowering dates of a large number of landraces grown in different seasons from 2020 to 2023, to contradistinguish PPS from photoperiod insensitive cultivars. Unlike other indices and models of photoperiod sensitivity, the index does not require the presumed duration of different life history stages of the rice plant but relies only on the flowering dates and the number of days till flowering of a rice cultivar sown on different dates to consistently identify photoperiod sensitive cultivars.

Keywords: *Aman*; *Aus*; *Boro*; Flowering; Landraces; Photoperiod sensitivity; Rice (*Oryza sativa* L.)

1. Introduction

Flowering in most indigenous rice (*Oryza sativa* L.) landraces is sensitive to seasonal photoperiod during the short day season. Among the cultivated rice, *japonica* cultivars tend to be more sensitive to temperature and less sensitive to photoperiod than *indica* cultivars [1]. South Asian rice landrace that flower during short, cooler days and are harvested in winter, are termed *aman* and *sali* in eastern India and Bangladesh, *samba* in southern India [2], *mayin* in Myanmar and *na bi* in Thailand [3]. Most of the short-day rice landraces are strongly photoperiod sensitive (PPS), flowering on about the same date every year

*CORRESPONDING AUTHOR:
Debal Deb, Centre for Interdisciplinary Studies, Kolkata, 700075, India; Email: debdebal@gmail.com

ARTICLE INFO
Received: 20 May 2023 | Revised: 4 July 2023 | Accepted: 7 July 2023 | Published Online: 13 July 2023
DOI: https://doi.org/10.30564/jbr.v5i3.5737

CITATION
Deb, D., 2023. A Farmer's Approach to Detecting Photoperiod Sensitivity in Rice (*Oryza sativa* ssp. *indica*) Landraces. Journal of Botanical Research. 5(3): 60-66. DOI: https://doi.org/10.30564/jbr.v5i3.5737

during the short-day season, regardless of the date of sowing. Some of the *aman* landraces that can also flower during the hotter long-day (termed *boro* and *aus*) seasons are insensitive to photoperiod [4].

Traditional farmers used to identify the degree of photoperiod sensitivity of their landraces by the invariance of either the date of anthesis or the date of 50% flowering. However, the precision of sensitivity to photoperiod is also variable in many landraces, and Yoshida (p. 44) [5] observed that "there is no sharp dividing line between the photoperiod-sensitive and photoperiod-insensitive varieties, and any definition would be based on arbitrary criteria"—accounting for an amorphous classification of strong, moderate and weak photoperiod sensitivity [5,6]. Rice biologists [5-7] have constructed a schema of growth phases of the rice plant, showing changes in the basic vegetative phase (BVP) and photoperiod sensitive phase (PSP) of the rice plant at short-day and long-day (> 11 h) seasons. **Figure 1** describes the growth phases of rice cultivars in the short day condition (*aman* season in South Asia), but sown on different days (e.g. 1 May and 20 May). If the cultivar flowers on about the same date despite considerably different sowing dates, the cultivar is PPS. If the flowering date is delayed proportionately by delayed sowing, the cultivar is photoperiod insensitive (PPI).

Several authors have developed a few indices to identify photoperiod-sensitive rice cultivars by considering the duration of the reproductive phase (RP) and vegetative growth phase [8-10], but "these models are only valid at the latitude where they have been calibrated" [10,11]. However, the actual anthesis date of many cultivars does not seem to match exactly with that predicted by the indices. We examine here the limitations of a most cited photoperiod-sensitivity index, and propose an alternative, simpler index, which takes into account only the degree of invariance of the date of anthesis in different years.

2. Materials and methods

Over 3 years from 2020 to 2022, we recorded the dates of sowing and the first flowering dates (FD) of 1114 rice landraces [12], among which we examine here 92 landraces that were repeat-sown in different years either in the same season or in different seasons. Eighty-one of these landraces were cultivated in the short-day season in different years, while 23 were cultivated in the long-day season, among which 12 were sown in both long-day and short-day seasons (detailed in Supplementary Material [13]). All these landraces were cultivated on the Basudha conservation farm (http://cintdis.org/basudha), located in Bissam Cuttack block, Rayagada district of Odisha. India (19°42'32.0" N, 83°28'8.4" E).

The deviation of the FD of each landrace grown during the short day season in different years was recorded. This difference in FD of a landrace between years (dFD) would indicate the degree of photoperiod sensitivity of that landrace, because an ideal, strongly PPS cultivars ought to show dFD ≈ 0 d. Conversely, a PPI cultivar would not only show a wide range of dFD (> 6 d) between years, but also flower in both short- and long-day seasons.

Using the flowering data of the landraces summarised in Supplementary Material [13], we develop an index of photoperiod sensitivity based on the relative invariance of FD:

$$PPSI = dFD / |dFD - dDTF| \quad (1)$$

where dFD is the actual seasonal difference in flowering dates = |FD*i* – FDE|;

DTF = Days till flowering, is the number of days from the sowing date (SD) till FD, or (FD – SD);

dDTF = |(DTF – DTFE)|;

FD*i* is the flowering date observed for the *i*th sowing date;

FDE is the earliest flowering date in a short day season of a given year;

DTFE is the number of days from the sowing of a cultivar to FDE, or (FDE – SD).

The index is zero if FD_i = FDE. To illustrate, if the FD1 of a cultivar is 10 Sep 2020, and FD2 of the same cultivar is 01 Sep 2021, then FDE is 01 Sep 2021; thus, dFD = 10 Sep – 01 Sep = 9 d.

The difference (in days) between |DTF*i* – DTFE| and |FD*i* – FDE| informs whether anthesis is delayed in response to a delay in the sowing date—a feature characteristic of PPI cultivars. This difference would

approximate zero for a purely PPI cultivar that comes to flowering exactly according to the sowing date, without changing the growth phase duration till maturity. Conversely, |FD*i* – FDE| is zero for strongly PPS cultivars. Based on this understanding, we estimate the range of PPSI values for all the landraces examined, based on the actual DTF, DTFE and dFD of all the landraces.

For an accurate estimation of the effective interval of one or more years ($Y > 0$) between the dates of anthesis, the following procedure was undertaken. For a cultivar flowering during the same season in different years, a factor of 365*Y* must be subtracted from the dFD, to calculate the *actual seasonal difference* (in days), because the interval between two successive *aman* (or *boro*) seasons is 365 d (except leap years, in which case the interval is 366 d). An *aman* cultivar, for instance, that flowers in September are likely to flower also on the same date in succeeding years (dFD = 0), exactly 365*Y* d later. If its anthesis occurs during the *boro* (long day) season, we calculate the difference between this interval and 365*Y*. For example, the FD1 (= FDE) of cultivar DD01, sown during *aman* season, was 03 September 2020, and FD2 was 16 September 2021 when sown in July 2021 (**Table 1** and Supplementary Material). In this instance, $Y = (2021 – 2020) = 1$, and dFD between the two *aman* seasons = |FDE – FD2| = (378 – 365 x 1) d = 13 d. The same cultivar was sown during *boro* season, and its flowering date FD3 was 28 April 2022; so the actual seasonal difference between the short-day and long-day flowering dates is |FDE – FD3| = |602 – 2 x 365| d = 128 d. All the calculations are shown in Supplementary Material [13].

3. Results

An illustrative data set presented in **Table 1**, drawn on the data of flowering of 91 rice landraces [13] shows that for the cultivar DD01, the earliest flowering date (FDE), marked during the short day season of any year, is 03 September, corresponding to its sowing date on 17 June. For cultivar N03, the FDE is 06 September, corresponding to its sowing date on 20 June.

The data of 92 landraces with their SD, FD, dFD and DTF, and the corresponding calculations of PPSI are presented in Supplementary Material [13]. It is common knowledge that strong photoperiod sensitivity is found in most short-day (*aman*) rice, and they do not flower beyond a "critical" photoperiod, usually > 11 h [6]. Thus, we identify the PPI landraces as those that flowered both during short- and long-day seasons, and their anthesis occurs after a fixed

Table 1. Identification of photo-period sensitivity based on sowing dates and flowering dates of illustrative rice cultivars (Excerpted from Supplementary Material [13]).

Cultivar & Year	SD	FD	DTF (d)	Factor to subtract from dFD	dFD (d)	|dFD – dDTF|	PPSI
***C04* (2020)**	17 JUN	22 SEP	97	0	8	17	0.47
C04 (2021)	04 JUL	14 SEP*	72	365 x 1			
C04 (2022)	03 FEB	11 APR	67	365 x 1	156	51	1.03
DD01 (2020)	17 JUN	03 SEP*	78	0			
DD01 (2021)	07 JUL	16 SEP	71	365 x 1	13	6	2.17
DD01 (2022)	03 FEB	28 APR	84	365 x 2	128	122	1.05
DD01 (2022)	29 MAR	21 JUN	84	365 x 2	74	68	1.09
S90 (2020)	17 JUN	18 SEP*	93	0	0		
S90 (2021)	08 JUL	18 SEP*	72	365 x 1	0	21	0
S90 (2022)	29 JUN	19 SEP	82	365 x 2	1	10	0.10

DTF = Days till flowering; DTFE = Days till earliest flowering during the short-day season; FD = Flowering date; FDE = Earliest date of flowering during the short-day season; dDTF = DTFi – dTFE; dFD = FDi – FDE; PPSI = Photoperiod sensitivity index. An asterisk (*) corresponds to the FDE of respective cultivars.

vegetative growth phase of the rice plant [6]. For these landraces in our dataset, PPSI is always found to exceed the value of 0.33. Conversely, many of the landraces that flowered only during the short-day season showed largely invariant FD, and were identified as strongly PPS. The PPSI for these landraces is seen to never exceed the value of 0.33.

4. Discussion

Previous analyses of photoperiod sensitivity in rice emphasized the different growth phases of the rice plant. In South Asia, most of the PPS winter (*aman*) landraces do not anthese in the long-day season, when the critical day PP exceeds 11 h. For example, the strong PPS landrace Latisail never flower in long day condition beyond 12 h of daylight [5]. However, if a cultivar can flowers in both seasons, its photoperiod sensitivity can be estimated as follows.

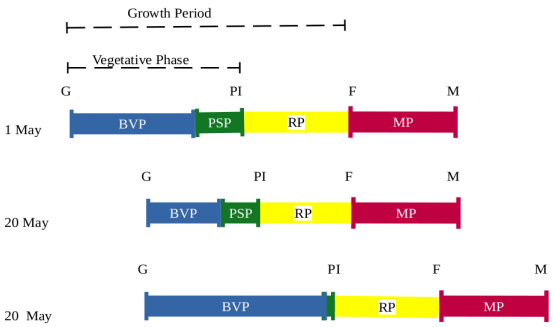

Figure 1. Schema of rice growth phase [7]: A vegetative period begins from germination (G) of the seedling until panicle initiation (PI), followed by a Reproductive Phase (RP) of a fixed duration (35 d) until flowering (F). The vegetative period consists of a Basic Vegetative Phase (BVP) and a photoperiod sensitive period (PSP), which ends at PI. The RP is followed by the grain Maturation Phase (MP) ranging from 30 d to 35 d, terminated at grain maturation (M). Different sowing dates are shown on the left.

"Maximum differences in growth duration can be obtained in the May and November plantings if temperatures are not too low for growth. If a rice's growth duration changes more than 30 d, agronomists usually consider it photoperiod sensitive or a seasonal cultivar." [6]. For instance, the PPS landrace Peta has DTF = 70 d at 10 h (winter) photoperiod, and DTF = 145 d at 16 h (summer) photoperiod [5]. With this data, the photoperiod sensitive phase (PSP) of the cultivar is calculated, assuming RP = 35 d:

$$\text{PSP} = \text{Longest DTF} - \text{Shortest DTF} = 145 - 70 = 75 \text{ d} \quad (2)$$

These calculations presuppose that Peta's PSP = 0 d in the short-day optimal photoperiod (as graphically shown in the study by Dinkhun and Asch [7], 1999, **Figure 1**):

Shortest DTF = BVP (35 d) + PSP (0 d) + RP (35 d) = 70 d

Longest DTF = BVP (35 d) + PSP (75 d) + RP (35 d) = 145 d

This assumption of PSP = 0 in short day condition implies that a strong PPS cultivar responds to the optimal photoperiod after PI. However, this contradicts the fact that only PPI cultivars can have a very short PSP, according to the "practical grouping" [6] (V&C) of rice varieties based on rice phenology (**Table 2**).

Table 2. Rice growth phases and corresponding phenological features (Vergara and Chang, 1985).

Response to day length	Phenological features
Photoperiod insensitive	Very short PSP (< 30 d) and BVP varying from short to long.
Weakly photoperiod-sensitive	Marked increase in growth duration when photoperiod is longer than 12 h; PSP may exceed 30 d, but flowering occurs under any long photoperiod.
Strongly photoperiod sensitive	Sharp increase in growth duration with increase in photoperiod; no flowering beyond critical photoperiod; BVP usually short (< 41 d).

4.1 Dissents to the schema

Collinson et al. [14] disagreed with the procedure of estimation of PSP. "The PSP [is] calculated as the difference between the duration from sowing to panicle emergence in short and long days, such that in optimal photoperiods (at which progress to panicle emergence is most rapid) the end of the BVP is assumed to coincide with the end of the vegetative phase; the duration of the reproductive phase is assumed to be 35 d, and so the BVP is assumed to be 35 d less than the duration from sowing to panicle emergence in optimal photoperiods. It would be re-

markable if this arbitrary 35 d period proved to be not only insensitive to temperature but also identical for different cultivars." (p. 340). They [14] further showed that RP may range from 30.2 to 52.9 d at different temperatures. However, the contention of a significant effect of post-PI photoperiod on the RP duration [6] was confirmed by other studies [15,16].

An alternative division of rice growth duration was also proposed [7], in which (i) a constant duration (30 d) of a reproductive phase (RP) is followed by a constant grain ripening phase (35 d); and (ii) BVP is "estimated by subtracting [RP =] 30 d from the duration to flowering at the sowing date associated with the shortest duration" [7] (p. 112). When measured as degree-days at a given temperature, the BVP appears to show a constant duration, regardless of the sowing date, and is measured following Equation (2), with RP = 30 d, instead of 35 d.

$$\text{BVP} = \text{Shortest DTF} - \text{RP} [= 30 \text{ d}] \quad (3)$$

Dinkhun and Asch [7] calculated photoperiod sensitivity "as the difference in duration of the photoperiod-sensitive phase (PSP) between 12.0 h and 12.5 h mean astronomic day length during PSP" (p. 116).

4.2 Conformity and confusion

Despite the "somewhat arbitrary" measurement of BVP and assumed length of PSP, the same method is followed in determining the degree of phoroperiod sensitivity in rice cultivars in various models of photoperiodism in rice [8,9]. This approach to determining phoroperiod sensitivity, based on the duration of BVP and PSP, instead of more direct proximity of the exact flowering date of a cultivar with different sowing dates, leads to some confusion. For all *aman* cultivars that do not flower in the long day (summer) season, PSP cannot be calculated from a difference in a cultivar's growth duration between short-day and long-day seasons, and therefore the extent of photoperiod sensitivity cannot be quantified.

This constitutes a conundrum, which makes an attempt to detect the degree of photoperiod sensitivity in different rice landraces with recourse to different life history stages and their phenological durations of the rice plant. This conundrum is built summarily on:

(i) The arbitrary choice of a constant 35 d [6] or 30 d [7] for RP, overlooking the wide variability (30 to 52.9 d) of the RP, already documented [7];

(ii) The assumption that PSP = 0 in the calculation of the shortest DTF of a PPS cultivar (Equation (2)), directly contradicting the "practical" consideration [6] (**Table 2**) that PPI cultivars have very short PSP;

(iii) The thumb rule that *boro* and *aus* landraces (flowering in long day periods of April and early June, respectively) are PPI, is vitiated by the fact that some of the PPS cultivars described by those authors (such as Peta) flower both during short and long day seasons; implying that either this classification or the identification of PPS based on estimation of PSP, is incorrect.

It is impossible to determine if a cultivar is PPS or PPI when the FD during the short-day season is unavailable. Therefore, the criterion of the difference between PSP of the cultivar sown on different dates may not give a reliable indication of the degree of photoperiod sensitivity. An index of photoperiod sensitivity, based on flowering dates during at least 1 short day season is required to contradistinguish the PPI from PPS cultivars, regardless of the availability of the data pertaining to PVP and RP durations.

4.3 A misleading index in vogue

Immark et al. [8] and Khotasena et al. [9] considered two flowering dates of the same cultivar sown on two different dates, and employed the ratio of the difference between two DTFs and the interval between two sowing dates (SD) as an index of photoperiod sensitivity:

$$\text{PSI} = |\text{DTF1} - \text{DTF2}| / |\text{SD1} - \text{SD2}|, \quad (4)$$

and classified the cultivars with PSI < 0.3 as PPI, and PSI > 0.7 as strongly PPS [9].

This index poses two kinds of problems. Firstly, in the trivial case of SD1 = SD2 during the same season [8], the PSI is indeterminately large (division by zero). Secondly, if a cultivar is sown in *aman* and

DTF1 = DTF2, but FD1 and FD2 are wide apart, the Equation (4) would always yield PSI < 0.3, leading to the exactly opposite, counterfactual inference that cultivars flowering on widely different dates are all PPS!

4.4 Resolving the conundrum with Occam's razor

Previous attempts at indexing the PPS cultivars seem to be inaccurate, primarily because they counted on various *durations*, namely, DTF, BVP, RP and PSP, which in turn are calculated by indirect means, based on certain assumptions, some of which are disputable. We contend here that a more parsimonious approach of reliance on the exact sowing and flowering dates, rather than any estimated duration of PSP and RP, maybe more fruitful—the approach taken by indigenous farmers over centuries. The PPSI threshold of 0.33 developed here is not arbitrarily determined based on any *a priori* assumptions, but empirically derived from the values obtained from the invariant flowering dates of cultivars that do not flower in the long day season (see calculations in Supplementary Material [13]).

5. Conclusions

The basic characteristic of a strongly PPS cultivar is that its flowering date would ideally not deviate from a fixed date in a given season, regardless of different sowing dates. Rice farmers do not sow their *aman* crop more than 2 months later, unlike experimental agronomists, and are reasonably confident of the relatively invariant flowering date, especially for rice grown during the short-day season. Traditional farmers of South Asia sow the same cultivar in successive years on different dates, contingent on the arrival of the monsoon rain. Thus, *aman* cultivars are sown usually in May-June, but the sowing date may sometimes be delayed in some years by a month. The farmers used to recognize that if an *aman* cultivar flowers every year on the same date (with a few days' deviation), despite widely different sowing dates, it is PPS. Conversely, if the flowering dates are widely (> 10 d) different from the mean FD, it is PPI. Our experience with more than 1400 PPS landraces cultivated on our conservation farm Basudha (http://cintdis.org/basudha) over 25 years indicates that BVP, RP and PSP seem to be irrelevant, from the farmer's perspective, to detect the photoperiod sensitivity of a cultivar, regardless of their physiological importance in orchestrating the plant's photoperiod response at the molecular level. We demonstrate this using our record [12] of actual sowing and flowering dates of PPS and PPI cultivars in different seasons and years.

Our index of photoperiod sensitivity PPSI simulates this traditional procedure, and relies only on the date of flowering and the DTF, rather than on any presumption of the length of PSP or constancy of duration of life history stages (BVP, RP), and is therefore independent of latitudinal differences in day length. This parsimony of factors for adequate explanation is an application of Occam's Razor. For all strongly PPS cultivars, PPSI < 0.33, such as S90, despite altered days of sowing. Conversely, all cultivars (e.g. AA03, C04, DD01, G32, and N03) with PPSI > 0.33 are PPI, and they all bloomed during both short day and long day seasons (**Table 1**). This categorical consistency of the index is its most reliable property.

Supplementary Material

Supplementary Material contains the author's original data and calculations, and is freely available from Harvard Dataverse, DOI: https://doi.org/10.7910/DVN/QRCNMD [13].

Conflict of Interest

There is no conflict of interest.

Funding

This work received no institutional funding.

Acknowledgement

I am grateful to Debdulal Bhattachary and Ma-

hendra Nauri of Basudha farm for their diligent assistance in recording all phenological data of rice landraces.

References

[1] Summerfield, R.J., Collinson, S.T., Ellis, R.H., et al., 1992. Photothermal responses of flowering in rice (*Oryza sativa*). Annals of Botany. 69(2), 101-112.

[2] Government of India, Rice Knowledge Management Portal [Internet] [cited 2023 Jul 12]. Available from: http://www.riceportal.in/extension-domain/national/production-know-how/seasons

[3] The Real Life of Thai Rice Farmers Who Produce to Feed the World [Internet]. Available from: https://www.landactionthai.org/english/item/142-the-real-life-of-thai-rice-farmers-who-produce-to-feed-the-world.html

[4] Gangulee, H.C., 1954. Types of flowering behaviour in rice 'oryza sativa linn.' and the distinctiveness of the aman type. Current Science. 23(3), 80-81.

[5] Yoshida, S., 1981. Fundamentals of rice crop science. International Rice Research Institute: Los Baños, Philippines.

[6] Vergara, B.S., Chang, T.T., 1985. The flowering response of the rice plant to photoperiod, 4th ed. International Rice Research Institute: Los Baños, Philippines.

[7] Dingkuhn, M., Asch, F., 1999. Phenological responses of *Oryza sativa*, O. glaberrima and inter-specific rice cultivars on a toposquence in West Africa. Euphytica. 110(2), 109-126.

[8] Immark, S., Mitchell, J.H., Jongdee, B., et al. (editors), 1997. Determination of phenology development in rainfed lowland rice in Thailand and Lao PDR. Proceedings of the International Workshop on Breeding Strategies for Rainfed Lowland Rice in Drought-Prone Environments; 1996 Nov 5-8; Ubon Ratchathani, Thailand. p. 89-96.

[9] Khotasena, S., Sanitchon, J., Chankaew, S., et al., 2022. The basic vegetative phase and Photoperiod Sensitivity Index as the major criteria for indigenous upland rice production in Thailand under unpredictable conditions. Agronomy. 12(4), 957.
DOI: https://doi.org/10.3390/agronomy12040957

[10] Abdulai, A.L., Kouressy, M., Vaksmann, M., et al., 2012. Latitude and date of sowing influences phenology of photoperiod-sensitive sorghums. Journal of Agronomy and Crop Science. 198(5), 340-348.

[11] Clerget, B., Sidibe, M., Bueno, C.S., et al., 2021. Crop photoperiodism model 2.0 for the flowering time of sorghum and rice that includes daily changes in sunrise and sunset times and temperature acclimation. Annals of Botany. 128(1), 97-113.
DOI: https://doi.org/10.1093/aob/mcab048

[12] Deb, D., 2022. Rice Flower Opening Time and Flower Opening Duration Data [Internet]. Available from: https://doi.org/10.7910/DVN/KYW1UC

[13] Deb, D., 2023. Flower Opening Time of Photoperiod Sensitive and Photoperiod Insensitive Rices on Sunny Days [Internet]. Available from: https://doi.org/10.7910/DVN/QRCNMD

[14] Collinson, S.T., Ellis, R.H., Summerfield, R.J., et al., 1992. Durations of the photoperiod-sensitive and photoperiod-insensitive phases of development to flowering in four cultivars of rice (*Oryza sativa* L.). Annals of Botany. 70(4), 339-346.

[15] Chandraratna, M.F., 1954. Photoperiod response in rice (*Oryza sativa* L.). I. Effects on inflorescence initiation and emergence. The New Phytologist. 53(3), 397-405.

[16] Yin, X., Kropff, M.J., 1998. The effect of photoperiod on interval between panicle initiation and flowering in rice. Field Crops Research. 57(3), 301-307.

BILINGUAL PUBLISHING GROUP
Tel:+65 65881289
E-mail: contact@bilpublishing.com
Website:https://journals.bilpubgroup.com

2630-5054 03
9 772630 505231